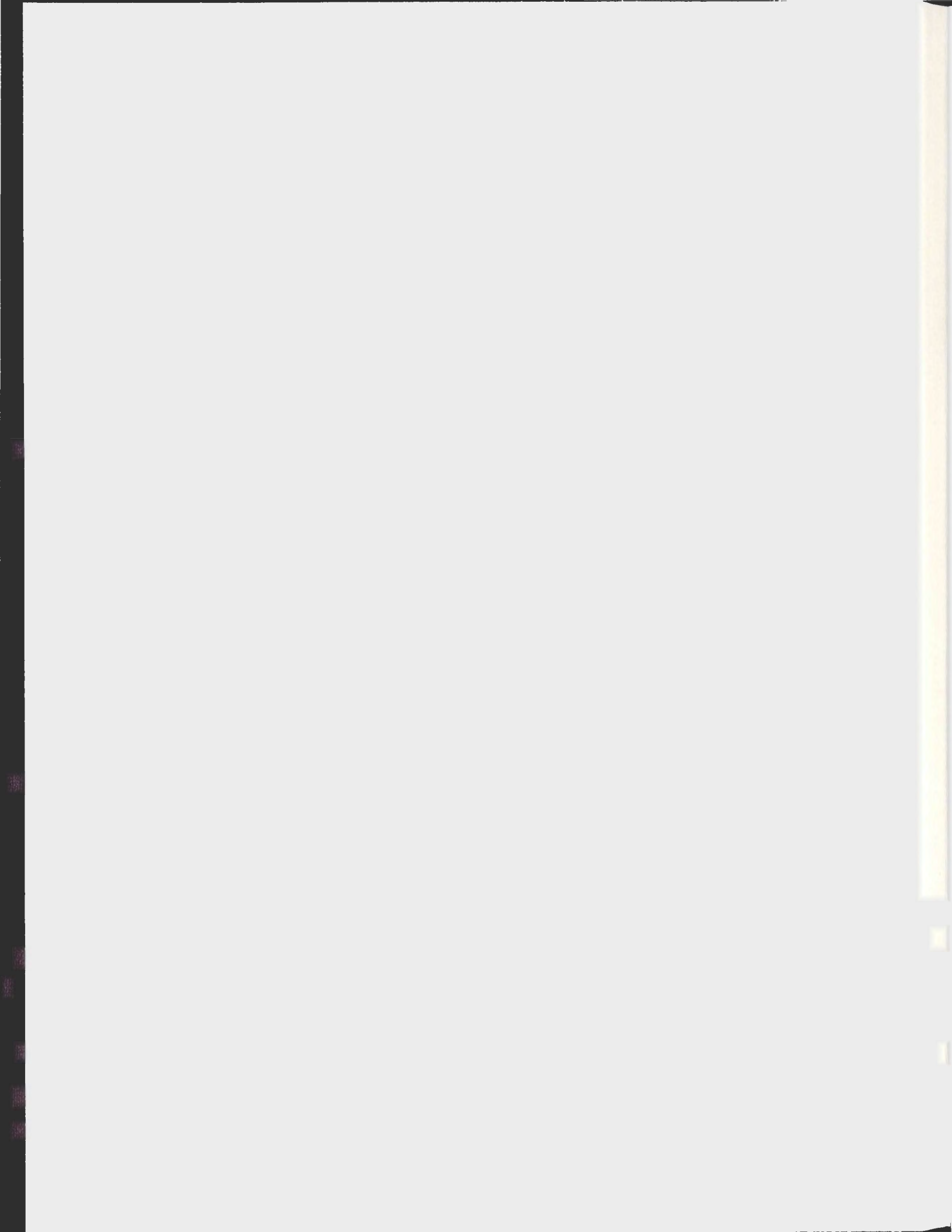


GLUTAMATERGIC ACTIVATION OF LOCUS  
COERULEUS INDUCES SELECTIVE NORADRENERGIC  
MODULATION OF MEDIAL AND LATERAL PERFORANT  
PATH EVOKED POTENTIALS IN THE DENTATE GYRUS  
OF THE ANAESTHETIZED RAT

HILARY T. EDISON





**GLUTAMATERGIC ACTIVATION OF LOCUS COERULEUS INDUCES  
SELECTIVE NORADRENERGIC MODULATION OF MEDIAL AND LATERAL  
PERFORANT PATH EVOKED POTENTIALS IN THE DENTATE GYRUS  
OF THE ANAESTHETIZED RAT**

by

**Hilary T. Edison**

A thesis submitted to the

School of Graduate Studies

in partial fulfillment of the

requirements for the degree of

**Master of Science (Experimental Neuroscience)**

Department of Psychology

Memorial University of Newfoundland

February, 2010

St. John's

Newfoundland

**Abstract**

Norepinephrine (NE) induces long-lasting potentiation of the medial perforant path (PP) and depression of the lateral PP input to dentate gyrus (DG) *in vitro*. *In vivo*, nucleus paragigantocellularis stimulation transiently potentiates the medial PP evoked population spike and depresses a lateral PP mediated synaptic potential in DG following locus coeruleus (LC) activation. In contrast, using glutamatergic activation of LC, this study in one experiment observed the expected potentiation of medial PP input to DG, but no depression of the lateral PP evoked potential (LOT stimulation, 60 s ISI) in DG post activation. A second experiment (10 s ISI) demonstrated significant potentiation of the lateral PP input to DG for 30 min immediately following LC activation, but no potentiation of the medial PP input. These results contrast with previous NE-induced *in vitro* and *in vivo* modulation of the lateral and medial PP, but resemble the long-term heterosynaptic interactions observed with tetanic stimulation of the medial and lateral PP, suggesting a competitive relationship between the medial and lateral PP inputs to DG in which the input paired most strongly and consistently with elevated LC-NE levels in the hippocampus controls the network.

**Acknowledgements**

I would like to thank Dr. Carolyn Harley for her support, supervision, and much patience over the past years, and for giving me the opportunity to enter the field of neuroscience. My thanks also to Dr. Charles Malsbury and Dr. John Evans for their assistance as members of my supervisory committee. And of course this thesis would not have been possible without the endless help of Dr. Susan Walling and Steve Milway in lab and out of it.

**Table of Contents**

Abstract	ii
Acknowledgements	iii
Table of Contents	iv
List of Figures	viii
List of Abbreviations	x
<b>Chapter 1: Introduction</b>	
1.1 Overview	1
1.2 Hippocampus and dentate gyrus	4
1.3 Entorhinal cortex	9
1.4 Perforant path	12
1.4.1 <i>Projections</i>	12
1.4.2 <i>Distinctions between medial and lateral perforant pathways</i>	12
1.4.3 <i>Stimulation of the LOT elicits lateral PP responses</i>	17
1.5 Locus coeruleus	20
1.5.1 <i>Anatomy</i>	20
1.5.2 <i>Afferent projections to LC</i>	21
1.5.3 <i>Efferent projections from LC</i>	22
1.6 Norepinephrine and adrenergic receptor localization	22
1.7 Noradrenergic modulation of hippocampal activity	23
1.8 Glutamatergic modulation of LC activity	27
1.9 Neural memory models: LTP and NE-LTP	28
1.10 Objectives	30

**Chapter 2: Experiment 1**

2.1	Introduction	33
2.2	Methods	36
2.2.1	<i>Subjects and surgical preparation</i>	36
2.2.2	<i>Recording and stimulation</i>	37
2.2.3	<i>Drugs and injection procedure</i>	38
2.2.4	<i>Histology</i>	38
2.2.5	<i>Data analysis</i>	39
2.3	Results	40
2.3.1	<i>PP-evoked population spike amplitude</i>	40
2.3.2	<i>PP-evoked EPSP Slope</i>	44
2.3.3	<i>PP-evoked latency to peak and EPSP slope paired-pulse ratio</i>	46
2.3.4	<i>LOT-evoked EPSPs</i>	52
2.3.6	<i>LOT-evoked latency to peak</i>	56
2.3.7	<i>Input-output analyses</i>	58
2.3.8	<i>E-S coupling ratio</i>	66
2.3.9	<i>Oscillation of PP- and LOT-evoked parameters</i>	69
2.3.10	<i>Histology and electrode placements</i>	71
2.4	Discussion	73

**Chapter 3: Experiment 2**

3.1	Introduction	79
3.2	Methods	82
3.2.1	<i>Subjects and surgical preparation</i>	82

3.2.2	<i>Procedures for recording, stimulation, and drug injection</i>	83
3.2.3	<i>Histology</i>	83
3.2.4	<i>Data analysis</i>	84
3.3	Results	85
3.3.1	<i>PP-evoked population spike amplitude</i>	85
3.3.2	<i>PP-evoked EPSP slope</i>	90
3.3.3	<i>PP-evoked latency to peak</i>	94
3.3.4	<i>LOT-evoked EPSP amplitude</i>	96
3.3.5	<i>LOT-evoked EPSP slope</i>	98
3.3.6	<i>LOT-evoked EPSP latency to peak</i>	100
3.3.7	<i>Input-output analyses</i>	102
3.3.8	<i>Histology and electrode placements</i>	107
3.4	Discussion	109
<b>Chapter 4: Discussion</b>		
4.1	Overview of new outcomes	114
4.2	Theoretical implications	116
4.2.1	<i>Spatial v. olfactory selectivity</i>	116
4.2.2	<i>Network resetting</i>	118
4.2.3	<i>Signal-to-noise ratio</i>	119
4.3	Other observations	121
4.3.1	<i>EPSP slope potentiation</i>	121
4.3.2	<i>ACSF controls</i>	122
4.3.3	<i>Competition in the present experiments</i>	123

4.3.4	<i>Heterosynaptic tetanic LTP and LTD of PP</i>	125
4.3.5	<i>Pairing of LC-NE and PP stimulation</i>	127
4.4	Conclusions	129
<b>Chapter 5: References</b>		131

## List of Figures

Figure 1.1	<i>Example PP-evoked waveform</i>	8
Figure 1.2	<i>Inputs and outputs of EC and hippocampal formation</i>	10
Figure 1.3	<i>Inputs to EC and DG</i>	15
Figure 1.4	<i>Example LOT-evoked waveform</i>	19
Figure 2.1	<i>Initial increase in PP-evoked population spike amplitude</i>	41
Figure 2.2	<i>Long-term increase in PP-evoked pop spike amplitude</i>	43
Figure 2.3	<i>No change in PP-evoked EPSP slope</i>	45
Figure 2.4	<i>Decrease in PP-evoked latency to peak</i>	47
Figure 2.5	<i>No initial change in PP-evoked latency to peak</i>	48
Figure 2.6	<i>PP-evoked EPSP slope paired-pulse ratio</i>	50
Figure 2.7	<i>PP-evoked EPSP slope paired-pulse ratio (ACSF control)</i>	51
Figure 2.8	<i>No change in LOT-evoked EPSP amplitude</i>	53
Figure 2.9	<i>No change in LOT-evoked EPSP slope</i>	55
Figure 2.10	<i>No change in LOT-evoked latency to peak</i>	57
Figure 2.11	<i>PP-evoked population spike amplitude I-O analysis</i>	59
Figure 2.12	<i>PP-evoked spike amplitude I-O analysis (ACSF control)</i>	60
Figure 2.13	<i>PP-evoked EPSP slope I-O analysis</i>	61
Figure 2.14	<i>PP-evoked EPSP slope I-O analysis (ACSF control)</i>	62
Figure 2.15	<i>LOT-evoked EPSP amplitude I-O analysis</i>	64
Figure 2.16	<i>LOT-evoked EPSP amplitude I-O analysis (ACSF control)</i>	65
Figure 2.17	<i>PP-evoked EPSP slope/population spike ratio</i>	67
Figure 2.18	<i>PP-evoked EPSP slope/population spike ratio (ACSF)</i>	68

Figure 2.19	<i>Example oscillations in PP-evoked population spike amplitude and LOT-evoked EPSP amplitude</i>	70
Figure 2.20	<i>Experiment 1 LC cannula ejection sites</i>	72
Figure 3.1	<i>PP-evoked population spike amplitude</i>	86
Figure 3.2	<i>No change in PP-evoked population spike amplitude</i>	88
Figure 3.3	<i>Decrease in PP-evoked population spike amplitude</i>	89
Figure 3.4	<i>No change in PP-evoked EPSP slope</i>	91
Figure 3.5	<i>PP-evoked EPSP slope paired-pulse ratio</i>	93
Figure 3.6	<i>No change in PP-evoked latency to peak</i>	95
Figure 3.7	<i>Increase in LOT-evoked EPSP amplitude</i>	97
Figure 3.8	<i>Increase in LOT-evoked EPSP slope</i>	99
Figure 3.9	<i>LOT-evoked EPSP latency to peak</i>	101
Figure 3.10	<i>PP-evoked EPSP slope I-O analysis</i>	103
Figure 3.11	<i>PP-evoked population spike I-O analysis</i>	104
Figure 3.12	<i>LOT-evoked EPSP amplitude I-O analysis</i>	105
Figure 3.13	<i>PP-evoked EPSP slope/population spike ratio</i>	106
Figure 3.14	<i>Experiment 2 LC cannula ejection sites</i>	108
Figure 4.1	<i>Diagram of stimulation and recording configuration</i>	115

**Abbreviations**

ACSF	artificial cerebrospinal fluid
ACTH	adrenocorticotrophic hormone
ANOVA	analysis of variance
CA1	cornu ammonis area 1 (region of hippocampus)
CA2	cornu ammonis area 2 (region of hippocampus)
CA3	cornu ammonis area 3 (region of hippocampus)
cAMP	cyclic AMP (adenosine monophosphate)
CNS	central nervous system
CRF	corticotropin-releasing factor
DG	dentate gyrus
EC	entorhinal cortex
EPSP	field excitatory postsynaptic potential
E-S	EPSP/population spike ratio
GABA	gamma amino-butyric acid
i.p.	intraperitoneal injection
I-O	input-output
ICV	intracerebroventricular
ISI	interstimulus interval
LC	locus coeruleus
LOT	lateral olfactory tract
LPP	lateral perforant pathway
LSD	least significant difference

LTD	long-term depression
LTP	long-term potentiation
MPP	medial perforant pathway
NE	norepinephrine/noradrenaline
NE-LTP	norepinephrine-induced long term potentiation
NMDA	<i>N</i> -methyl-D-aspartate
PGi	nucleus paragigantocellularis
PKA	protein kinase A
PP	perforant pathway

## **Chapter 1: Introduction**

### **1.1 Overview**

The existence of long-lasting and reversible modifications in synaptic strength is essential to the encoding of new information in the brain, and underlies models of the cellular basis for learning and memory. Enhancement or depression of synaptic transmission can take the form of activity dependent long-term potentiation (LTP) or long-term depression (LTD) of synaptic efficacy in neural networks. The processes underlying learning and memory are thought to be initiated through persistent changes of neuronal responses (Hebb, 1949).

The effect of locus coeruleus (LC)-produced norepinephrine (NE) upon the dentate gyrus (DG) of the hippocampus may play a role in the acquisition and storage of memory and in attentional processes (Woodward et al., 1979). Many of the connections in the hippocampus proceed unidirectionally, and the DG is the first hippocampal region to receive cortical sensory input from the entorhinal cortex (EC), making it the first step in the processing of sensory information in the hippocampus. Because the DG receives input from different sensory modalities, it possibly uses that sensory information to mark spatial locations and thus more efficiently represent spatial information, reducing redundancy and orthogonalizing output (Kesner, Lee, & Gilbert, 2004). The medial and lateral perforant paths (PP), composed of axons whose cell bodies are located in the medial and lateral EC, provide the main input to the DG (McNaughton & Barnes, 1977).

Differential effects of NE upon the responses of the medial and lateral PP may be

functionally important as different input is relayed through the medial and lateral PP. The lateral PP contains projections from the lateral EC which terminate in the outer third of the granule cell dendrites, after receiving input from central olfactory and subcortical structures (Steward, 1976; McNaughton & Barnes, 1977; Colino & Malenka, 1993). Non-olfactory cortical sensory areas project to the medial EC, which in turn projects to the middle third of granule cell dendrites (Steward, 1976), indicating a division in function between the two pathways.

The DG receives noradrenergic projections from the LC (Moore & Bloom, 1979), and an association has been shown between noradrenergic activation and LTP of the DG evoked potential (Neuman & Harley, 1983). The LC, the primary source of noradrenergic projections to the hippocampus, is stimulated by novelty in the environment, and enhances detection and fidelity of sensory events (Segal & Bloom, 1976). These qualities support a role for the LC and NE involvement in facilitation of responses to sensory input and in memory and attention (Harley, 1991).

Following the initial report of NE-induced potentiation of PP input to the DG, later studies *in vitro* and *in vivo* found evidence that potentiation effects were selective and seen only with pairing of NE and medial PP input while depression occurred when NE was paired with lateral PP input (Dahl & Sarvey, 1989; Babstock & Harley, 1993). Babstock and Harley (1993) used electrical stimulation of the nucleus paragigantocellularis (PGi) to provide excitatory input to the LC, the source, as noted, of NE innervation to the DG. Their study aimed to observe NE modulatory selectivity *in vivo* by examining medial and

lateral PP responses following PGi stimulation. Stimulation of the lateral olfactory tract (LOT) was used to selectively elicit lateral PP responses. LOT-evoked fEPSPs were found to be depressed immediately (with a prime conditioning latency of 40 ms) following stimulation of the PGi, while the medial PP evoked population spike was enhanced at the same time point. Steward (1976) had demonstrated earlier that the LOT EPSP in DG depended on the integrity of the lateral EC.

These *in vivo* findings were consistent with *in vitro* studies such as that of Dahl and Sarvey (1989), in which a long-lasting (more than 45 min) depression of lateral PP and enhancement of medial PP evoked DG potentials was seen following a 30 min perfusion of NE. There were, however, differences, besides time course, in the effects seen *in vivo* and *in vitro*. *In vivo* only the medial PP population spike was potentiated and the associated EPSP did not change, while *in vitro* both EPSP and population spike potentiated. This difference was explained as possibly a combination of lateral EPSP depression and medial EPSP enhancement in stimulation of the combined pathway *in vivo*. The explanation was consistent with the LOT depression observed *in vivo*. While the brief time-restricted pairing of LC activation and PP stimulation, such as that used by Babstock and Harley (1993), has some physiological relevance it did not yield long-term effects which are more critical for our understanding of learning and memory. In other studies, anatomically selective, burst activation of the LC with glutamate has produced immediate and enduring potentiation of the medial PP (Harley & Milway, 1986; Harley, Milway, & Lacaille, 1989; Klukowski & Harley, 1994; Walling & Harley, 2004). Thus, it is of interest to investigate the hypothesized selective effects of NE release on PP inputs

to the DG *in vivo* with glutamatergic activation of LC.

The following introduction reviews the anatomy of the hippocampus proper and the DG, the hippocampal inputs originating in the EC, and the features of noradrenergic innervation of the DG from the LC, focusing on evidence for its role in synaptic plasticity of the DG.

## **1.2 Hippocampus and dentate gyrus**

Memorial processes are considered to be initiated as persistent modifications of neuronal responses, and the hippocampus plays a well-documented role in acquisition and storage of spatial memories (Kesner, Lee, & Gilbert, 2004). Although object recognition is processed by the perirhinal cortex, the hippocampus is key in the recognition of the spatial configuration of objects, by comparing incoming stimuli to stored information and functioning as a novelty detector (Kemp & Manahan-Vaughan, 2006). The three main subregions of the hippocampus (DG, CA3, and CA1) cooperate extensively, but also demonstrate individual specificity of function (Kesner, Lee, & Gilbert, 2004).

In the rat, the hippocampal formation forms a banana-shaped structure that extends from the septal nuclei to the temporal cortex. In general, the hippocampus consists of a tri-synaptic loop, with inputs passing from DG to CA3 to CA1. The fields CA1, CA2, and CA3 make up the hippocampus proper, while the DG consists of the fascia dentata and the hilus. The DG is the first stage of the hippocampal circuit, with the PP providing its primary input from the EC to the DG, and granule cells of the DG project through the

mossy fibers to the hilus and CA3. From CA3 the Schaffer collaterals project to area CA1. Projections from the lateral EC also terminate in the distal part of CA1 and proximal part of the subiculum, while fibers from the medial EC terminate in proximal CA1 and distal subiculum. Area CA3 also receives projections from the lateral EC (Sewards & Sewards, 2003). Because many of the connections in the hippocampus are unidirectional, and the EC is a source of cortical sensory information, the DG becomes the first step in the processing of sensory information in the hippocampus (Amaral, Scharfman, & Lavenex, 2007).

The DG is composed of three layers: the molecular layer, the granule cell layer, and the polymorphic layer. In the rat, closest to the hippocampal fissure is the relatively cell-free molecular layer, which is about 250  $\mu\text{m}$  in depth and contains the granule cells' dendrites, along with fibers of the PP. Below the molecular layer is the granule cell layer, which mostly consists of closely packed granule cells, in a layer approximately 60  $\mu\text{m}$  in depth. Together these two layers form a V- or U-shaped structure that encloses the polymorphic cell layer (or hilus). Along the boundary of the granule cell layer and the polymorphic layer are the cell bodies of dentate pyramidal basket cells and within the polymorphic cell layer are mossy cells and other cell types (Amaral, Scharfman, & Lavenex, 2007).

The granule cell is the principal cell type of the DG, characterized by its cone-shaped dendritic arborization, with branches oriented toward the superficial part of the molecular layer, and distal dendritic tips ending at the hippocampal fissure or ventricular surface. The distinctive unmyelinated axons of the granule cells are known as the mossy fibers,

synapsing on mossy cells in the polymorphic layer and pyramidal cells in region CA3 of the hippocampus. DG cells are suggested to act as a competitive learning network to reduce redundancy of and orthogonalize outputs, working in conjunction with CA3 to support spatial pattern separation (distinguishing partially overlapping activation patterns to facilitate retrieval of one pattern separate from others); the low probability of any pair of CA3 neurons receiving mossy fiber input from a similar set of DG cells is theorized to accomplish the separation of patterns, with DG cells working as a competitive learning network to produce sparse, orthogonal outputs and reduce redundancy (Kesner, Lee, & Gilbert, 2004). The pyramidal cells of CA3 project mainly to fields CA1 and CA2 along the Schaffer collaterals, but some projections return to the hilus. Region CA1 sends output to layer V of the EC and the subiculum; the subiculum also outputs to layer V of the EC, as well as other structures.

The pontine nucleus LC sends a prominent noradrenergic input to the DG, and the noradrenergic fibers terminate primarily in the polymorphic layer, but also in the molecular layer. Serotonergic projections from the raphe nuclei also terminate in the polymorphic layer, on interneurons that influence the distal dendrites of granule cells (Amaral & Witter, 1995).

When recording in the granule cell layer of the DG, population spike amplitude in response to PP stimulation is an index of granule cell excitability (or loss of interneuron inhibition), while fEPSP slope demonstrates synaptic strength. Sustained increases in the amplitude of granule cell EPSPs and population spikes evoked by PP stimulation that are

modulated by NE depend upon  $\beta$ -adrenoceptor activation (Harley, 1991). The phenomena of high frequency stimulation-induced LTP and NE-induced long-lasting potentiation are seen as changes in the amplitude of granule cell EPSPs and population spikes (see Figure 1.1) evoked by PP stimulation (Bliss & Lømo, 1973; Neuman & Harley, 1983), although *in vivo* PP-evoked population spikes are potentiated by NE more reliably than EPSPs (Neuman & Harley, 1983).

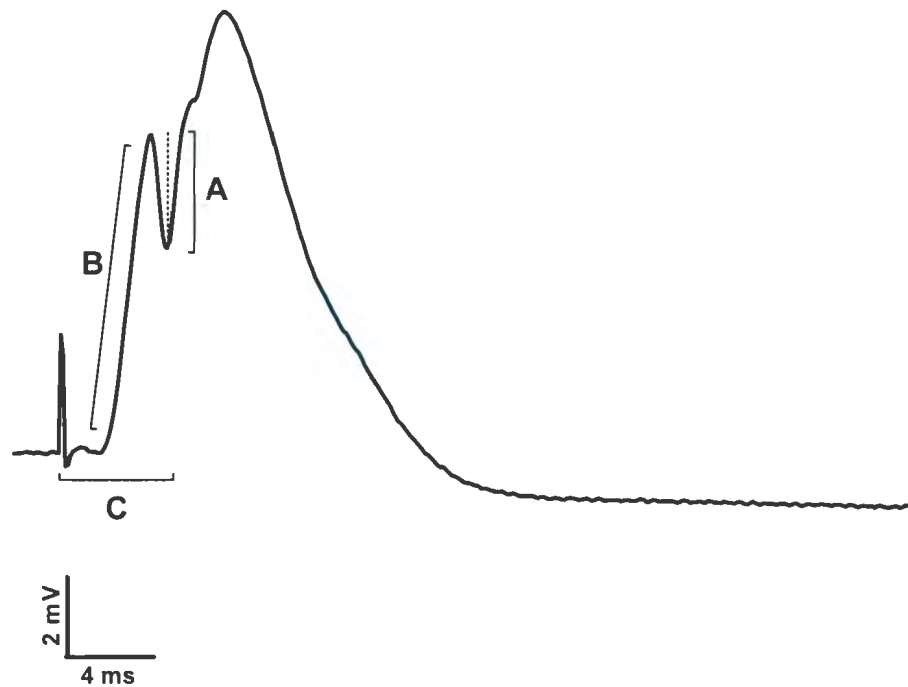


**Figure 1.1 Example PP-evoked waveform**

Example PP-evoked waveform recorded in DG from animal with glutamatergic activation of LC, recorded 1 min post-activation.

**A:** Population spike amplitude. **B:** EPSP slope. **C:** Latency to peak, measured from stimulus artifact to the deepest point of the population spike.

### **1.3 Entorhinal cortex**

The EC consists of six layers, and is subdivided into two general areas, the medial and lateral entorhinal areas. Cortical inputs to the EC form two groups, those terminating in the superficial layers, and those terminating in the deeper layers. The inputs to superficial layers I-III reach entorhinal neurons that project to the DG, hippocampus, and subiculum (Steward & Scoville, 1976). The deeper layers IV-VI receive information returning from the hippocampal fields and project back to other cortical regions. Olfactory projections input substantially to the superficial layers, while limbic and paralimbic cortices project to the deeper layers IV-VI of EC (Amaral & Witter, 1995).

The fibers forming the PP arise mainly from the stellate cells in Layer II and the pyramidal cells in layer III, as well as other projections, including GABA-ergic neurons, to various hippocampal subfields from the EC (Amaral & Witter, 1995). The projection of PP to the DG primarily originates in layer II, although a minor component arises from the deeper layers (IV-VI) (Steward & Scoville, 1976).

The EC is involved in the pre-processing and selection of information directed to the hippocampus, and evidence suggests that the medial and lateral EC have distinct functions in the pre-processing of EC output to the hippocampus (Kerr et al., 2007). Functional studies indicate that the medial EC contributes spatial information, while the neurons of the lateral EC demonstrate less spatial specificity (Fyhn et al., 2004). These functional differences are consistent with the neuroanatomy of projections to the EC (see Figure 1.2).

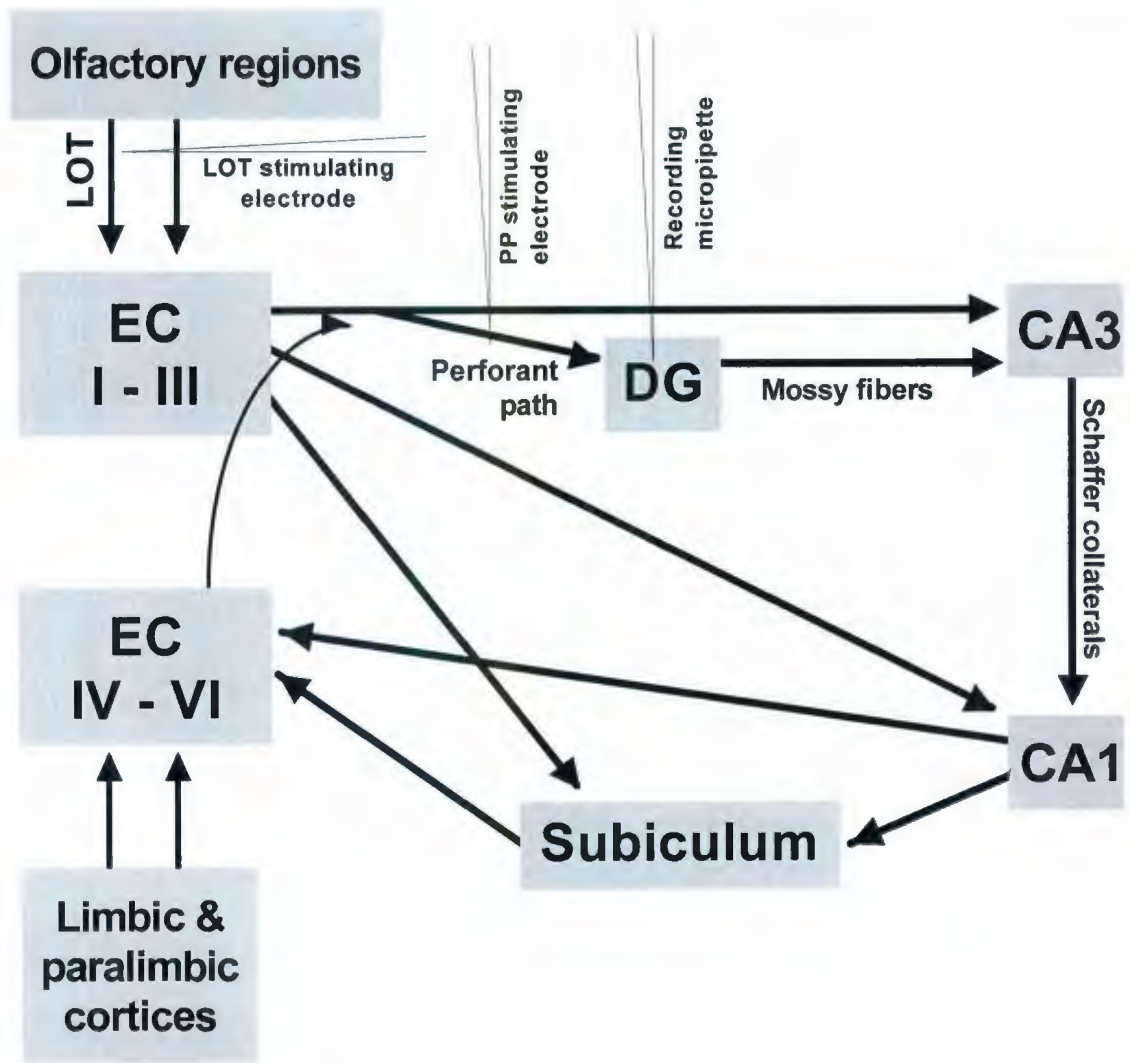


**Figure 1.2 Inputs and outputs of entorhinal cortex and hippocampal formation**

Olfactory regions output to superficial regions of EC through LOT. Limbic and paralimbic cortices output to deep layers of EC. Superficial EC outputs to DG (through PP), CA3, and subiculum. DG outputs to CA3 through mossy fibers. CA outputs to CA1 through Schaffer collaterals. CA1 outputs to subiculum and deep layers of EC. Positions of stimulating electrodes and recording micropipette indicated.

The medial EC receives its primary projections from visual association cortex, posterior parietal cortex, cingulate cortex, and dorsal thalamus, all of which are implicated in spatial learning and memory (Kerr et al., 2007). The lateral EC receives heavier cortical projections than the medial EC, which originate primarily in the piriform and insular cortices, and lesser inputs from the visual, posterior parietal, and retrosplenial cortices (Burwell & Amaral, 1998; Kerr et al., 2007). The medial EC receives a larger proportion of cingulate, parietal, and occipital input, including visual and visuospatial areas, than the lateral EC (Burwell & Amaral, 1998).

Place cells in the hippocampus and grid cells in the medial EC form parts of the brain circuit that represents self-location. Most of the medial EC displays spatially confined grid-like firing, and grid cells are topographically organized so that the scale of the grid increases with anatomical distance from the dorsal border of the medial EC. Principal cells of layer II are grid-like, and deeper layers also contain grid cells (Brun et al., 2008). The heavy influence of posterior parietal and visual association areas on the dorsocaudal medial EC may account for the distinctive spatial firing pattern of the cells here (Kerr et al., 2007).

For successful place learning, input from the medial EC, but not the lateral EC, is required. Following medial PP lesioning in a discriminative fear conditioning to context task an amygdala-like low fear effect (absence of fear response to either chamber in the task, indicating lack of association between chamber and shock) was observed, whereas lesioning of the lateral PP led to enhanced conditioning to context and discriminative

freezing (Ferbinteanu, Holsinger, & McDonald, 1999). The lateral EC receives projections from the perirhinal and postrhinal cortices, which receive uni- and polymodal associational input, representing highly-processed sensory information. The medial EC receives mainly non-sensory, non-specific information from the pre- and parasubiculum, amygdala, cingulate cortex, and retrosplenial cortex (Ferbinteanu, Holsinger, & McDonald, 1999). Because anatomical data does not support a total selectivity of projections, the segregation of sensory input of the lateral and medial EC is considered relative, not absolute (Ferbinteanu, Holsinger, & McDonald, 1999).

## **1.4 Perforant path**

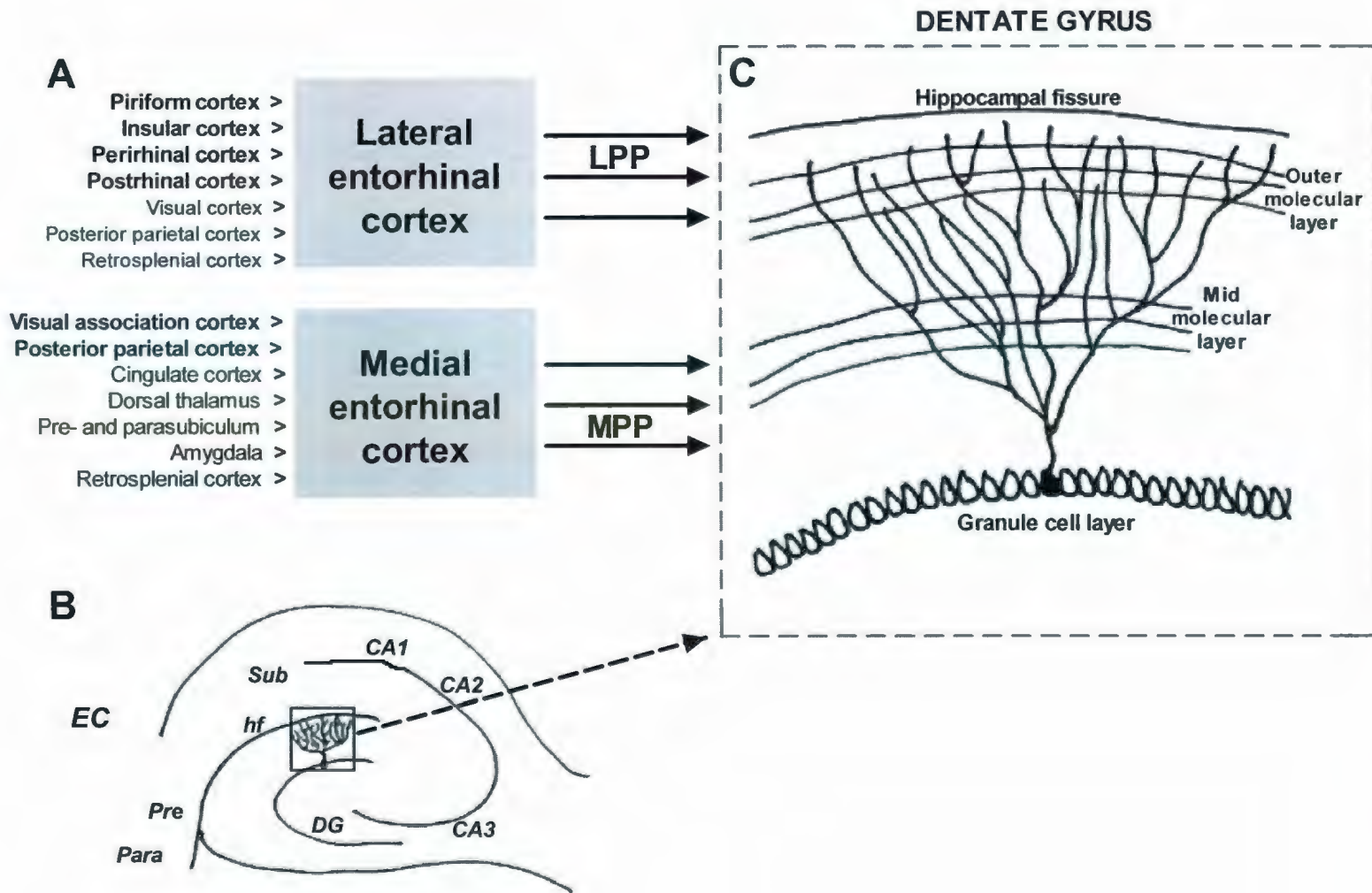
### ***1.4.1 Projections***

The PP consists of projections from the EC to the hippocampal formation. It mainly arises from entorhinal layers II and III, and proceeds in a laminar fashion, with cells in layer II projecting to the DG and area CA3, while cells in layer III project to CA1 and the subiculum (Steward & Scoville, 1976; Sowards & Sowards, 2003). In rats, the glutamatergic fibers projecting from the pyramidal and stellate cells of layer II form physiologically and pharmacologically distinct medial and lateral pathways. Cells in lateral and caudal locations of the EC project to septal levels of DG, while medially and rostrally located EC cells project more temporally (Dolorfo & Amaral, 1998).

### ***1.4.2 Distinctions between medial and lateral perforant pathways***

On the basis of degeneration studies, Hjorth-Simonsen and Jeune (1972) and Hjorth-Simonsen (1972) suggested that the rat PP is composed of two distinct fiber systems

(McNaughton & Barnes, 1977). Again as noted earlier, the terminals of the medial and lateral PP are topologically separated in the molecular layer (McNaughton, 1980; Hjorth-Simonsen, 1973). Fibers of the medial PP form synapses onto the middle one-third of the molecular layer of the DG, while fibers of the lateral PP synapse onto the outer one-third (Steward, 1976; McNaughton & Barnes, 1977; Colino & Malenka, 1993). The lateral EC receives projections primarily from piriform and insular cortex, while non-olfactory sensory areas project to the medial EC (Burwell & Amaral, 1998; Kerr et al., 2007) (see Figure 1.3).



McNaughton (1980) observed that at the midpoint of the medial to lateral range of input *in vitro*, a distinct transition in response properties happened, and this transition exactly corresponds to the border of the medial and lateral termination zones in the outer two-thirds of the molecular layer, indicating that the PP consists of two physiologically distinct subdivisions.

McNaughton and Barnes (1977) found that stimulating the dorsomedial or ventrolateral aspects of the PP resulted in quantitatively different extracellular EPSPs in the DG of the rat. When recording with an extracellular electrode in the hilus of the DG, the evoked population EPSP varies in waveform depending on the location of the stimulus along the medio-lateral axis of the PP (Abraham & McNaughton, 1984).

Responses elicited from lateral stimulation sites, involving synaptic activation in the outer third of the molecular layer, demonstrate greater latency to peak and width at half-amplitude (the width of the EPSP at one half its height above baseline; McNaughton & Barnes, 1977) than responses from medial stimulation, which involves synaptic activation of the middle third of the molecular layer (McNaughton, 1980). Responses to medial fiber stimulation reached maximum negativity about 100 to 180  $\mu\text{m}$  deeper in the molecular layer than responses to lateral stimulation. When stimulating intermediate locations, double spikes were frequently elicited from the granule cell population (McNaughton & Barnes, 1977).

Pharmacological differences between the medial and lateral aspects of the PP have also

been observed. Bramham, Errington, and Bliss (1988) used electrically-induced LTP to demonstrate a difference in lateral and medial PP responses. Naloxone, an opioid receptor antagonist, blocked the induction, but not the maintenance, of LTP in the lateral PP, while production of LTP in the medial PP was unaffected. *In vitro*, LTP in both pathways is *N*-methyl-D-aspartate (NMDA) receptor-dependent, but *in vivo*, only LTP of the medial PP is completely NMDA receptor-dependent (Bramham, Milgram, and Srebro, 1991). However, application of propranolol (a  $\beta$ -noradrenergic antagonist) blocks the induction of LTP in both the medial and lateral PP inputs to the DG (Bramham, Bacher-Svendsen, & Sarvey, 1997). Rush, Rowan, & Anwyl (2001) also demonstrated that plasticity evoked by *in vivo* application of NMDA is pathway specific, inducing LTP of the medial PP and LTD of the lateral PP.

#### ***1.4.3 Stimulation of the LOT elicits lateral PP responses***

The LOT arises from the olfactory bulbs and projects to the piriform cortex and the rostral portion of the EC; LOT fibers and associative fibers originating in the piriform cortex primarily terminate in the superficial layers of the lateral EC. Because the lateral and medial EC are not interconnected, olfactory afferents cannot be transmitted to the medial EC via the lateral EC (Biella & de Curtis, 2000). No associative response is seen in the medial EC following LOT stimulation, demonstrating that the projections arising from the piriform cortex do not project to the medial EC, and that there is a complete separation between the medial and lateral EC regarding olfactory input (Biella & de Curtis, 2000).

Electrical stimulation of the lateral EC or of the olfactory tract evokes EPSPs limited to

the terminal area of the lateral PP (the apical one-third of the molecular layer), while auditory-evoked potentials are recorded only in the terminal area of the medial PP (the middle one-third of the molecular layer) (Dahl & Sarvey, 1989). Thus stimulation of the LOT can be used to selectively elicit lateral PP responses; electrical stimulation of the olfactory tract or lateral EC evokes EPSPs in the apical one-third of the molecular layer, where the lateral PP terminates (Steward & Scoville, 1976; Dahl & Sarvey, 1989).

Stimulation of LOT fibers results in long latency (14-20 ms) evoked responses in the ipsilateral DG (see Figure 1.4). Lesions of the lateral EC eliminate this DG response, indicating that LOT stimulation activates DG through a multisynaptic pathway relaying in the lateral EC (Wilson & Steward, 1978). LOT stimulation induces short-latency responses in the lateral EC, but not the medial EC. However, the medial EC can be polysynaptically activated after hippocampal activation; with strong or repetitive LOT stimulation, an efferent signal re-enters the deep medial EC from the hippocampal loop (Biella & de Curtis, 2000).

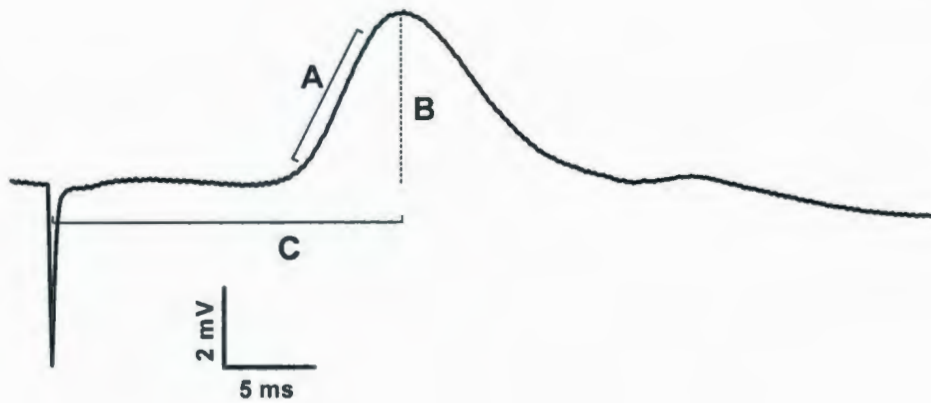


**Figure 1.4 Example LOT-evoked waveform**

Stimulation of LOT fibers results in long latency (14-20 ms) evoked potentials in DG. Example LOT-evoked waveform from animal with glutamatergic activation of LC, recorded 1 min post LC activation.

**A:** EPSP slope. **B:** EPSP amplitude. **C:** Latency to peak.

## **1.5 Locus coeruleus**

### ***1.5.1 Anatomy***

The LC nucleus is the source of the forebrain's major noradrenergic system. In the mammalian brain NE originates from several nuclei, including the LC, and the lateral tegmental NE system, whose nuclei of origin include the dorsal motor nucleus of the vagus, nucleus tractus solitarius and adjacent tegmentum, and lateral tegmentum (Moore & Bloom, 1979). NE was traditionally assumed to affect the signal-to-noise ratio, enhancing the signal it is paired with, while depressing the noise (Segal & Bloom, 1976). The activity of neurons of the LC varies in response to sensory stimuli, increasing especially to novelty, and with the sleep-wake cycle, being more active during waking. The properties of LC-NE neurons have led to hypotheses of roles in sleep, attention, memory, and vigilance (Aston-Jones et al., 1995).

The name "locus coeruleus", meaning "blue spot", is taken from the nucleus's appearance in unstained primate tissue. However, unlike the LC of humans and monkeys, the neurons of the rat LC are unpigmented. In Nissl-stained sections the rat LC is identified as a cluster of darkly-stained cells in the rostral rhombencephalic tegmentum (Aston-Jones et al., 1995). The LC extends for 1.2 mm along the ventrolateral border of the fourth ventricle, and meets the trigeminal nerve at the medial side of its mesencephalic nucleus. The number of neurons in the rat LC is estimated to range between 1400 and 1800 unilaterally, depending on the staining method used (Aston-Jones et al., 1995).

Several cell types are located within the LC, which differ not only in size and shape but

also in dendritic orientation. Medium-sized fusiform cells, larger multipolar neurons, and a third class of ovoid-shaped cells have been distinguished in the rat LC. The arborization of small fusiform cells is primarily in the sagittal and horizontal planes, while multipolar LC neurons have dendritic arborizations mainly in the frontal plane. Despite their morphological differences, most neurons in the rat LC contain NE (Aston-Jones et al., 1995).

### ***1.5.2 Afferent projections to LC***

Neuropharmacological studies have indicated that LC neurons are strongly influenced by a range of neurotransmitters, including inhibition by  $\alpha_2$ -adrenergic agonists, GABA, and  $\mu$ -opiate agonists, and excitation from glutamate, substance P, ACTH, vasopressin, and CRF, while neurotensin and serotonin have more complex effects. Because these studies indicate that the LC receives a variety of inputs, and the LC projects extensively throughout the brain, it is likely that multiple levels of the CNS provide regulation of the LC (Aston-Jones et al., 1995).

Two rostral medullary areas provide the major afferents to the LC nucleus, the lateral paragigantocellularis (PGi) and the prepositus hypoglossi, with the PGi being the most prominent afferent. Other minor afferents come from the paraventricular hypothalamic nucleus, the intermediate zone of the spinal grey, and the central nucleus of the amygdala (Aston-Jones et al., 1995).

### ***1.5.3 Efferent projections from LC***

Neurons of the LC send ascending efferent projections to olfactory structures, hippocampus, neocortex, thalamus, basal forebrain, preoptic area, hypothalamus, and the midbrain. Descending projections from the LC reach the cerebellum, pons and medulla, and spinal cord. At least 40% of LC neurons send their projections to the olfactory bulb, of which the LC provides the sole adrenergic input, and the primary olfactory cortex is also heavily innervated by LC projections. The rat LC projects substantially to all areas and layers of the neocortex, and the projections are almost exclusively ipsilateral (Aston-Jones et al., 1995).

The entire NE input to the hippocampal formation comes from the LC, and the projections primarily originate in the dorsal third of the LC. The DG receives a substantial projection from the LC (Swanson and Hartman, 1975; Jones and Moore, 1977). The noradrenergic LC projection to the hippocampal formation is 75-90% ipsilateral (Loy et al., 1980). LC axons follow three routes to the hippocampal formation: the ventral amygdaloid pathway (which innervates the entire hippocampal gyrus and midseptotemporal and ventral regions of the DG), and more bilateral projections from the fornix (innervating the septal pole of the DG) and cingulum bundle, which innervates the ventral DG (Loy et al., 1980; Aston-Jones et al., 1995).

### **1.6 Norepinephrine and adrenergic receptor localization**

Adrenergic receptors are divided into two classes,  $\alpha$  and  $\beta$  receptors. The  $\alpha$ -adrenergic receptors are divided into two subtypes,  $\alpha_1$  and  $\alpha_2$ . Autoradiographic studies found  $\alpha$ -

adrenergic receptors throughout the brain, with higher levels in olfactory regions, parts of the cerebral cortex and DG, the LC and nucleus tractus solitarii, medial parts of the hypothalamus and thalamus and portions of the spinal cord, with the distribution of  $\alpha 1$  and  $\alpha 2$  receptors differing in certain areas. For example, higher densities of  $\alpha 2$  receptors were observed in the LC, while  $\alpha 1$ -receptor densities there were low (Young & Kuhar, 1980). In the hippocampal formation  $\alpha$ -adrenergic binding sites are relatively concentrated in the DG, correlating with the distribution of NE innervation, while  $\beta$ -adrenergic receptors are more evenly distributed throughout the hippocampal gyrus (Crutcher & Davis, 1980).

In the DG of the rat, NE acts primarily on  $\beta$ -adrenergic receptors, which are located postsynaptically on the dendrites and spines of granule cells and on some astrocytes, as well as select interneurons and presynaptic processes (Milner, Shah, & Pierce, 2000). Activation of these receptors is necessary for the induction of LTP at medial and lateral PP synapses, and physiological studies find that NE release sites are near  $\beta$ -adrenergic receptors (Milner, Shah, & Pierce, 2000).

### **1.7 Noradrenergic modulation of hippocampal activity**

In 1970 Seymour Kety proposed that NE and the aroused state induced by novel stimuli facilitate the processing of novel or significant stimuli while suppressing non-significant stimuli, and that this state initiates persistent facilitation of active synapses. Foote, Freedman, and Oliver (1975) tested the effect of NE on auditory cortex neurons of squirrel monkeys, finding that a dose of NE reduced spontaneous activity (non-significant

stimuli) more than activity evoked by species-specific vocalizations (significant stimuli).

Segal and Bloom (1976) proposed that LC-NE acted to screen stimuli by enhancing responses to significant stimuli and reducing excitatory responses to non-significant stimuli, in effect increasing the signal-to-noise ratio in hippocampus. They found that electrical stimulation near the LC had reinforcing properties and inhibited spontaneous activity of hippocampal cells. The authors also demonstrated an inhibitory response of some hippocampal pyramidal cells to loud auditory stimuli, suggesting that those responses were mediated by NE, and possibly by LC activation. They suggested that arousing stimuli could cause the inhibitory response, and that this arousal is accompanied by the generation of hippocampal theta rhythm, which is observed with LC stimulation. Because the inhibitory hippocampal response became excitatory when the stimulus was significant (associated with a positive reinforcer), they proposed that LC-NE increased the signal-to-noise ratio in hippocampus (1976).

As summarized, the noradrenergic innervation of the hippocampus arises primarily from cells of the LC. By injecting 6-hydroxydopamine into the LC, Bliss, Goddard, and Riives (1983) found that NE levels were depleted, and the magnitude of LTP of the fEPSP in the DG was reduced, although LTP of granule cell excitability (measured by population spike amplitude) was unaffected by NE depletion. Munro et al. (2001), using  $\beta$ -adrenergic receptor antagonists, also blocked LTP of the fEPSP while the population spike LTP remained unchanged. Because  $\beta$ -adrenergic receptors are linked to adenylate cyclase, NE likely acts through a mechanism similar to dopamine, leading to activation of PKA via an

increase in cAMP levels (Bliss, Collingridge, & Morris, 2007).

Electrical stimulation of the LC enhances PP-evoked cell firing in the DG (Assaf, Mason, & Miller, 1979; Dahl & Winson, 1985), and activation of LC by glutamate (Harley & Milway, 1986), NE superfusion of hippocampal slices (Lacaille & Harley, 1985; Stanton & Sarvey, 1985), and iontophoresis of NE to the cell body layer (Neuman & Harley, 1983) all lead to increases in DG population spike amplitude, a measure of granule cell excitability.

Studies in the hippocampal slice have shown the NE enhancement of CA1, CA3, and DG evoked potentials to be dependent upon  $\beta$ -receptor activation, since effects are blocked by beta antagonists (Mueller, Hoffer, & Dunwiddie, 1981; Mueller, Kirk, Hoffer, & Dunwiddie, 1982; Lacaille & Harley, 1985; Stanton & Sarvey, 1985). As well, beta-receptor antagonists block the effects of endogenous NE releasers and LC activation (Segal & Bloom, 1974; Harley & Milway, 1986) *in vivo*, indicating that the electrophysiological enhancement effects are again attributable primarily to beta receptor activation (Harley, 1987).

However, Harley, Milway, and Lacaille (1989) used electrical stimulation of the LC 40 ms prior to PP stimulation to cause a short-lasting potentiation of the DG population spike amplitude. With 50 LC-PP pairings using the same 333 Hz, 15 ms pulse to the LC, a long-lasting potentiation (over 30 min following LC stimulation) was observed in about half of experiments. While propranolol (a  $\beta$ -adrenergic antagonist) suppressed the potentiating

effect of glutamatergic stimulation of LC, it failed to block the potentiating effect of LC electrical stimulation. This suggests that there is both a  $\beta$ -NE-dependent and  $\beta$ -NE-independent system in or near the LC capable of acting on and inducing long-lasting potentiation of the PP-evoked DG potential.

Dahl and Sarvey (1989) first demonstrated *in vitro* pathway-selective modifications of synaptic responses in the DG, with a low concentration of NE inducing potentiation of medial PP-evoked EPSPs and population spikes, and depression of those evoked by the lateral PP, with both responses blocked by the  $\beta$ -adrenergic antagonist propranolol. This was the first indication that NE can have differential effects on the medial and lateral pathways projecting to the DG. Pelletier et al. (1994) later demonstrated that *in vitro* application of isoproterenol, a  $\beta$ -noradrenergic receptor agonist, induces long-lasting potentiation of the medial PP and long-lasting depression of the lateral PP, confirming the selectivity of medial and lateral PP responses.

Lacaille and Harley (1985) and Dahl and Sarvey (1990) conducted *in vitro* investigations of a pairing requirement for PP-evoked NE potentiation, and failed to see a requirement for stimulation of PP input to be paired with NE. Long-lasting effects occurred after NE application and washout although no PP stimulation was applied during NE. Reid and Harley (2009) tested the pairing requirement for LC activation and PP stimulation *in vivo* and found that PP stimulation paired with LC activation only induced long-lasting potentiation of both EPSP slope and population spike when they co-occurred. When PP stimulation was interrupted for 10 minutes pre- and post-LC activation, potentiation of

the DG-evoked potential did not occur. The authors concluded that since delaying PP stimulation for 10 min prevented NE-LTP of PP input, pairing of NE and PP activation must occur within at least a 10 min window. They suggested the negative results *in vitro* were due to prolonged activation of the cAMP system by bath applications of NE.

### **1.8 Glutamatergic modulation of LC activity**

Palamarchouk et al. (2000) (with *in vivo* voltammetry) demonstrated that glutamate infusion (100 nl of 0.1 M glutamate infused over 60 s) into the LC increased the NE-like oxidation current in the rat hippocampus with a delay of approximately 30 s and peaking within 90 s of glutamate application. This response to glutamate was augmented by pre-treatment with an NE reuptake inhibitor (desmethyylimipramine), suggesting that the changes in current were due to changes in NE.

Harley and Sara (1992) investigated cellular changes in the LC produced by glutamate activation. DG population spike amplitude increased with LC glutamate ejections, and movement of the LC recording electrode in the region of the LC was, in some cases, sufficient to initiate potentiation of population spike amplitude. It took an average of 34 s following glutamate ejection for spikes to exceed the maximum control spike, with nearly all increases occurring within the first minute. EPSP slope increases occurred with 22/34 ejections, while population spike latency was unaffected by glutamate ejection. The PP was stimulated 1/10 sec.

Increases in population spike amplitude were produced by glutamate ejections

accompanied by an audible increase in cell activity (with LC unit activity played through an audio monitor), but some increases in cell activity did not produce changes in spike amplitude (when volumes of < 50 nl glutamate were used), indicating that the number of LC cells activated was a factor in the initiation of hippocampal potentiation (Harley & Sara, 1992). This is consistent with a later study (Harley, Lalies, & Nutt, 1996) showing that the concentration of NE in the DG was a determining factor in whether or not long-term spike potentiation occurred. Intravenous injections of clonidine (an  $\alpha_2$ -agonist) silenced or depressed LC cell firing for 3 to 5 minutes; clonidine injections produced either no change or a mild depression of EPSP slope and population spike amplitude. That LC inactivation was uncorrelated with DG potentiation indicates that the LC burst is critical in initiating spike potentiation (Harley & Sara, 1992). While glutamate ejections in the LC potentiated the PP potential in DG, potentiation was never produced by ejections outside the LC (Harley & Sara, 1992).

### **1.9 Neural memory models: LTP and NE-LTP**

Hippocampal LTP has been the most widely studied model of neuronal plasticity. LTP, a lasting increase in cellular responses to specific inputs and an example of activity-dependent plasticity, was first demonstrated *in vivo* (Bliss & Lømo, 1973; Bliss & Gardner-Medwin, 1973) and provides an attractive model of learning and memory as it can be induced by brief, relatively physiological stimuli, while lasting long enough to account for some types of memory (Sarvey, Burgard, & Decker, 1989). LTP is typically induced through application of high-frequency trains of electrical stimulation. Neurotransmitters and neuromodulators, including NE, can affect the threshold for

induction, magnitude, or duration of hippocampal LTP (Chaulk & Harley, 1998).

Along with LTP, which is produced by high-frequency stimulation and manifests as a long-lasting increase in population spike amplitude and EPSP slope in the DG evoked potential, exposure to  $\beta$ -adrenergic agonists produces, as we have seen, a similar long-lasting effect in the DG, termed NE-induced long-term potentiation (NE-LTP) (Neuman & Harley, 1983; Lacaille & Harley, 1985; Stanton & Sarvey, 1985b; Stanton & Sarvey, 1987). NE-LTP is heterosynaptic, involving both glutamatergic and noradrenergic signals. Like LTP, NE-LTP is NMDA-dependent (Burgard, Decker, & Sarvey, 1989; Sarvey, Burgard, & Decker, 1989) and LTP in DG can be blocked by  $\beta$ -adrenergic antagonists and chronic depletion of NE (Stanton & Sarvey, 1985b; Stanton & Sarvey, 1987).

Bramham, Bacher-Svendsen, and Sarvey (1997) first demonstrated that NE is required for activity-dependent high frequency stimulation-induced LTP as well as for NE-LTP, finding that propranolol (a  $\beta$ -noradrenergic antagonist) blocks the induction of LTP in both the medial and lateral PP inputs to the DG. This indicated that NE has a dual function in regulating both activity-dependent depression and activity-independent LTP in the lateral PP.

Walling and Harley (2004) assessed the effect of glutamatergic activation of the LC upon EPSP slope and population spike amplitude of PP-evoked DG potentials for 3 hours post-activation and at 24 hours post-activation. During the 3 hour period immediately following LC activation, a long-lasting increase in population spike amplitude was

observed, while EPSP slope did not vary. This increase in population spike amplitude was prevented by application of propranolol (a  $\beta$ -receptor antagonist). At 24 hours, EPSP slope had increased in glutamate-activated animals, demonstrating a long-term change in plasticity (Walling & Harley, 2004).

A second experiment comparing parameters at 24 hr post-LC activation to baseline mean demonstrated this long-term NE-induced change in plasticity to be dependent on protein synthesis. While animals with glutamate-activated LC alone demonstrated the significant increase in both EPSP slope and population spike amplitude, animals which had first received intraventricular anisomycin (a protein synthesis inhibitor) prior to LC activation demonstrated no change in EPSP slope or population spike amplitude. ICV application of anisomycin without LC activation had no effect on either parameter, indicating that baseline synaptic efficacy is not affected by inhibition of protein synthesis in the absence of LC activation (Walling & Harley, 2004).

Walling and Harley (2004) first demonstrated an LC activation-dependent persistent facilitation of synaptic strength *in vivo*, implicating the LC's role in a mechanism for memory. However, EPSP slope, the index of synaptic strength, remained unchanged in the 3 hours immediately post-LC activation, but increased at 24 hours, suggesting that LC activation supports a long-term, not short-term, synaptic memory mechanism.

### **1.10 Objectives**

NE modulatory selectivity has been reported with both memory-like (*in vitro*) and

attention-like (*in vivo*) durations, with NE application eliciting LTP of the medial PP-evoked potential and LTD of the lateral PP-evoked potential in the DG *in vitro*, and NE release via LC activation eliciting corresponding short-term medial PP potentiation and LOT depression *in vivo*.

Whether NE enhances one hippocampal input over another (spatial v. olfactory) to produce long-term changes in DG responses *in vivo* has yet to be determined. The following experiments, using methods previously associated with long-lasting medial/mixed PP-evoked DG effects (e.g. Walling and Harley, 2004) and short-term NE modulatory selectivity effects (Babstock and Harley, 1993), investigates the effects of NE on the modification of DG inputs by exploring long-term alterations in the LOT- and PP-evoked DG potentials following LC-NE release.

The present study uses glutamate burst activation of LC *in vivo* combined with both PP stimulation and LOT activation to ask whether LTP and LTD are seen when a robust LC stimulation mode is employed *in vivo* as has been reported with bath application of NE *in vitro*. By examining the effects of NE release following glutamatergic activation of LC upon the medial and lateral PP inputs in the anaesthetized rat, this study aims to reproduce the original immediate and transient *in vivo* effects and to elicit longer-term DG responses in the 3 hours following LC activation.

Two separate experiments investigate these modulatory effects of NE on inputs to the DG, a region previously implicated in memory and the orthogonalization of sensory inputs

(Kesner, Lee, & Gilbert, 2004). The first explores modulation of the LOT- and PP-evoked potentials in the DG over several hours following endogenous release of NE evoked by application of glutamate in the LC. Failure to see the expected depression of the LOT-evoked potential in the first experiment led to a second experiment to observe effects of more frequent pairings of NE and LOT inputs by increasing the rate of PP and LOT stimulation, a critical factor in long-term effects as described by Reid and Harley (2009).

## Chapter 2: Experiment 1

### 2.1 Introduction

LC-NE is hypothesized to play a role in hippocampal memory and attentional processes by improving the signal-to-noise ratio through enhancement of the signal, suppression of noise, or both (Woodward et al., 1979). The medial and lateral PP provide the main input to the DG, the first hippocampal region to receive sensory input from the EC. Differential effects of LC-NE upon the medial and lateral PP, which relay primarily spatial and olfactory information, respectively, may be functionally important by selectively enhancing one input over the other.

*In vitro* studies demonstrated long-term (> 30 min) potentiation of DG evoked potentials with pairing of medial PP stimulation and NE application, and long-term depression with pairing of NE and lateral PP stimulation (Dahl & Sarvey, 1989), effects also seen with the application of isoproterenol, a  $\beta$ -noradrenergic agonist (Pelletier et al., 1994). These long-term effects support a learning or memory-type change in processing.

Using electrical stimulation of PGI to provide excitatory input to the LC, an *in vivo* study demonstrated an effect similar to that seen *in vitro*. Pairing of LOT stimulation (used to selectively elicit lateral PP responses) and PGI-LC-NE depressed DG evoked potentials, while medial PP stimulation paired with PGI (LC) activation enhanced medial PP evoked population spikes. Both effects were found immediately following a conditioning pulse with a 30-40 ms latency, and were no longer present after 70 ms unless again paired with a prior LC burst (Babstock & Harley, 1993). This short-term modulation supports an

attentional effect of NE as selectively enhancing spatial information and depressing olfactory information, consistent with the longer-term memory-like medial PP potentiation and lateral PP depression shown *in vitro*.

While effects with memory-like (*in vitro*) or attentional-like (*in vivo*) durations have thus far been demonstrated, whether NE selectively enhances one hippocampal input over another (spatial v. olfactory) to produce long-term changes in DG responses *in vivo* has yet to be determined. The following experiment investigates the effects of NE on the modification of inputs to the DG by exploring alterations in LOT- and PP-evoked DG potentials over several hours following endogenous NE release evoked by glutamatergic activation of LC.

Here LOT stimulation is used to selectively elicit lateral PP responses (Steward & Scoville, 1976), and is alternated with PP stimulation, which elicits a medial PP population spike as defined by latency (McNaughton & Barnes, 1977), at 60 s intervals. Along with the experimental group of animals receiving glutamatergic activation of LC, the responses of a control group receiving ACSF ejection to LC were also followed. In this group DG responses were recorded for an initial period of 4 hours (comparable to the total 1 hr pre- and 3 hr post-LC activation recording period of the experimental group) before ACSF ejection through the LC cannula, and responses were recorded for an additional 3 hr post-ACSF (comparable to the 3 hr post-LC activation recording period of the experimental group). The initial 4 hr recording period allowed for comparison of rising baseline and anesthetic drift effects with the experimental group, while the

additional 3 hr recording post-ACSF provided a comparison for mechanical stimulation of the LC region.

## **2.2 Methods**

### ***2.2.1 Subjects and surgical preparation***

Thirteen male Sprague Dawley rats (Memorial University of Newfoundland Vivarium) weighing 250-350 g were used. Experimental procedures were conducted within the light phase of the animals' cycle, and in accordance with the Canadian Council of Animal Care guidelines following a protocol approved by the Institutional Animal Care Committee.

Rats were anaesthetized with 15% urethane (10 ml/kg, i.p.), had their heads shaven, and were placed in a stereotaxic instrument in the skull-flat position. Local anaesthetic (0.25 ml marcaine) was used on the scalp before making a midline incision, the scalp was retracted to expose the skull, and the plane between bregma and lambda leveled to horizontal. Holes were drilled for a glass recording micropipette (3.5 mm posterior to bregma and 2.0 mm lateral, ~ 2.5 mm ventral from brain surface), PP bipolar stimulating electrode (7.2 mm posterior, and 4.1 mm lateral, ~ 3.0 mm ventral), LOT bipolar stimulating electrode (5.0 mm anterior, and 1.5-1.6 mm lateral, ~ 5.8-6.0 mm ventral from brain surface), and LC cannula (12.5 mm posterior to bregma, 1.0 mm lateral, ~ 4.5mm ventral). The LC cannula made of 22-gauge stainless steel (Plastics One) was angled 20° from the vertical to bypass the sagittal sinus and anchored to a jeweler's screw in the skull with dental acrylic. A second jeweler's screw on the anterior portion of the skull served as reference electrode.

The recording pipette and PP stimulating electrode were lowered until the DG field EPSP and population spike were maximized, before positioning the LOT stimulating electrode.

The LOT stimulating electrode was first positioned 4.5 mm ventral to the brain surface, before lowering in 50  $\mu\text{m}$  increments to a depth that produced the maximal stable EPSP (5.8 to 6.0 mm ventral from surface). Once electrodes were placed, LOT and PP were stimulated at 1 min intervals until evoked potentials appeared stable (approximately 30 to 60 min) before beginning data recording.

### ***2.2.2 Recording and stimulation***

During baseline and test period recording, PP stimulation consisted of a single, 0.2 ms square wave pulse (ISI 60 s) at the intensity that elicited a population spike approximately 50% of maximum (400-800  $\mu\text{A}$ ) during the I-O curve. Stimulation of LOT consisted of a 800-1000  $\mu\text{A}$  pulse (intensity chosen to produce maximal stable EPSP) with duration of 0.2 to 0.5 ms (duration chosen to maximize consistency between waveforms) and 60 s ISI. PP and LOT pulses were alternated with a 30 s ISI. The input-output current intensity relationship (I-O curve) was determined at the beginning of each recording session. I-O stimulation consisted of increasing current intensities (100-1000  $\mu\text{A}$ , 10 s ISI, 100  $\mu\text{A}$  increments). For PP stimulation, I-O data was collected using paired-pulse stimuli at intervals of 30, 70, and 200 ms, collecting two samples at each interval at each current level; paired-pulse ratio data was used to assess the medial-lateral fiber composition of the PP. In the present study, only data from the 30 ms ISI were analyzed to assess PP fiber composition. For LOT stimulation, three samples were collected at each current level; paired pulse stimuli were not used. Evoked potentials were amplified and stored by Datawave software for later analysis.

The final experimental group consisted of eight animals. After recording I-O curves, responses to PP and LOT stimulation were recorded until 1 hr of stable baseline was obtained. 200 nl 0.5M glutamate was injected through the LC cannula (see below). After injection, an additional 3 hr of recording was followed by I-O curves.

The control group consisted of five animals. Following initial I-O curves, 4 hours of baseline responses were obtained before 200 nl of ACSF were injected through the LC cannula. Responses were recorded for an additional three hours following injection, followed by I-O curves.

### ***2.2.3 Drugs and injection procedure***

Monosodium-L-glutamate mixed in sterile saline (500 mM) was injected into the LC through a 28 gauge internal cannula attached to a 1  $\mu$ l syringe by autoanalyzer tubing. The internal cannula was positioned in the LC 2 min prior to injection. Glutamate (200 nl) was injected over 30 s, and the internal cannula was left in place for 5 min before removal. The 30 s timing pairs one LOT stimulus and one PP stimulus with drug ejection in LC. The same procedure was used for injecting 200 nl ACSF (147mM NaCl, 3mM KCl, 1mM MgCl<sub>2</sub>, 1.3mM CaCl<sub>2</sub>) in the control group.

### ***2.2.4 Histology***

Following post-injection I-O curves, 200 nl of methylene blue (2%) were injected into the LC through the guide cannula to mark the injection site. A 0.5 mA, 2 s lesion was made to mark the placement of the LOT stimulating electrode. Following lesioning, rats were

decapitated and brains frozen in chilled methylbutane and stored at  $-70^{\circ}\text{C}$ . A cryostat-microtome was used to take  $30\ \mu\text{m}$  sagittal sections through the region of LC. Alternate sections were stained with 1% cresyl violet and the others left unstained. To locate electrode tracks in LOT, DG, and PP,  $30\ \mu\text{m}$  coronal sections were taken and glycogen phosphorylase staining used.

### ***2.2.5 Data analysis***

Three parameters of PP evoked potentials (EPSP slope, population spike amplitude, and latency to pop spike peak) and three parameters of LOT evoked potentials (maximum amplitude, EPSP slope, and time to maximum) were measured. All parameters were reduced to 5-minute means for analysis. Parameters in glutamate-injected animals were normalized to the 1 hr pre-glut baseline mean. Parameters in ACSF animals were normalized to both 1-hr and 4-hr pre-ACSF baseline means. I-O curves for individual animals were normalized to the largest mean EPSP slope or population spike of the pre-LC activation I-O curve of each individual. Two-way repeated measures ANOVAs were used to assess possible interactions of group and time for each parameter, and post-hoc LSD analyses were used to further investigate any interactions.

## **2.3 Results**

### ***2.3.1 PP-evoked population spike amplitude***

LC activation initiated a long-term increase in the amplitude of the PP-evoked population spike in all animals. The average baseline amplitude of 2.4 mV (in the 1 hr pre-LC activation) increased to 4.0 mV (mean of the 3 hr post-activation period) with LC-PP stimulation (a 65% enhancement, ranging from 31% to 109%). ACSF control animals, starting from a baseline mean spike amplitude of 4.79 mV in the first 1 hr of recording, showed a non-significant 13% increase (ranging from -8% to 30%) from 6.6 to 7.5 mV from 1 hr pre-injection to 3 hr post-injection.

To analyze possible changes in the period immediately around drug ejection, a two factor (group, time) mixed-effects ANOVA comparing all 1 min samples in the 30 min following LC activation to a 15 min pre-activation baseline revealed a significant group X time interaction ( $F(44,396) = 1.88, p < .001$ ). A post-hoc LSD analysis showed the population spike amplitude of glutamate-injected animals to differ significantly from baseline beginning immediately after LC activation (see Figure 2.1).

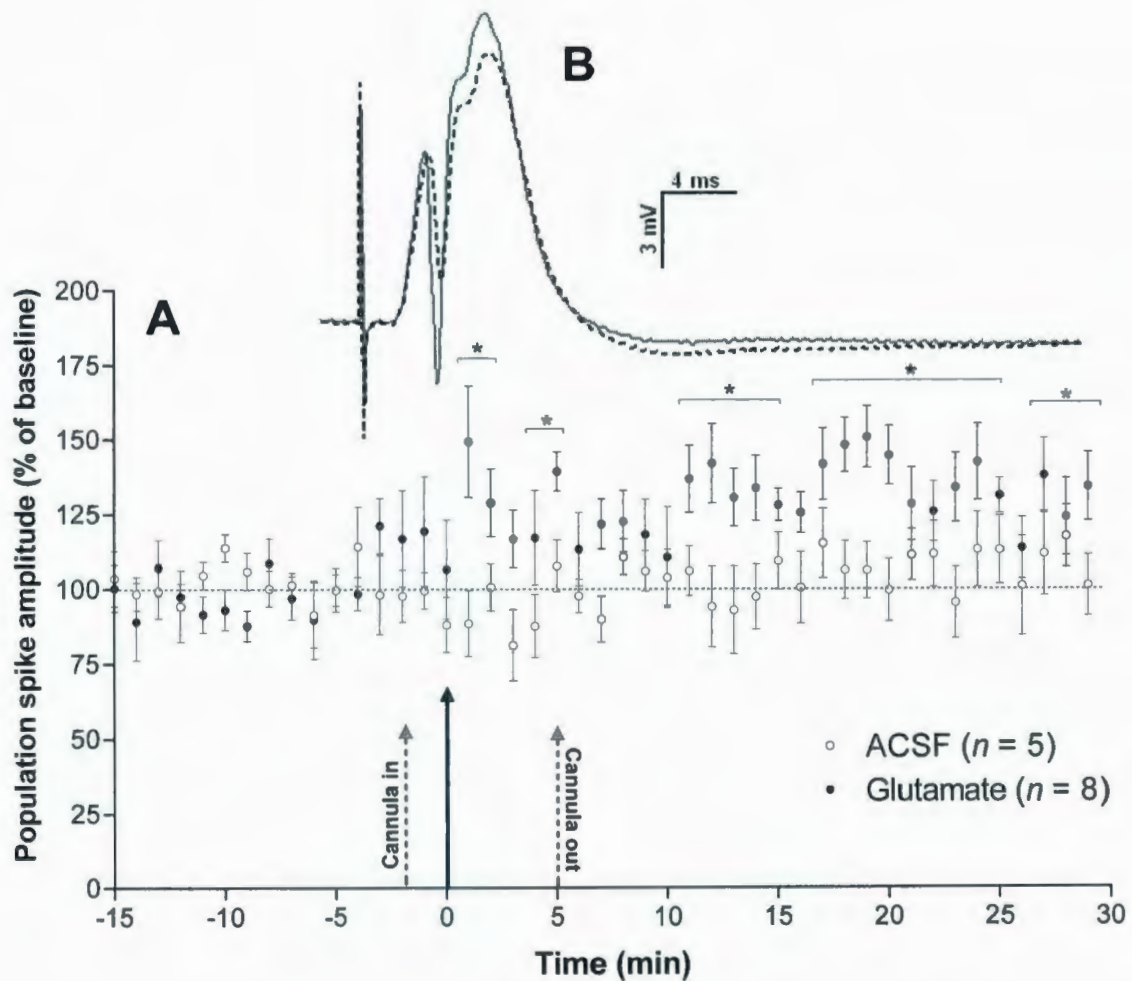


**Figure 2.1 Initial increase in PP-evoked population spike amplitude.**

A. An increase in population spike amplitude immediately followed drug application in glutamate animals. Arrow indicates drug ejection. Group means of 1 min samples, standard error bars indicated. \* indicates  $p < 0.05$ .

B. Example PP-evoked waveforms recorded in DG from animal with glutamatergic activation of LC. Dashed line is waveform recorded during pre-LC activation baseline. Solid line is waveform recorded 210 min post-LC activation.

To analyze the entire 4 hr recording period of the glutamate group and the corresponding 4 hr period in the ACSF group, a two factor (group, time) mixed-effects ANOVA was also carried out to examine the effects of group and time on PP-evoked population spike amplitude over the 1 hr before and 3 hr after LC activation. A significant group X time interaction was present ( $F(47,470) = 4.48, p < .001$ ), and post-hoc LSD analysis showed 5-min means in test animals following LC glutamate injection to differ significantly both from equivalent time points in ACSF animals and from all points on glutamate baseline ( $p < 0.05$ ; see Figure 2.2).

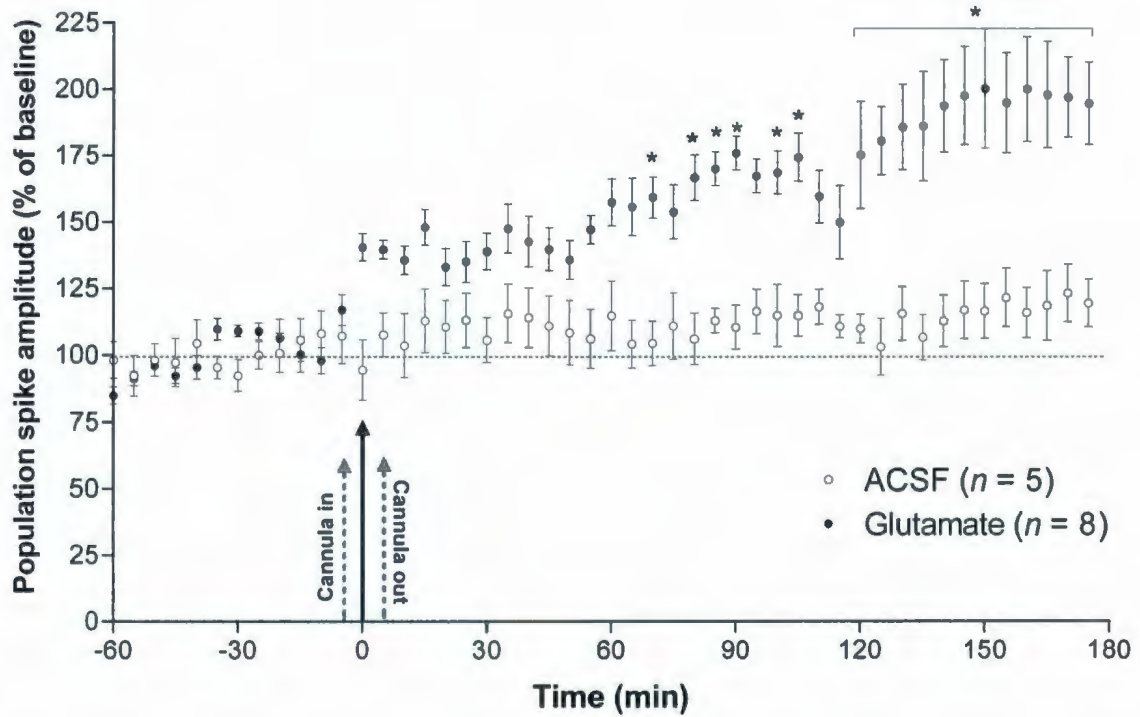


**Figure 2.2 Long-term increase in PP-evoked population spike amplitude.**

An average increase of 65% in PP-evoked population spike amplitude was observed in the 3 hr following LC activation. Arrow indicates time of drug ejection in LC. In glutamate animals, a pop-up in spike amplitude is seen following cannula insertion. 5 min means, standard error bars indicated.

\* indicates  $p < 0.05$ .

### **2.3.2 PP-evoked EPSP Slope**

In the glutamate group the mean PP-evoked EPSP slope increased from 3.39 mV/ms at baseline to a mean of 3.5 mV/ms in the 3 hr after LC activation. PP-evoked EPSP slope increased in 6 glutamate-injected animals and decreased in 2, but did not reach significance. ACSF animals (with a mean EPSP slope of 5.6 mV/ms in the first 1 hr of recording) similarly showed no change, decreasing from 6.0 mV/ms in the hour before injection to 5.95 mV/ms in the 3 hr post-LC activation (see Figure 2.3). A between-groups ANOVA of 5 min means in the 3 hr post-injection period showed no significant difference between ACSF and glutamate animals ( $F(35, 385) = 0.327, p = 1.0$ ) for PP-evoked EPSP slope.

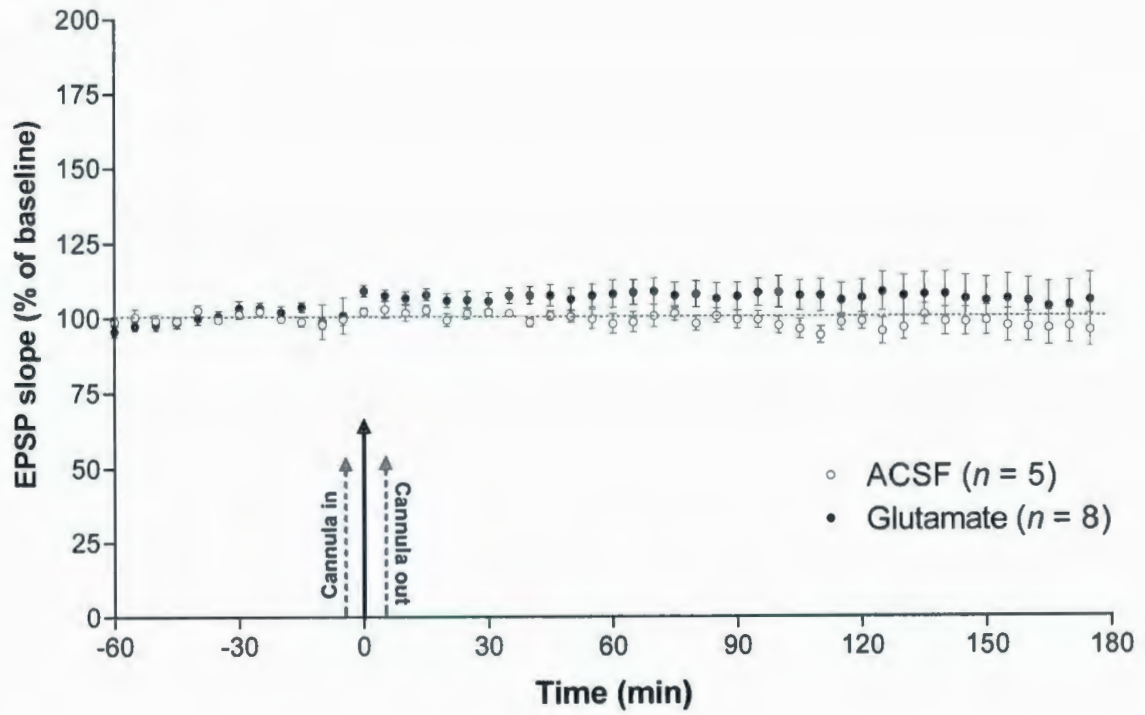


**Figure 2.3 No change in PP-evoked EPSP slope.**

No significant change in PP-evoked EPSP slope was observed. Arrow indicates time of drug ejection in the LC. 5 min means, standard error indicated.

### **2.3.3 PP-evoked latency to peak and EPSP slope paired-pulse ratio**

A significant main effect for time ( $F(47,517) = 6.05, p < 0.001$ ) and group  $\times$  time interaction ( $F(1, 47) = 1.51, p = 0.018$ ) were found for latency to population spike peak in the PP-evoked potential. Latency to peak decreased over time, and a post-hoc LSD analysis found 5-min means in glutamate animals differed significantly from all baseline points beginning approximately 1 h post LC activation (see Figure 2.4). In the glutamate group, latency decreased from 4.05 ms in the 1 h pre LC activation to 3.93 ms in the 3 hr post activation (3.87 ms in the final 1 hr of recording, a 4.5% decrease from the 1 hr baseline mean). In the ACSF group, latency decreased from 3.91 ms in the 1 hr before ACSF ejection to 3.87 in the 3 hr post activation (3.85 in the final 1 hr of recording, a 1.5% decrease from the 1 hr baseline mean). In the first hour of the 7 hr ACSF recording, the latency to peak was 4.01 ms, similar to the starting value of glutamate animals.

To compare with initial PP-evoked population spike amplitude changes over the same time period, latency to peak in the 30 min following drug ejection was compared to the 15 minutes pre-ejection in both groups. No significant differences were found between groups or over time for that period (see Figure 2.5).

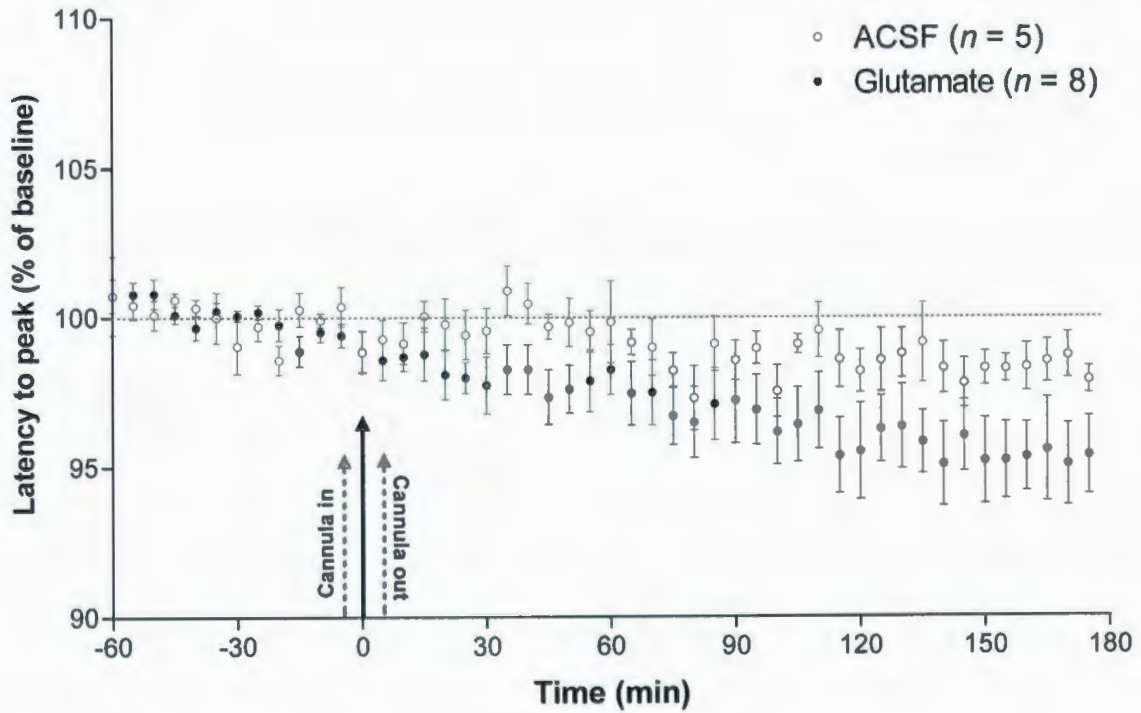


**Figure 2.4 Decrease in PP-evoked latency to peak**

A mean decrease of 4.5% in PP-evoked latency to peak was observed from the first 1 hr to the final 1 hr of recording in glutamate animals. ACSF animals decreased 1.5% over the same time period. 5 min means, standard error bars indicated. Solid arrow indicates time of drug ejection.

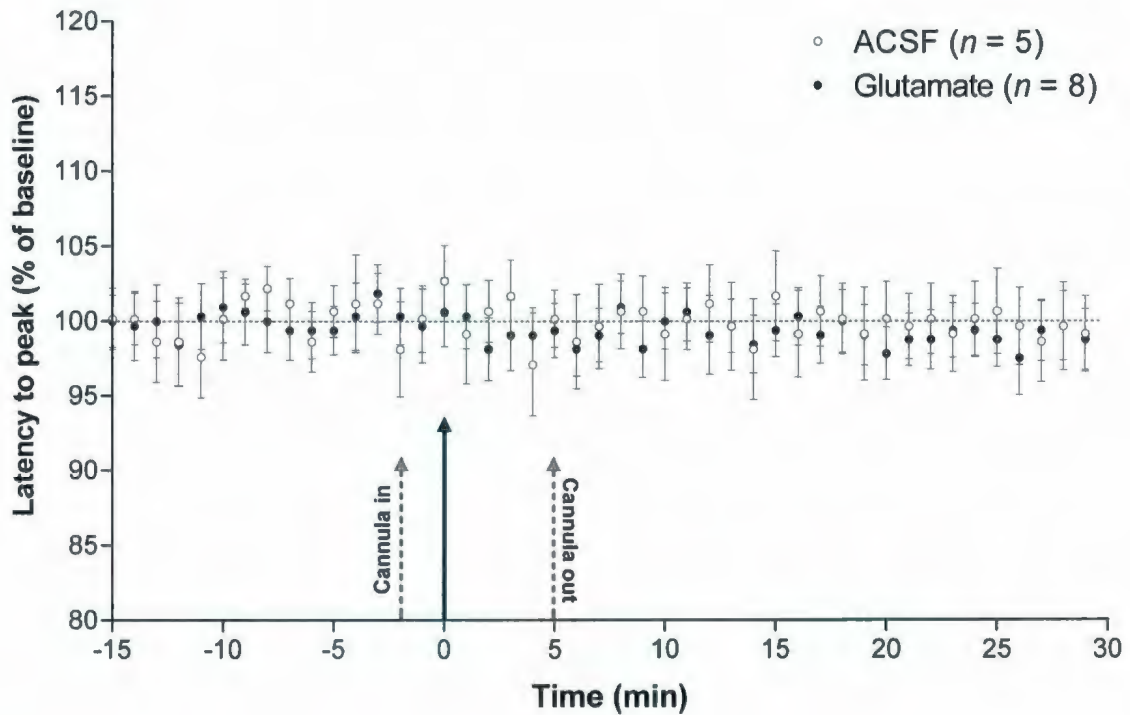


**Figure 2.5 No initial change in PP-evoked latency to peak**

No initial change in PP-evoked latency to peak is observed following glutamate or ACSF ejection in comparison to 15 min pre-ejection baseline. 1 min intervals, standard error bars indicated. Solid arrow indicates time of drug ejection.

Animals in both the glutamate and ACSF groups had a slightly higher post-LC ejection EPSP slope paired pulse ratio compared to pre-ejection (see Figures 2.6 and 2.7), although this difference was not significant, and glutamate and ACSF groups did not differ significantly from each other. In both groups, the 30 ms paired-pulse ratio at low stimulation intensities (100 to 300  $\mu\text{A}$ ) was above 1, and below 1 at higher stimulation intensities (500 to 1000  $\mu\text{A}$ ). The 30 ms paired pulse ratio is indicative of PP fiber composition, with ratios below 1 indicating more activation of medial PP fibers, as opposed to lateral PP (McNaughton, 1980).

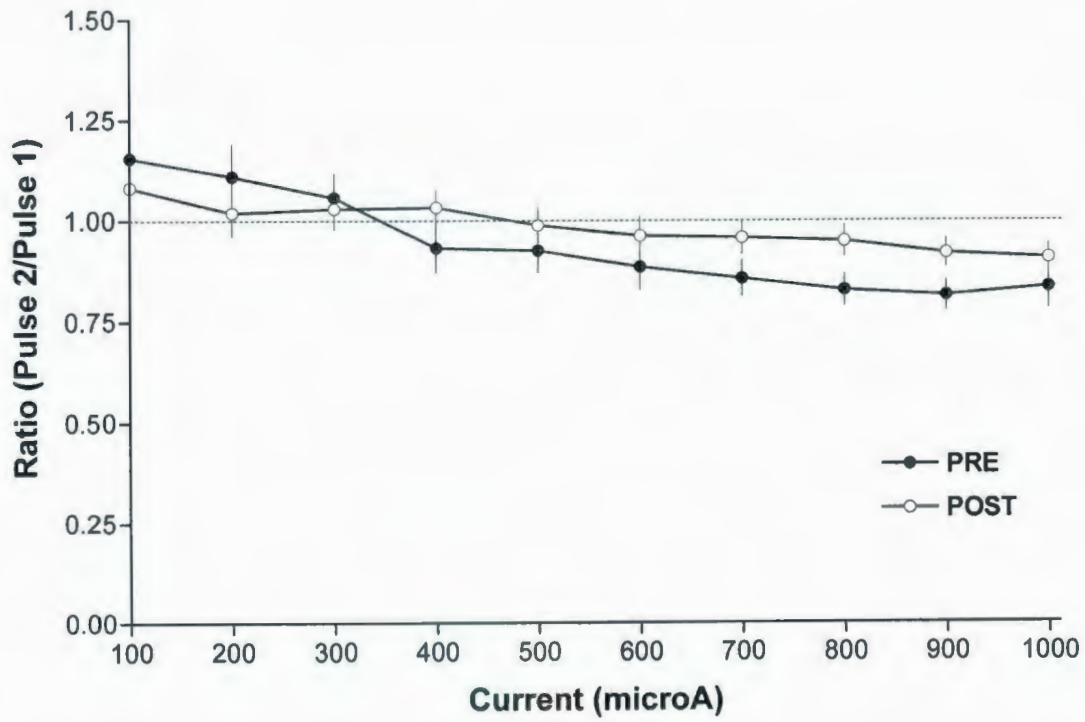


**Figure 2.6 PP-evoked EPSP slope paired-pulse ratio (glutamate)**

PP-evoked EPSP slope paired-pulse ratio (30ms ISI) taken 1 hr pre- and 3 hr post-LC activation ( $n = 6$ ).

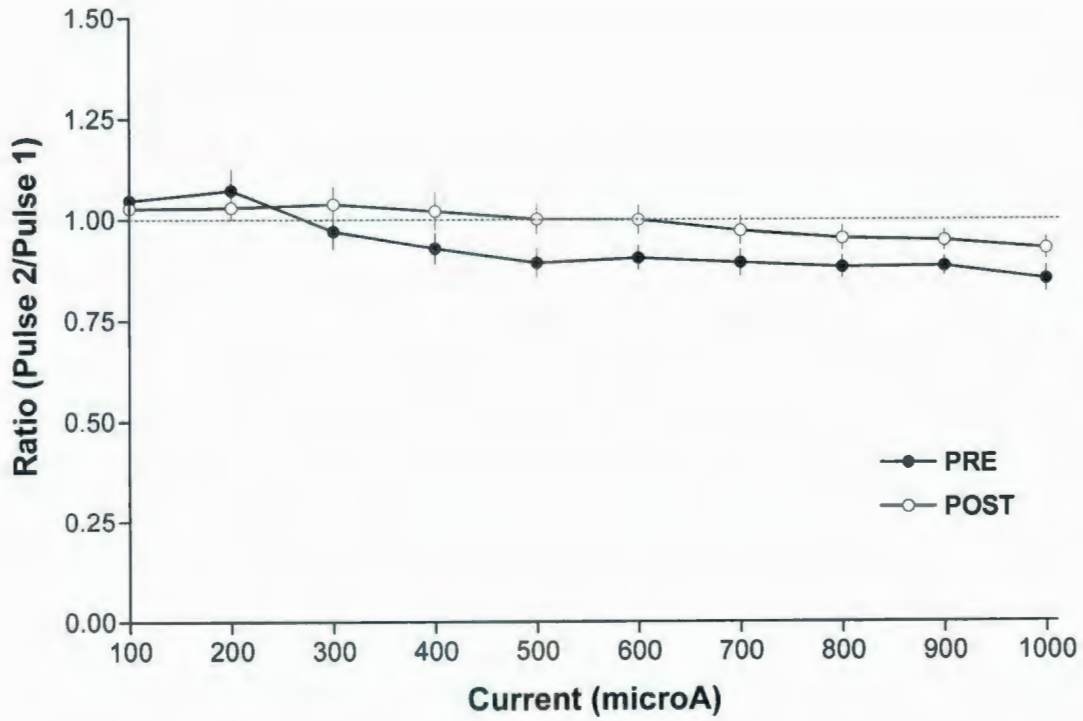


**Figure 2.7 PP-evoked EPSP slope paired-pulse ratio (ACSF)**

PP-evoked EPSP slope paired-pulse ratio (30ms ISI) taken 4 hr pre- and 3 hr post-ACSF ejection ( $n = 5$ ).

#### **2.3.4 LOT-evoked EPSPs**

No significant group  $\times$  time interaction was found for LOT-evoked EPSP amplitude ( $F(35, 385) = 0.588, p = 0.97$ ; between-groups repeated measures ANOVA, 5-min means post-ejection). The average amplitude increased from a 1 hr baseline mean of 1.7 mV to a mean of 2.2 mV in the 3 hr following glutamatergic stimulation of LC, a non-significant enhancement of 27% (ranging from 3% to 82%). In ACSF control animals, with a baseline mean amplitude of 1.72 mV in the first 1 hr of recording, amplitude increased from 2.88 mV in the 1 hr prior to injection to 2.96 mV in the 3 hr after (amplitude increased in 3 and decreased in 2 animals, with an average non-significant increase of 3%; see Figure 2.8).

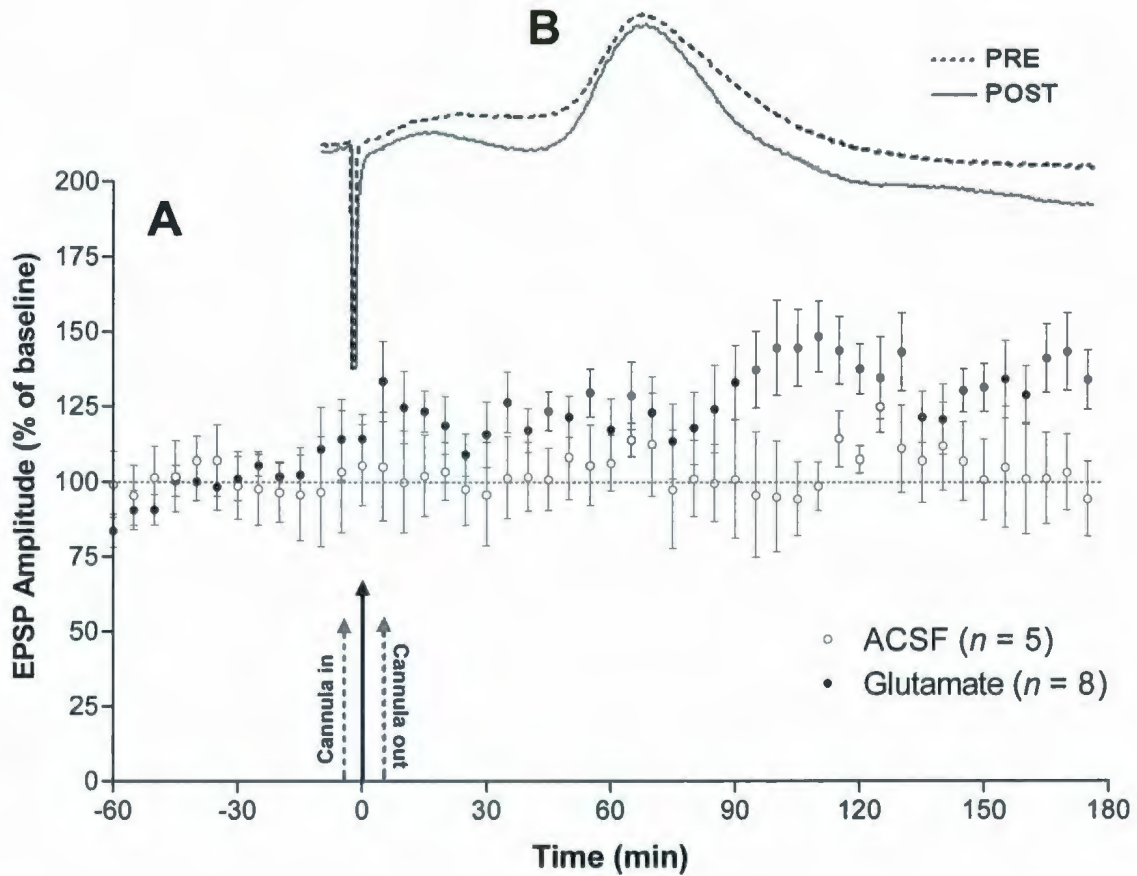


**Figure 2.8 No change in LOT-evoked EPSP amplitude.**

**A.** No significant interaction between group and time was observed for LOT-evoked EPSP amplitude. 5 min means, standard error bars indicated. Arrow indicates time of drug ejection in the LC.

**B.** Example LOT-evoked waveforms from animal with glutamatergic activation of LC. Dashed line is LOT-evoked potential recorded during pre-LC activation baseline. Solid line is LOT-evoked potential recorded 210 min post-LC activation. Amplitude measured from baseline at stimulus artifact.

A non-significant increase of LOT-evoked EPSP slope from a 1 hr baseline mean of 0.36 mV/ms to 0.48 mV/ms (a 34% increase, ranging from 6% to 110%) in the 3 hr post-LC activation was observed. In ACSF control animals, starting with a baseline mean slope of 0.33 mV/ms in the first 1 hr of recording, an average increase of 6% was observed (from 0.59 mV/ms in the 1 hr prior to injection to 0.63 mV/ms in the 3 hr after, with individual changes in slope ranging from -6% to 22% (see Figure 2.9). However, these changes in LOT-evoked EPSP slope remained non-significant for both the ACSF and glutamate groups ( $F(35, 385) = 0.498, p = 0.99$ ; between-groups repeated measures ANOVA, 5-min means post-ejection).

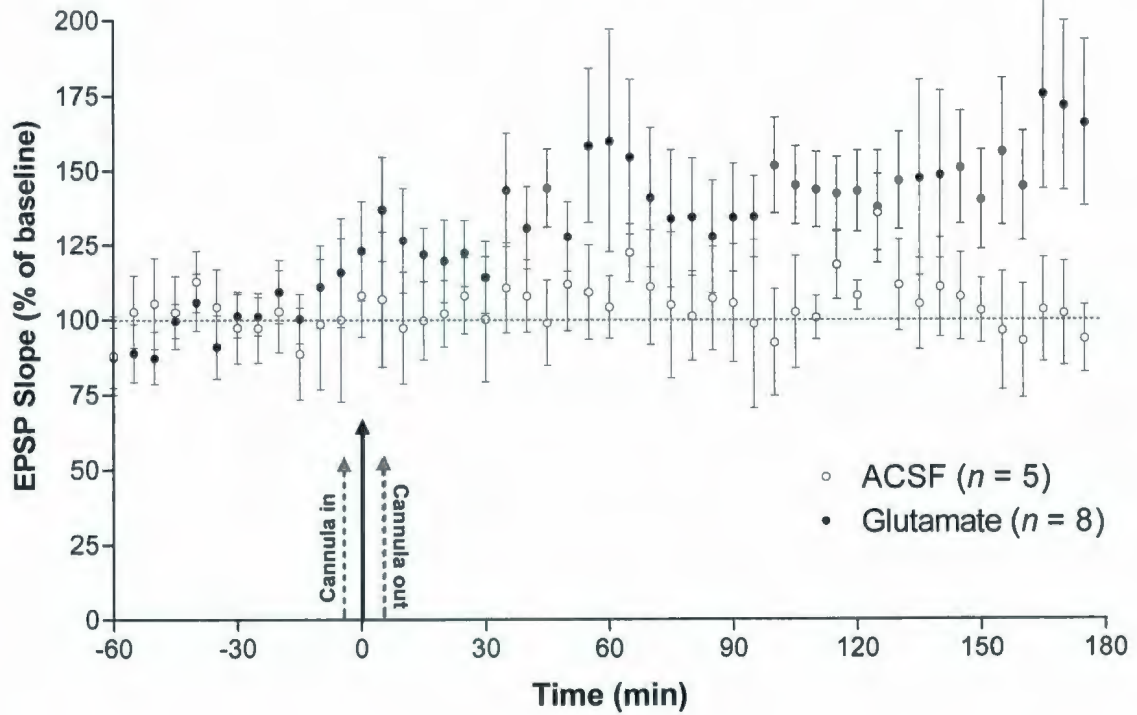


**Figure 2.9 No change in LOT-evoked EPSP slope**

No significant group X time interaction in LOT-evoked EPSP slope was observed. 5 min means, standard error indicated. Arrow indicates time of drug ejection through LC cannula.

### ***2.3.6 LOT-evoked latency to peak***

A between-groups ANOVA of 5 min means in the 3 hr post-injection found no significant effects for LOT time to peak ( $F(35, 385) = 0.923, I = 0.60$ ). The average latency was 18.4 ms in glutamate-injected animals before and after LC stimulation, and 18.7 ms in ACSF control animals (see Figure 2.10).

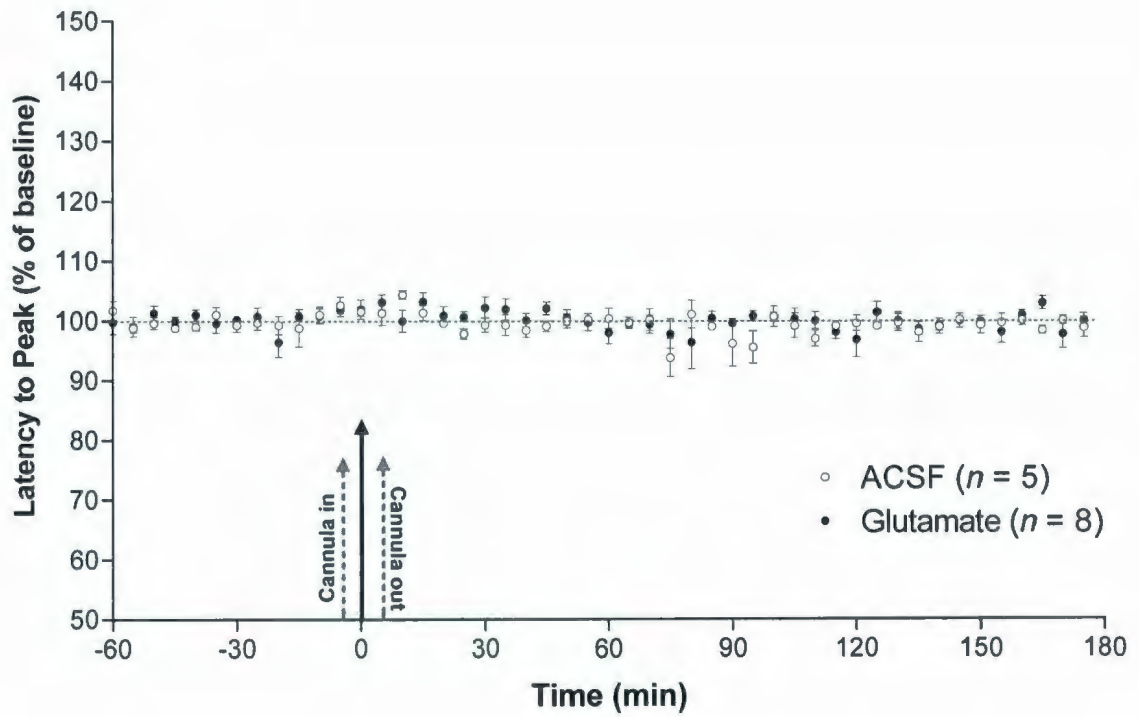


**Figure 2.10 No change in LOT-evoked latency to peak.**

No significant effects for LOT-evoked latency to peak were found.

Arrow indicates time of drug ejection in the LC. 5 min means,

standard error bars indicated.

### **2.3.7 Input-output analyses**

I-O current intensity relationships for animals with glutamatergic stimulation of LC ( $n = 8$ ) showed an increase in population spike amplitude following LC activation (see Figure 2.11). Post-recording I-O measures of PP-evoked population spike (see Figure 2.12) and EPSP slope (Figures 2.13 and 2.14) were also greater than pre-recording I-O curves in the ACSF group ( $n = 5$ ).

While both groups exhibited an increase in I-O relationships from initial to final I-O curves, the PP-evoked population spike of LC-activated animals showed an increase to 200-250% of initial I-O maximum at higher current levels (800-1000  $\mu\text{A}$ ) over the 4 hr period between I-O curves, whereas the ACSF group demonstrated a smaller increase of 125% over a longer (7 hr) period between initial and final I-O curves. This difference in elapsed time between collection of initial and final I-O data in the experimental (4 hr) and control groups (7 hr) prevents a direct statistical comparison.

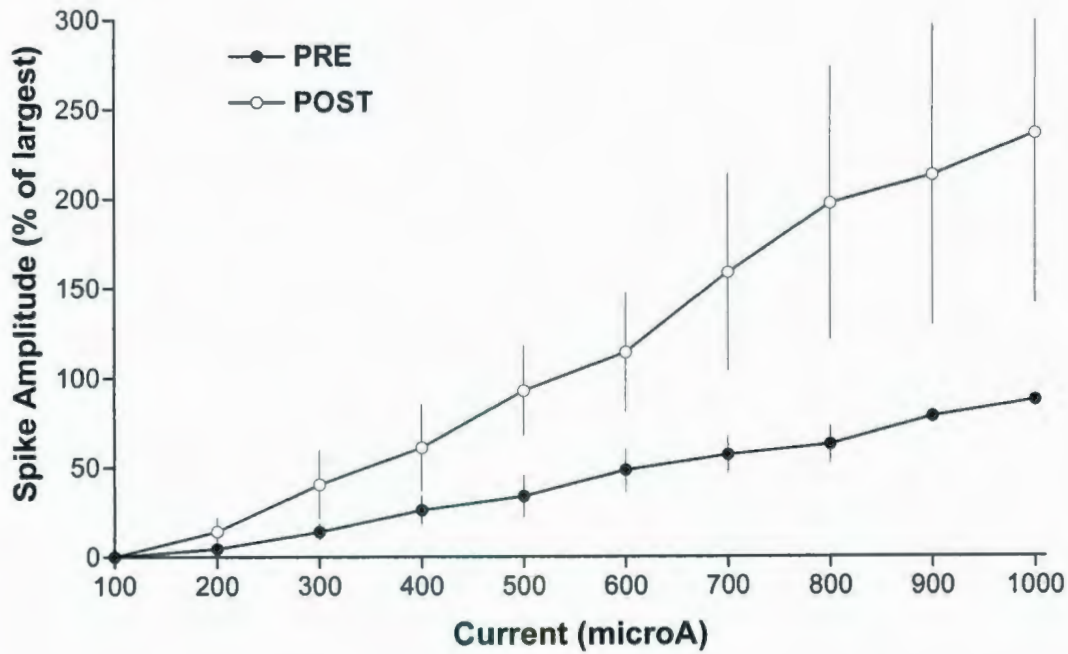


**Figure 2.11 PP population spike amplitude input-output analysis (glutamate).**

I-O curves 1 hr pre- and 3 hr post-LC activation ( $n = 6$ ). The mean population spike amplitude for each current intensity was converted to a percentage of the largest mean spike amplitude obtained during the pre-activation I-O curve for each animal. Data represent the group mean with SEM.

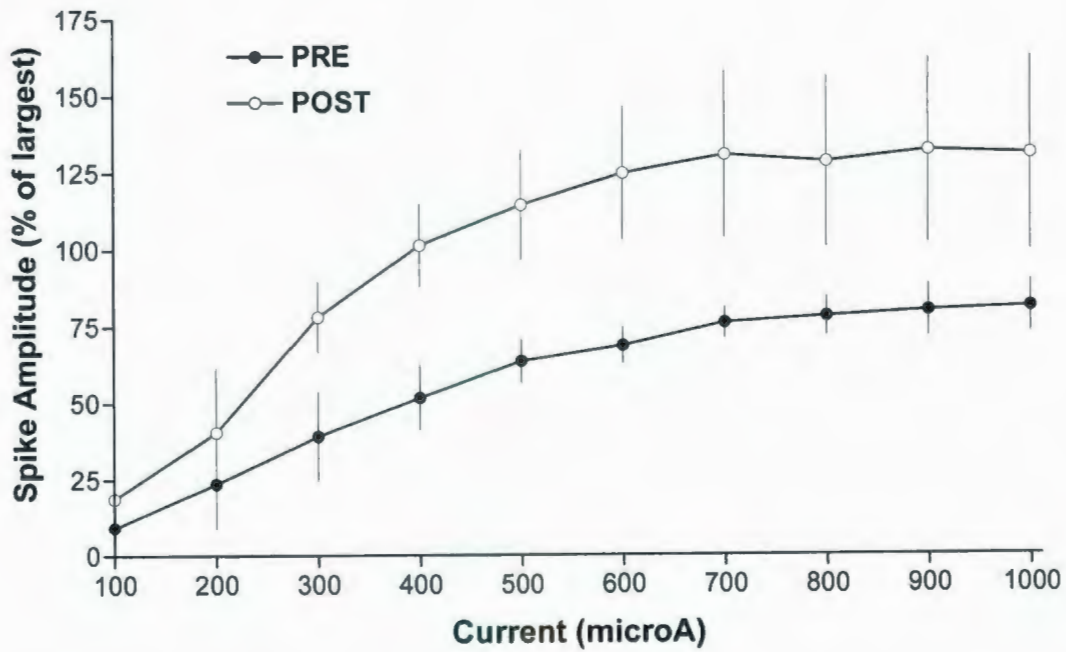


**Figure 2.12 PP-evoked spike amplitude I-O analysis (ACSF control).**

I-O curves taken 4 hr pre- and 3 hr post-LC ejection ( $n = 5$ ). The mean population spike amplitude for each current intensity was converted to a percentage of the largest mean spike amplitude obtained during the pre-activation I-O curve. Data represent the group mean with SEM.

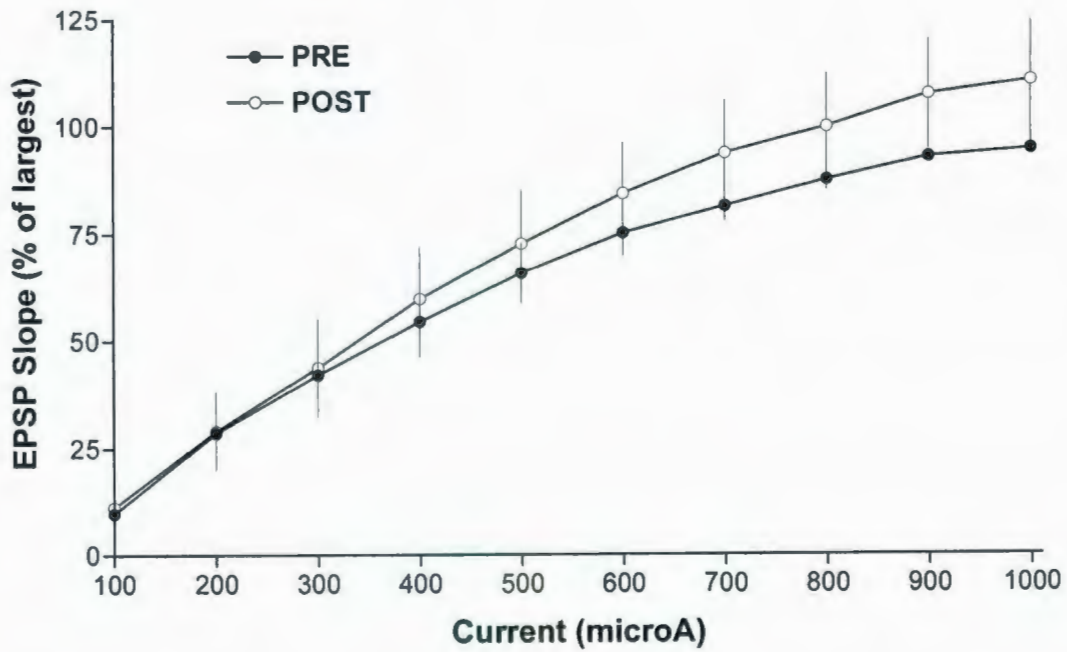


**Figure 2.13 PP-evoked EPSP slope input-output analysis (glutamate).**

I-O curves taken 1 hr pre- and 3 hr post-LC activation ( $n = 6$ ). The mean PP-evoked EPSP slope for each current intensity was converted to a percentage of the largest mean EPSP slope obtained during the pre-activation I-O curve. Data represent the group mean with SEM.

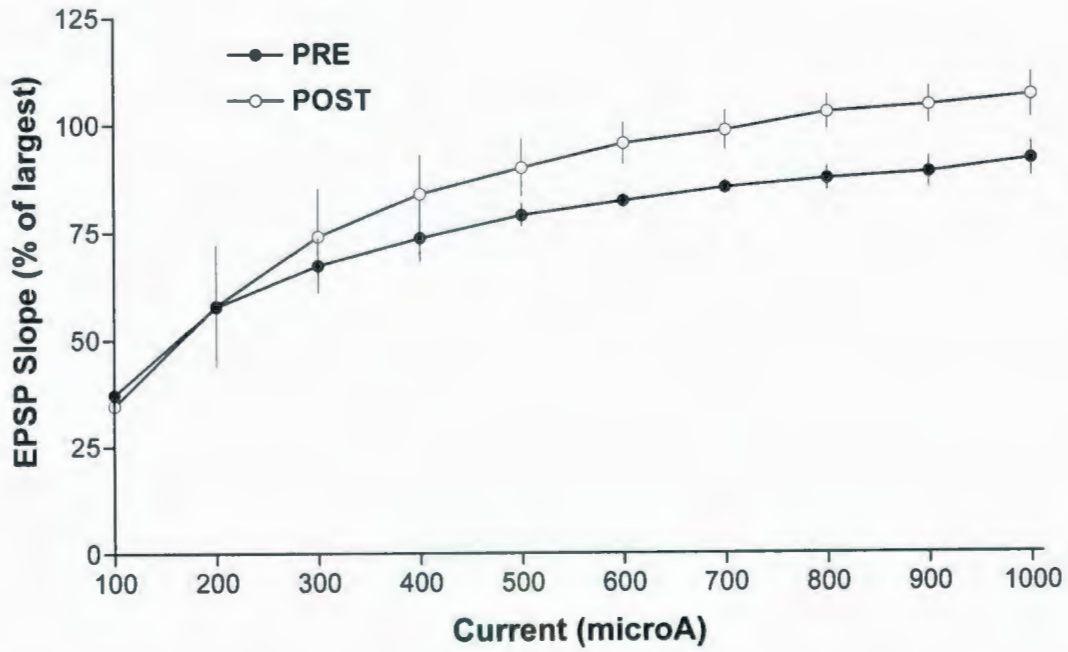


**Figure 2.14 PP-evoked EPSP slope I-O analysis (ACSF control).**

I-O curves taken 4 hr pre-ACSF ejection and 3 hr post-ACSF ( $n = 5$ ).

The mean PP-evoked EPSP slope for each current intensity was converted to a percentage of the largest mean EPSP slope obtained during the pre-activation I-O curve. Data represent the group mean with SEM.

Analysis of I-O data for LOT-evoked EPSP amplitude indicates an increase between pre- and post-LC activation measurements at all current levels (group X current interaction:  $F(9,90) = 4.07, p < 0.001$ ; see Figure 2.15). A 2-way ANOVA showed a significant interaction between group (ACSF-pre, ACSF-post, glutamate-pre, glutamate-post) and current level ( $F(27,162) = 2.43, p < 0.001$ ). Post-hoc LSD analyses showed that pre-glutamate and pre-ACSF I-O curves were not significantly different between ACSF and glutamate groups (see Figure 2.16). However, for both ACSF and glutamate groups, all points on the pre-injection baseline were significantly different from points at current levels 600 to 1000  $\mu\text{A}$  post-injection, suggesting a non-specific increase in EPSP over time, unrelated to LC activation.

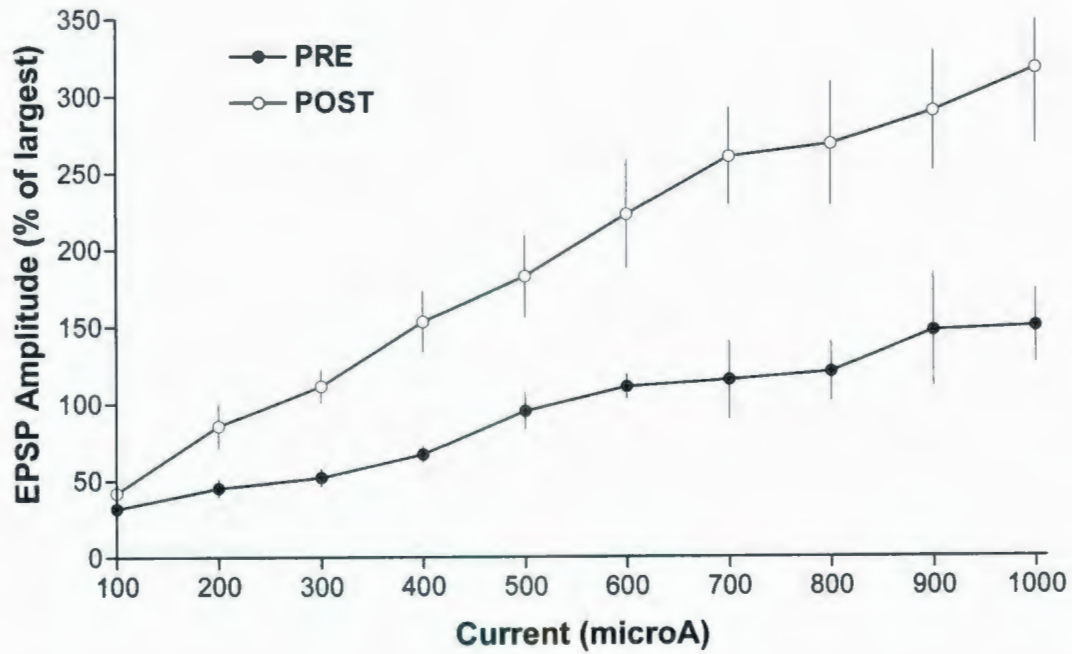


**Figure 2.15** LOT-evoked EPSP amplitude input-output analysis (glutamate).

I-O curves taken 1 hr pre- and 3 hr post-LC activation ( $n = 6$ ). The mean EPSP amplitude for each current intensity was converted to a percentage of the largest mean amplitude obtained during the pre-activation I-O curve. Data represent the group mean with SEM.

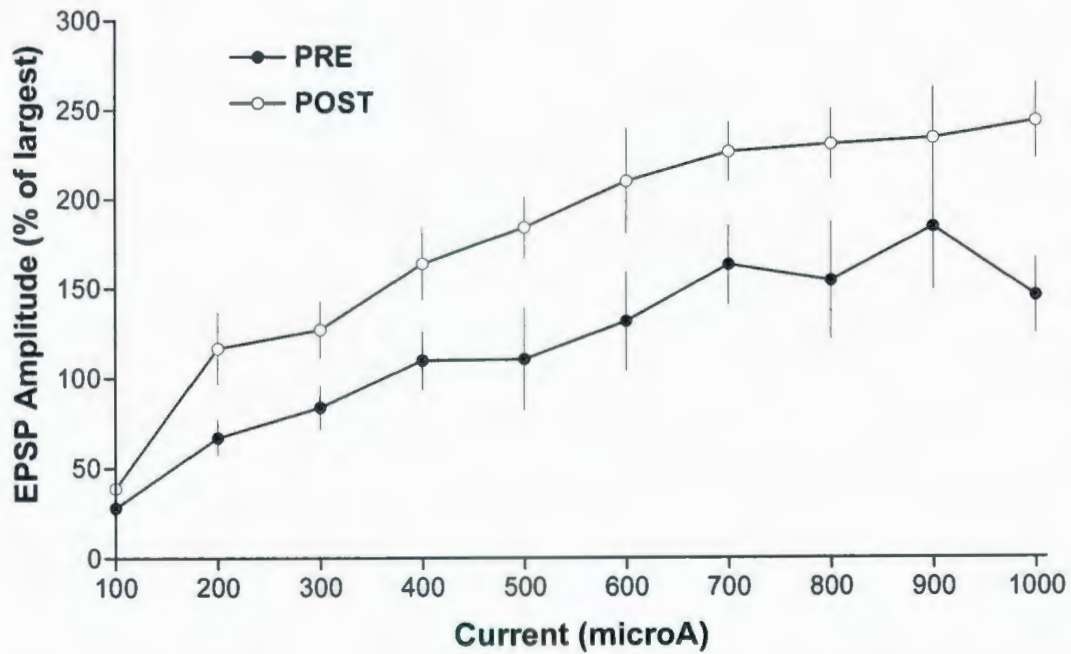


**Figure 2.16** LOT-evoked EPSP amplitude I-O analysis (ACSF control).

I-O curves 4 hr pre- and 3 hr post-LC ejection ( $n = 5$ ). The mean EPSP amplitude for each current intensity was converted to a percentage of the largest mean amplitude obtained during the pre-activation I-O curve. Data represent the group mean with SEM.

### ***2.3.8 E-S coupling ratio***

An increase in population spike amplitude unaccompanied by a change in EPSP slope led to a leftward shift in the PP-evoked EPSP slope/population spike ratio occurring following LC activation (see Figure 2.17), consistent with the change in baseline spike but not EPSP slope. A shift in the slope/spike ratio was also observed in the 7 hr ACSF control animals (see Figure 2.18), suggesting an additional non-specific excitability increase over time.

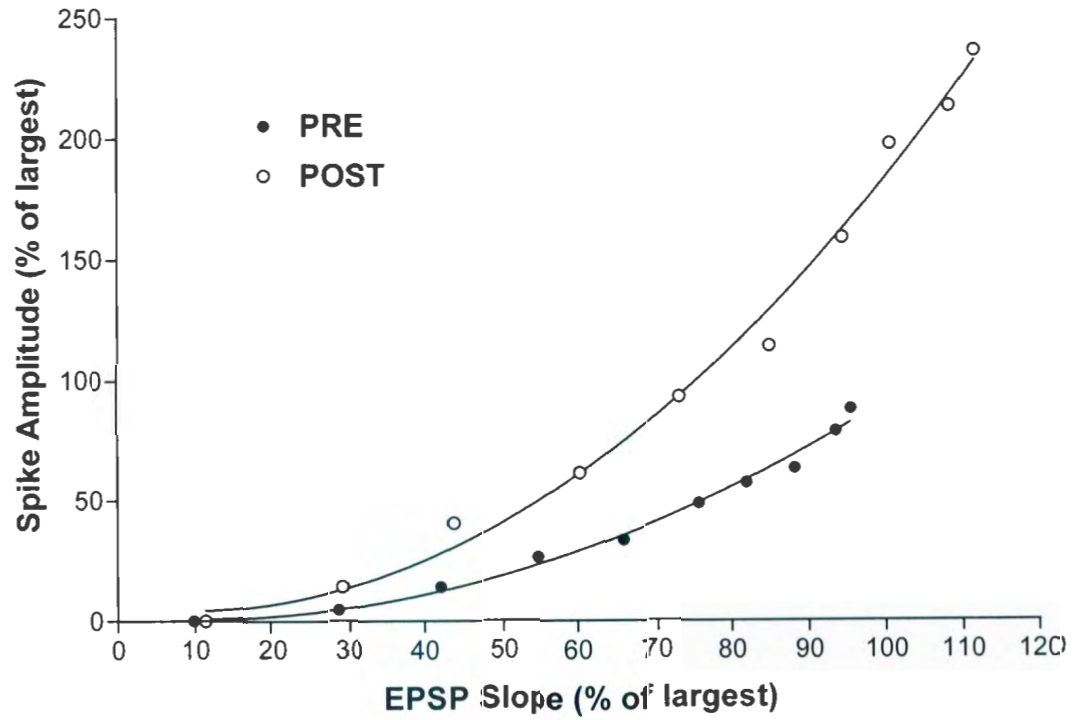


**Figure 2.17 PP-evoked EPSP slope/population spike ratio (glutamate)**

E-S coupling ratio for glutamate animals ( $n = 6$ ). A leftward shift in E-S coupling occurs post-LC activation.

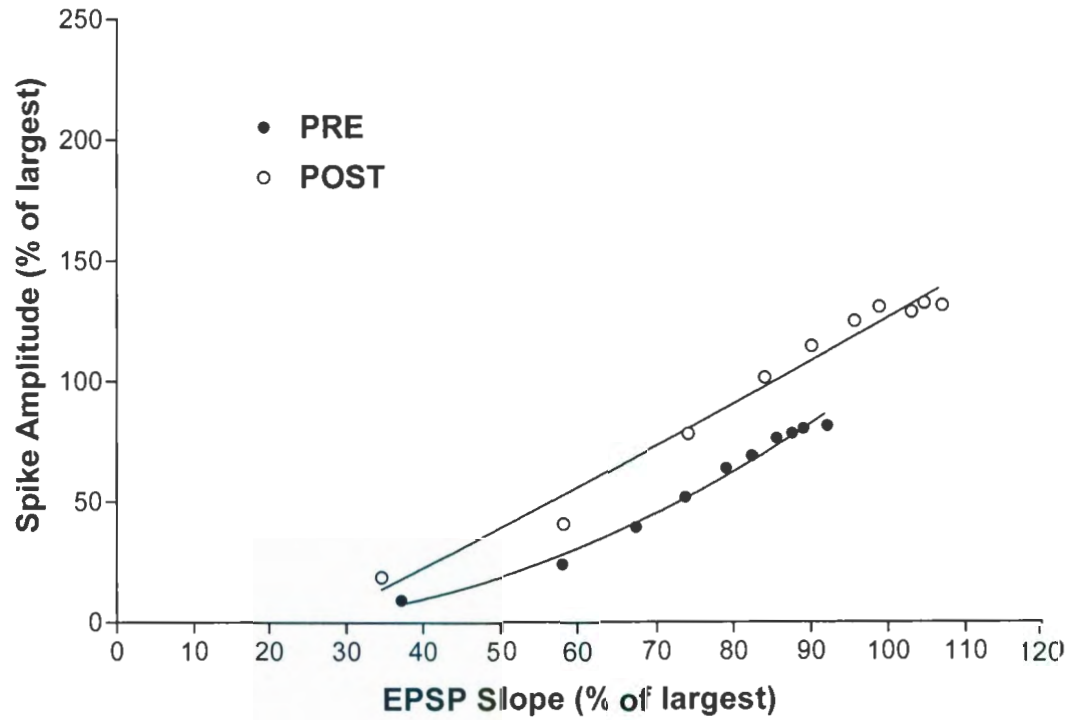


**Figure 2.18 PP-evoked EPSP slope/population spike ratio (ACSF)**

E-S coupling ratio for ACSF control animals ( $n = 5$ ). PRE and POST measures taken 4 hr pre- and 3 hr post-ACSF ejection, respectively.

Same scale as Figure 2.15.

### **2.3.9 Oscillation of PP- and LOT-evoked parameters**

The 7 hr recordings of individual ACSF animals appeared to demonstrate an inverse relationship between PP-evoked population spike amplitude and LOT-evoked EPSP amplitude. Figure 2.19 shows an example of this relationship ( $n = 1$ ) in which a significant negative correlation between corresponding 5 min means of the two parameters was found ( $r = -.222, p = 0.04$ ). The mean correlation of the group ( $n = 5$ ) was  $r = -0.103$ , with two additional animals demonstrating significant negative correlations ( $r = -.236, p = 0.03$ ;  $r = -.207, p = 0.05$ ), and no significant relationship found between parameters of the remaining two animals ( $r = -0.004, p = 0.97$ ;  $r = 0.157, p = 0.15$ ). The parameters also seem to exhibit an oscillation in values with a period of 1 hr. These individual effects were masked in the group mean due to time differences in the onset of the oscillation between animals.

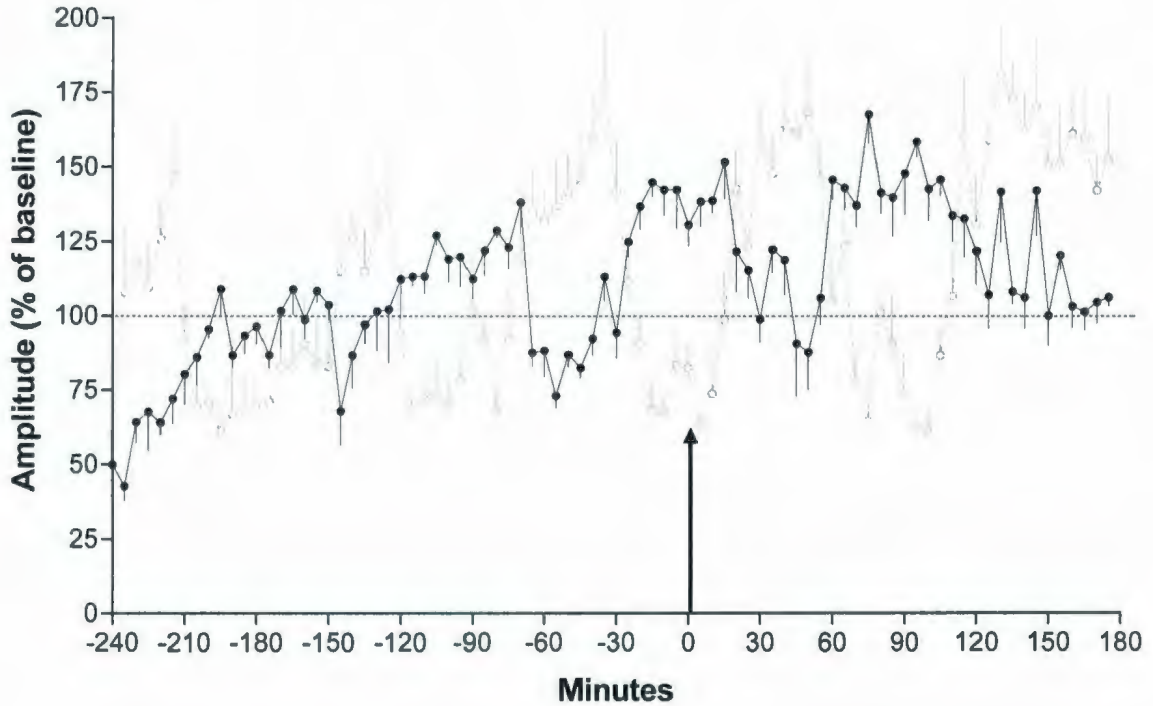


**Figure 2.19 Example oscillations in PP-evoked population spike amplitude and LOT-evoked EPSP amplitude ( $n = 1$ )**

A negative correlation between PP-evoked population spike amplitude and LOT-evoked EPSP amplitude was observed in individual animals. Data from one ACSF animal recorded over 7 hr with ACSF injection at 4 hr. Dark points represent PP-evoked population spike amplitude 5 min means with standard error indicated; light points represent LOT-evoked EPSP amplitude 5 min means with standard error indicated.

### ***2.3.10 Histology and electrode placements***

Animals were included in the study on the basis of proximity of dye injection to LC (see Figure 2.18). Based on previous experience cannula tips located within 300  $\mu\text{m}$  of the Nissl-identified nucleus of the locus coeruleus were considered successful. Dye proximity to LC was measured in 30  $\mu\text{m}$  sagittal tissue sections and compared to adjacent cresyl violet-stained sections. In the glutamate group, cannula placements were within LC in 4 animals, 200  $\mu\text{m}$  posterior in 1 animal, and 180  $\mu\text{m}$  lateral in 2 animals (one of those placements was also 100  $\mu\text{m}$  dorsal of LC). In the ACSF group, 2 cannula placements were within LC, 2 were 100  $\mu\text{m}$  posterior, and one was 100  $\mu\text{m}$  anterior of LC. LOT potentials were similar, although variable, in all animals, and lesions were present within LOT in all subjects.

Electrophysiological data (positive-going waveform with negative-going population spike) indicated recording micropipette positions within the granule cell layer of the DG in all animals. Population spike latencies were indicative of PP stimulating electrode placements within the medial perforant path.



**Figure 2.20 Experiment 1 LC cannula ejection sites**

Locations of dye marking cannula ejection sites near LC, determined with 30 micron sagittal sections through brainstem/cerebellum.

## **2.4 Discussion**

In Experiment 1 activation of noradrenergic input to the DG *in vivo* initiated a potentiation of the medial PP population spike in glutamate animals immediately following LC activation and lasting the duration of recording (3 hr), while the LOT-evoked EPSP at the same site did not differ significantly from baseline.

The expected immediate and long-lasting (3 hr) increase in amplitude of the medial PP-evoked population spike is consistent with the report of immediate increase seen by Babstock and Harley (1993), and similarly a decrease in PP-evoked latency to peak following LC activation was also observed.

Similar to Walling and Harley (2004), while a long-lasting increase in the PP-evoked population spike amplitude was observed, the PP-evoked EPSP slope of Experiment 1 remained unchanged in the 3 hr post LC activation. The increase in PP-evoked population spike (an index of granule cell excitability) without a corresponding increase in EPSP slope (a measure of synaptic drive) suggests that NE alters the coupling between EPSP and spike generation (Neuman & Harley, 1983). This increase has been observed in past studies of LTP (Bliss & Lømo, 1973) and NE-LTP (Neuman & Harley, 1983).

Previous studies have similarly failed to observe a consistent potentiation of the EPSP slope, when using electrical (Assaf, Mason, & Miller, 1979) or glutamatergic stimulation of the LC (Harley & Milway, 1986). The EPSP component of the PP-evoked DG response may contain a mix of medial and lateral inputs, so potentiation of the EPSP slope in the

medial PP could be masked by depression in the lateral PP (Reid & Harley, 2009). However, the properties of the PP-evoked waveform (peak latency, half-width, and rise time) indicated a primarily medial mix of fibers was stimulated in Experiment 1.

The decrease observed in latency to peak of the PP-evoked population spike would seem to indicate a change in EPSP consistent with the masking hypothesis. However, this decrease was only observed when comparing the entire 3 hr post-recording period to the 1 hr baseline mean; when examining the latency measure within 30 min of LC ejection, no change in latency is apparent, arguing against a change in synaptic drive. Additionally, the I-O current relationship measures of PP-evoked EPSP slope in both the glutamate and ACSF groups did not differ significantly from initial to final I-O curves. The 30 ms paired-pulse ratio (less than 1) observed in both experimental and control groups in Experiment 1 also did not differ significantly between pre- and post-recording I-O collection, as would be expected in the glutamate group if the medial PP input were stronger. Nor is there any suggestion of a depression at the lower current levels where the paired pulse ratio was more than 1.

Comparison between the I-O data of experimental and control groups is difficult because of the difference in duration of the recording period. Animals receiving glutamatergic activation of LC had 4 hr elapse between the recording of pre and post I-O curves, while 7 hr elapsed between pre and post I-O data collection in the ACSF control group.

While ACSF control animals are not typically used in studies involving LC activation due

to the possibility of activating LC through mechanical stimulation alone, changes in parameters following ACSF ejection in the LC were not observed. Increases in PP-evoked population spike amplitude seemed time-dependent (rising consistently over the 7 hr period) and were unaffected by ACSF ejection. The rising baseline measurements account for the differences in responses at initial and final I-O data collection and suggest an increase in excitability over time which would make some contribution to the overall increase in the experimental group, but which cannot account for the magnitude of the effects observed.

A study on the stability of baseline recording in the DG of urethane-anaesthetized rats noted a consistent upward drift in both the population spike amplitude and EPSP slope over the duration of recording (Gilbert & Mack, 1999). Over the first 2 to 4 hr of recording, large time-dependent increases in population spike amplitude (70-80%) are observed. Smaller increases in EPSP slope (20-30%) were also observed, stabilizing within 1 to 2 hr of recording. While in Experiment 1 the LOT and PP were stimulated for a period of 30-60 min prior to initial I-O data collection to allow baseline to stabilize, any additional time-dependent increases in parameters following the start of recording would be exaggerated in the final I-O curve of the ACSF control group in comparison to the glutamate animals because of the additional 3 hr of time elapsed.

Babstock & Harley (1993) demonstrated an immediate and short-term depression of the LOT-evoked DG potential with a 40 ms latency conditioning pulse, and Dahl and Sarvey (1989) and Pelletier et al. (1994) demonstrated long-lasting depression of the lateral PP

input to DG following *in vitro* application of NE or isoproterenol (a  $\beta$ -noradrenergic agonist), respectively, with concurrent potentiation of medial PP-evoked responses. Both *in vitro* and *in vivo* results supported selectivity of NE modulation of inputs to the DG.

However, in Experiment 1 the amplitude and slope of the LOT-evoked EPSP following LC activation did not differ significantly from baseline or from ACSF controls, in contrast to the decreases in lateral PP-evoked potentials previously mentioned. While Experiment 1 did not provide further evidence for depression of the lateral PP, the potentiation of medial PP parameters with no accompanying change in lateral PP evoked potentials does partially support selectivity.

This weaker selectivity of inputs (potentiation of the medial input, without accompanying depression of the lateral input) may be due to the features of temporal pairing of NE and PP or LOT stimulation used in this experiment. Reid and Harley (2009) demonstrated an associativity requirement for NE release and PP stimulation *in vivo*, finding that when PP stimulation was interrupted 10 min before and after LC activation, LC-induced long-term potentiation of the PP-evoked population spike and EPSP slope failed to occur. Thus degree of input activation in association with LC activation is an important parameter in long-term effects of LC activation.

The spacing of PP and LOT stimulation in Experiment 1 would have led to a weaker pairing of LC activation and consequent NE release with PP and LOT stimulation than that of Babstock and Harley's (1993) study using PGI stimulation. It was also a weaker

pairing than used in previous studies of glutamate LC activation and PP pairing, in which PP was normally stimulated every 10-30 s instead of every 60 s. The failure to observe depression of the LOT evoked potential may also have resulted from the use of a weaker input (EPSP only) paired less frequently with elevated NE. NE levels decline rapidly over minutes with LC activation (Palamarchouk et al., 2000).

Interestingly, the 7 hr recordings of the ACSF control group seem to demonstrate a spontaneous selectivity of responses, with the amplitude of PP- and LOT-evoked potentials varying in opposition. Statistical analysis of this oscillatory pattern revealed a significant negative correlation between the two parameters (PP-evoked population spike amplitude and LOT-evoked EPSP amplitude) over the duration of the 7 hr recording period. The PP-evoked population spike amplitude in the DG cycled from a lower to a higher level over the duration of recording, with a period of approximately 60-90 min. The LOT-evoked EPSP amplitude varied similarly, but attained its highest levels when PP spike amplitude was lowest, and vice versa.

Sleep-like cycling of hippocampal EEG states under urethane anaesthesia in the rat has been demonstrated by Clement et al. (2004), who found the alternations were not reflective of fluctuations in anaesthetic level. However, the period of the fluctuations between active and deactivated EEG patterns was approximately 9 min, whereas the fluctuations in PP- and LOT-evoked potentials in Experiment 1's ACSF animals had a much longer period of approximately 60-90 min.

To further examine possible *in vivo* depression of the lateral PP input to DG, Experiment 2 used a similar procedure to Experiment 1 with increased pairing of LOT stimulation and NE.

## Chapter 3: Experiment 2

### 3.1 Introduction

NE has been shown to differentially modulate medial and lateral PP input to the DG of the hippocampus *in vitro* and *in vivo*. *In vitro*, long term (> 30 min) potentiation of the medial PP and depression of the lateral PP evoked potentials is observed with extended perfusion of NE or the  $\beta$ -agonist isoproterenol (Dahl & Sarvey, 1989; Pelletier et al., 1994). *In vivo*, an immediate and transitory potentiation (< 70 ms) of the medial PP and depression of the LOT-evoked DG potential are observed following electrical stimulation of PGi, which provides the excitatory input to the LC, the source of NE innervation to the DG (Babstock & Harley, 1993).

In contrast, while Experiment 1 demonstrated the expected long-term (3 hr) potentiation of the medial PP population spike following LC activation, no change in the LOT-evoked DG potential was observed. This NE modulation of medial and lateral PP responses indicates a weaker modulatory selectivity than that seen immediately following PGi stimulation of LC *in vivo*.

In Experiment 1 LOT stimulation was used to selectively activate the fibers of the lateral PP, and produced only an EPSP in DG, in contrast with the stronger medial PP input, producing a population spike. The failure to observe depression of the LOT-evoked DG potential in Experiment 1 may have resulted from the combination of a weaker input and less frequent pairing of LOT stimulation with the period of peak NE release.

Microdialysis data indicates that increased hippocampal NE is only present for minutes following LC activation (orexin or glutamate stimulation of LC raised hippocampal NE levels in first 20 min sample, but not in the following samples; Walling et al., 2004), while voltammetry has shown a decline of NE levels to baseline within 10 min of glutamatergic LC activation (Palamarchouk et al., 2000). Reid and Harley (2009) have shown failure to obtain medial PP long-term potentiation if LC is not stimulated during PP stimulation. With the longer interstimulus interval (60 s) of Experiment 1, LOT stimulation was paired with raised hippocampal NE levels relatively few times.

Additionally, Experiment 1 did not pair LOT stimulation with peak NE release consistently, as presumably occurred with the 30-40 ms delay between PGi stimulation of LC and stimulation of the LOT in Babstock and Harley (1993). Babstock and Harley (1991) demonstrated a 30-40 ms latency between electrical stimulation of PGi and modulation of PP and LOT inputs consistent with a likely temporal interval for peak NE release from terminals in the hippocampus. This putative NE modulation returned to baseline levels by 70 ms (Babstock & Harley, 1991).

Potentiation of the PP evoked population spike is dependent upon a critical level of NE release, with the duration of changes related to the concentration of NE achieved in the DG (Harley, Lalies, & Nutt, 1996). As a threshold level of NE is needed in DG to produce NE-LTP, again the less frequent stimulation of LOT during the period of NE release in hippocampus may have been responsible for the failure to observe depression of the LOT-evoked potential in DG in Experiment 1.

Experiment 2 further examines possible *in vivo* depression of the lateral PP evoked DG potential by following a similar procedure to Experiment 1 but with increased pairing (10 s ISI) of LOT stimulation with LC-evoked NE release.

## **3.2 Methods**

### ***3.2.1 Subjects and surgical preparation***

Five male Sprague Dawley rats (Memorial University of Newfoundland Vivarium) weighing 240-300 g were used. Experimental procedures were conducted within the light phase of the animals' cycle, and in accordance with the Canadian Council of Animal Care guidelines following a protocol approved by the Institutional Animal Care Committee.

Surgical preparation followed the same procedure as Experiment 1. Rats were anaesthetized with 15% urethane (10 ml/kg, i.p.), had their heads shaven, and were placed in a stereotaxic instrument in the skull-flat position. Local anaesthetic (0.25 ml marcaine) was used on the scalp before making a midline incision, the scalp was retracted to expose the skull, and the plane between bregma and lambda leveled to horizontal. Holes were drilled for a glass recording micropipette (3.5 mm posterior to bregma and 2.0 mm lateral, ~ 2.5 mm ventral from brain surface), PP bipolar stimulating electrode (7.2 mm posterior, and 4.1 mm lateral, ~ 3.0 mm ventral), LOT bipolar stimulating electrode (5.0 mm anterior, and 1.5-1.6 mm lateral, ~ 5.8-6.0 mm ventral from brain surface), and LC cannula (12.5 mm posterior to bregma, 1.0 mm lateral, ~ 4.5mm ventral). The LC cannula made of 22-gauge stainless steel (Plastics One) was angled 20° from the vertical to bypass the sagittal sinus and anchored to a jeweler's screw in the skull with dental acrylic. A second jeweler's screw on the anterior portion of the skull served as reference electrode.

The recording pipette and PP stimulating electrode were lowered until DG field EPSP and population spike were maximized, before positioning the LOT stimulating electrode. The

LOT stimulating electrode was first positioned 4.5 mm ventral to the brain surface, before lowering in 50  $\mu$ m increments to a depth that produced the maximal stable EPSP (5.8 to 6.0 mm ventral from surface). Once electrodes were placed, LOT and PP were stimulated at 1 min intervals until evoked potentials appeared stable (approximately 30 to 60 min) before beginning recording.

### ***3.2.2 Procedures for recording, stimulation, and drug injection***

I-O curves were determined using the same procedure as Experiment 1. During baseline and test period recording, shorter PP and LOT stimulation ISIs of 10 s were used, so that PP and LOT stimuli alternated every 5 s. PP stimulation consisted of a single, 0.2 ms square wave pulse at the intensity that elicited a population spike approximately 50% of maximum during the I-O curve. Stimulation of LOT consisted of a 0.2 ms 800-1000  $\mu$ A pulse, using the intensity that produced the maximal stable EPSP. Evoked potentials were amplified and stored by Datawave software for later analysis.

Following the initial I-O curve, test period recording for all animals consisted of obtaining 1 hr of stable baseline, followed by a 200 nl injection of 0.5 M glutamate through the LC guide cannula. The 30 s ejection paired 3 LOT stimuli and 3 PP stimuli with immediate drug ejection. After the injection, an additional 30 min of recording was obtained before determining I-O curves for PP and LOT evoked potentials.

### ***3.2.3 Histology***

Histological analyses followed the procedure described in Experiment 1. Following post-

injection I-O curves, 200 nl of methylene blue (2%) was injected into the LC through the guide cannula to mark the injection site. A 0.5 mA, 2 s lesion was made to mark the placement of the LOT stimulating electrode. Following lesioning, rats were decapitated and brains frozen in chilled methylbutane and stored at -70°C. A cryostat-microtome was used to take 30  $\mu$ m sagittal sections through the region of LC. Alternate sections were stained with 1% cresyl violet and the others left unstained. To locate electrode tracks in LOT, DG, and PP, 30  $\mu$ m coronal sections were taken and glycogen phosphorylase staining used.

#### ***3.2.4 Data analysis***

Three parameters of PP evoked potentials (EPSP slope, population spike amplitude, and latency to peak) and three parameters of LOT evoked potentials (maximum amplitude, EPSP slope, and latency to peak) were measured. All parameters were reduced to 1- and 2-minute means for analysis, and normalized to 30 min pre-glut baseline mean. I-O curves for individual animals were normalized to the largest mean EPSP slope or population spike of the pre-LC activation I-O curve of each individual. Data was analyzed using repeated-measures ANOVAs, and post-hoc LSD analyses were used to further investigate any significant differences.

### **3.3 Results**

#### ***3.3.1 PP-evoked population spike amplitude***

The PP-evoked population spike amplitude of the group as a whole showed a non-significant 3% increase from 2.60 mV pre-LC activation to 2.69 mV post-activation. A repeated-measures ANOVA was used to compare 1 min means for the time from 30 min prior to LC activation to 15 min post-activation. As a group ( $n = 5$ ), PP-evoked population spike amplitude did not differ significantly from baseline (see Figure 3.1). However, among individual animals spike amplitude remained unchanged in two (3.75 mV pre- to 4.42 mV post-activation, 18% non-significant increase;  $F(45, 90) = 0.69, p = 0.92$ ) and decreased in the remaining three from 1.8 mV to 1.5 mV, a -17% change ( $F(45,90) = 2.15, p = 0.001$ ). Direction of change was unrelated to placement of LC cannula.

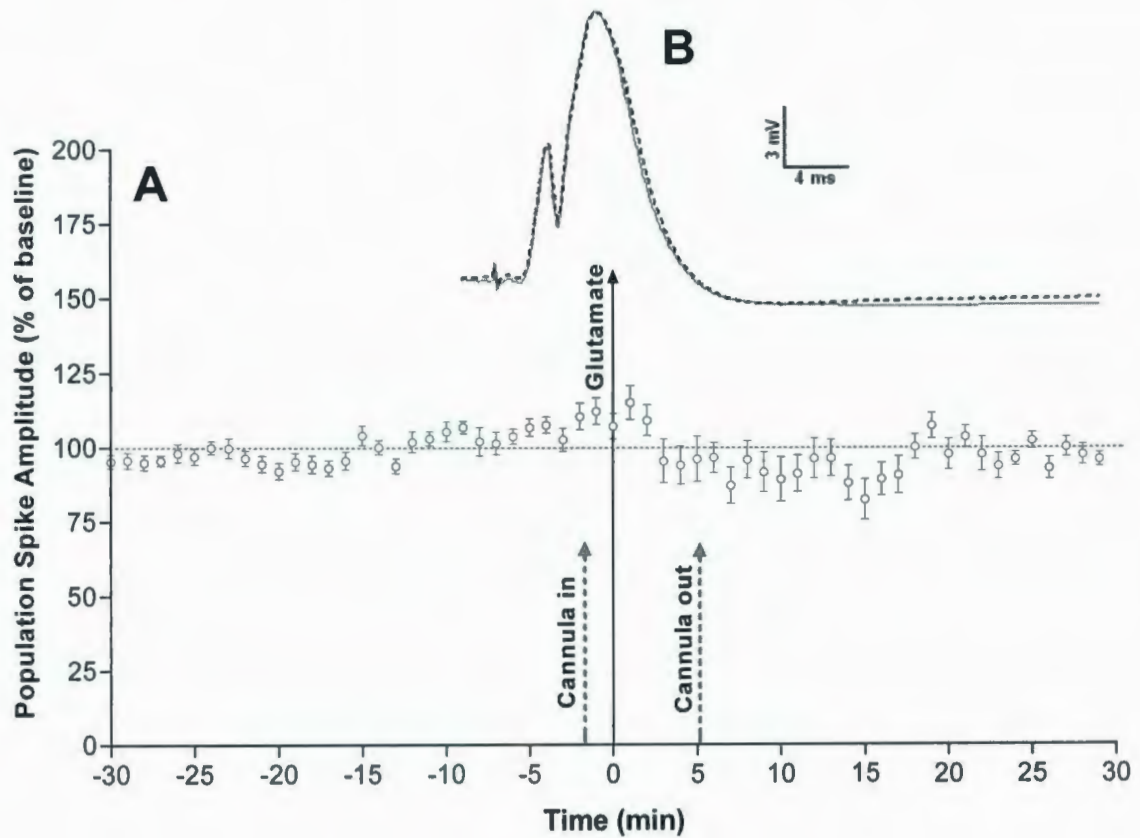


**Figure 3.1** PP-evoked population spike amplitude ( $n = 5$ ).

**A.** PP-evoked population spike amplitude following LC activation did not differ significantly from baseline. A slight pop-up in spike amplitude is seen at cannula insertion. 1 min means, standard error bars indicated.

**B.** Example PP-evoked waveforms recorded in DG from animal with glutamatergic activation of LC. Dashed line is waveform recorded during pre-LC baseline. Solid line is waveform recorded 25 min post-LC activation.

A second repeated-measures ANOVA compared 2 min means for the entire recording period (from 30 min pre-activation to 30 min post-activation), similarly finding a non-significant positive change in two animals (see Figure 3.2) and a significant reduction in three animals ( $F(29,58) = 1.97, p = 0.01$ ; see Figure 3.3) over the longer time period. Post-hoc LSD analysis showed the reduction in amplitude had returned to baseline levels in the latter subgroup by 20 min post-injection.

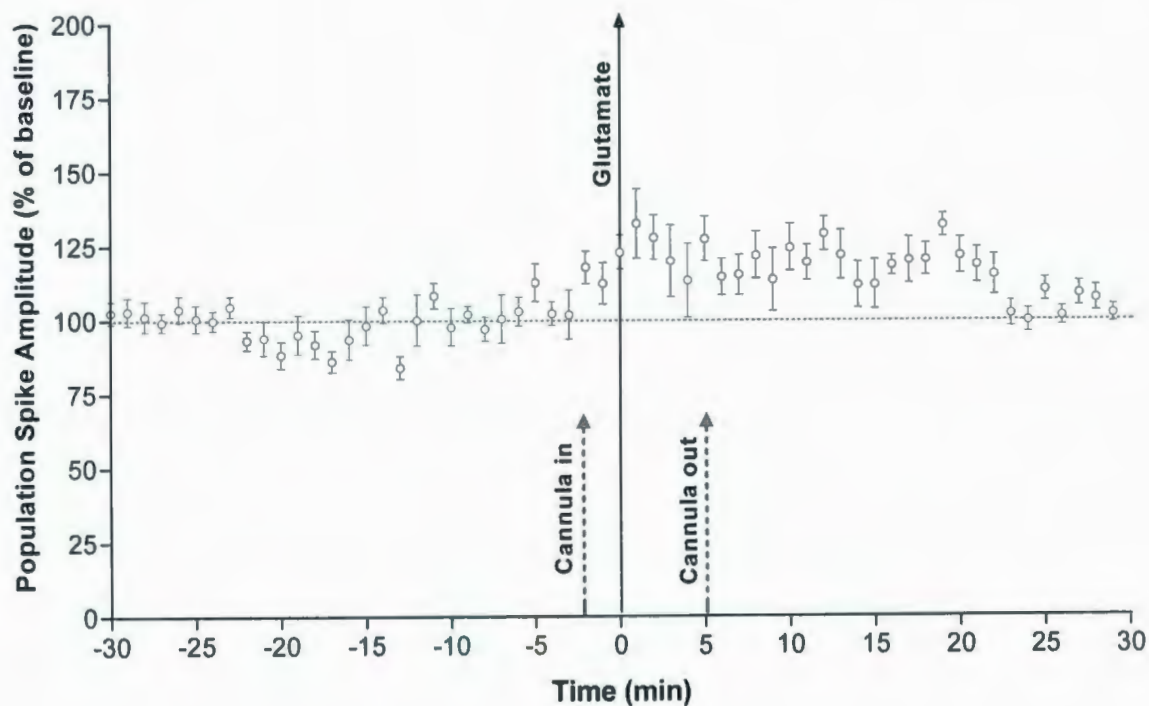


**Figure 3.2 No change in PP-evoked population spike amplitude ( $n = 2$ ).**

A non-significant increase in population spike amplitude (18% of baseline) was observed in two animals following LC activation. A slight pop-up in spike amplitude is seen at cannula insertion. 1 min means, standard error bars indicated.

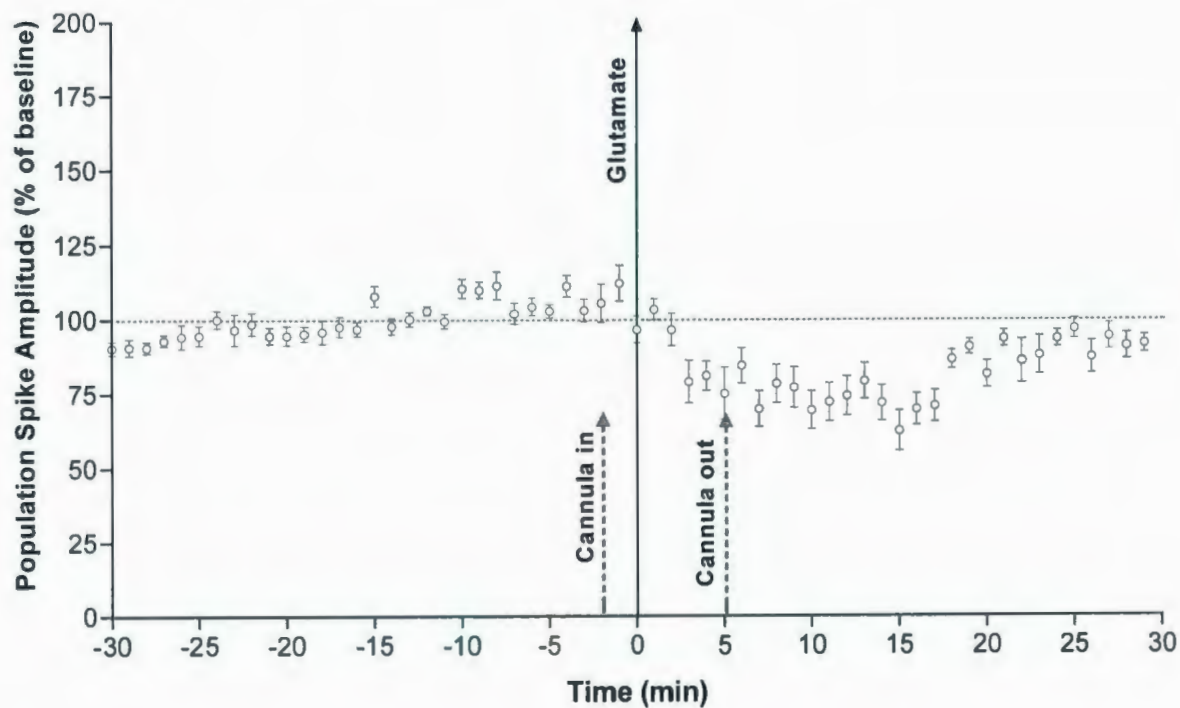


**Figure 3.3 Decrease in PP-evoked population spike amplitude ( $n = 3$ ).**

A 17% decrease in population spike amplitude was observed in three animals compared to baseline. 1 min means, standard error indicated.

### **3.3.2 PP-evoked EPSP Slope**

PP-evoked EPSP slope post-LC activation did not differ significantly from baseline (see Figure 3.4), increasing slightly from 3.03 to 3.08 mV/ms with LC activation (a 1.7% non-significant increase). A repeated-measures ANOVA was used to compare 1 min means for the time from 30 min prior to LC activation to 15 min post-activation ( $F(45,180) = 1.09$ ,  $p = 0.35$ ). A second repeated-measures ANOVA compared 2 min means from 30 min pre-activation to 30 min post-activation ( $F(29, 116) = 1.15$ ,  $p = 0.29$ ).

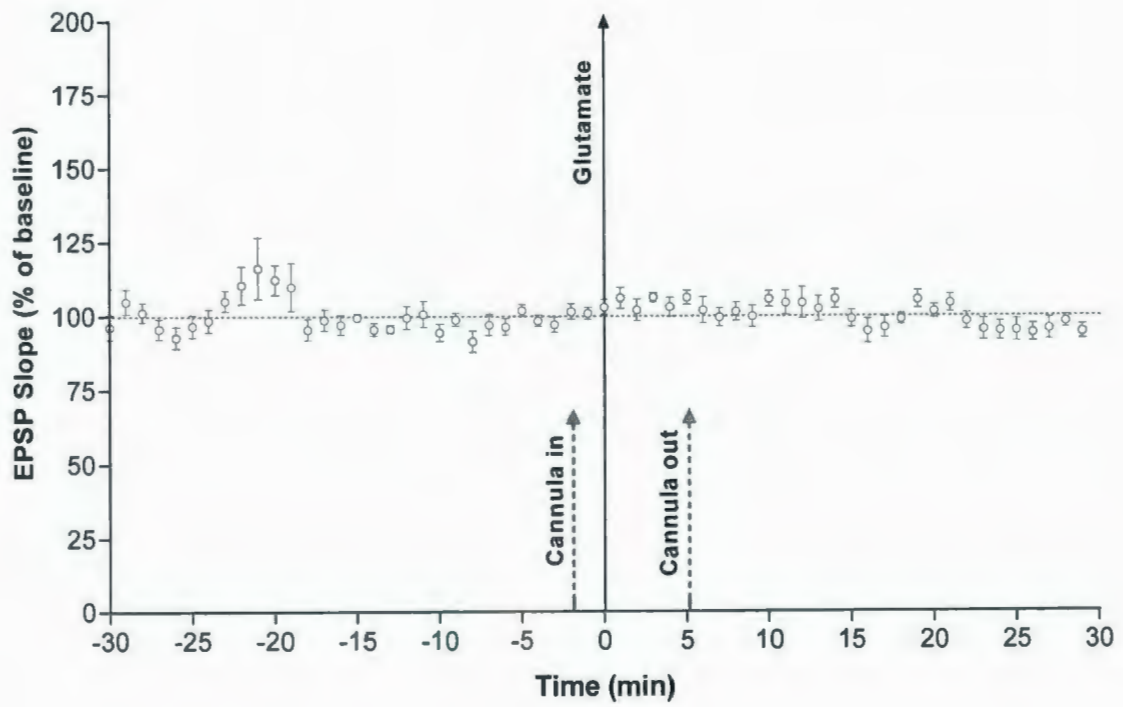


**Figure 3.4 No change in PP-evoked EPSP slope ( $n = 5$ ).**

No significant change in PP-evoked EPSP slope was observed following LC activation. 1 min means, standard error indicated.

The paired-pulse ratio (30 ms ISI) of PP-evoked EPSP slope remained unchanged from the initial to the final I-O curve. At the lowest current level (100  $\mu\text{A}$ ) and highest levels (800 to 1000  $\mu\text{A}$ ) the ratio was less than 1; in the intermediate range (200 to 700  $\mu\text{A}$ ) the ratio exceeded 1 (see Figure 3.5).

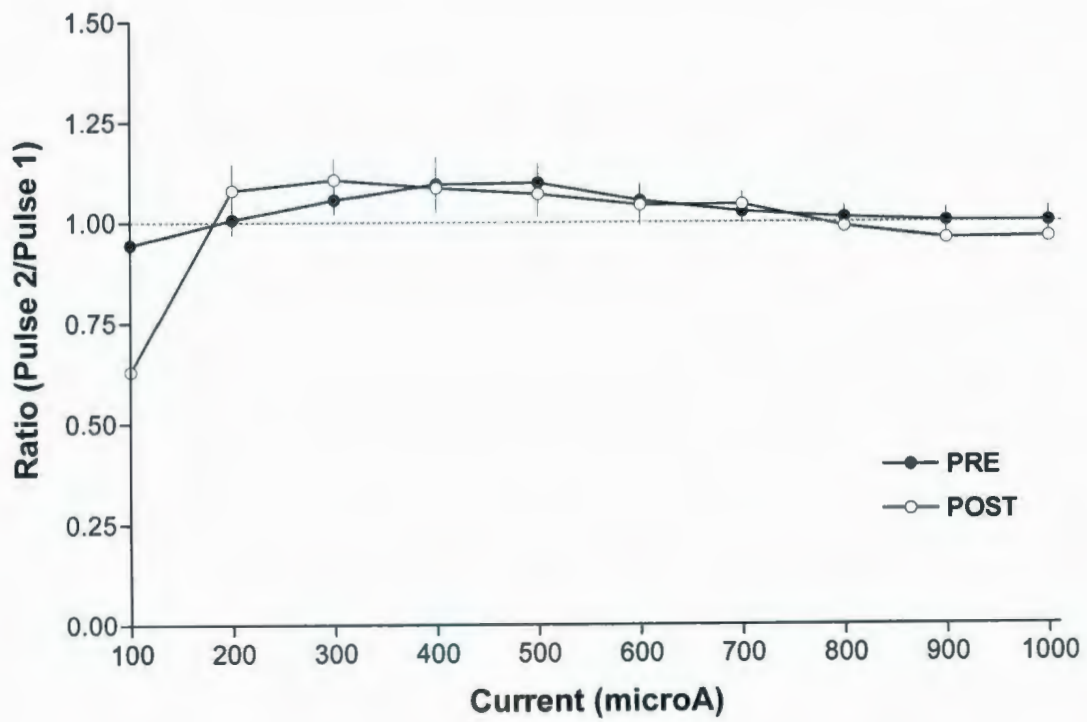


**Figure 3.5 PP-evoked EPSP slope paired-pulse ratio**

PP-evoked EPSP slope paired-pulse ratio (30ms ISI) taken 1 hr pre- and 30 min post-LC activation ( $n = 5$ ).

### ***3.3.3 PP-evoked latency to peak***

No change in PP-evoked latency to peak was observed. A mean latency of 4.19 ms was observed in the 30 min prior to LC activation, with a mean latency of 4.17 ms in the 30 min post-activation, a non-significant decrease of 0.4% (see Figure 3.6).

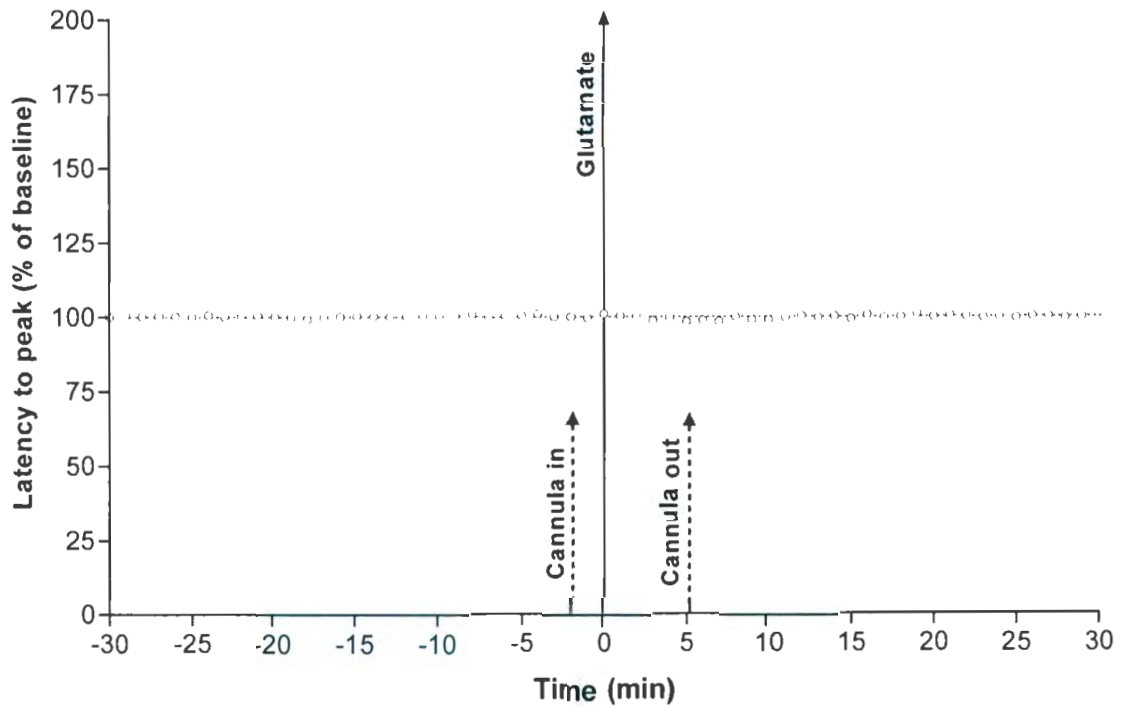


**Figure 3.6 No change in PP-evoked latency to peak ( $n = 5$ ).**

No change in PP-evoked latency to peak was observed in the 30 min following LC activation. 1 min means, standard error bars indicated (SE smaller than icon size).

### **3.3.4 LOT-evoked EPSP amplitude**

LOT-evoked EPSP amplitude (see Figure 3.7) increased in all animals, with the average amplitude of 1.6 mV increasing to 2.4 mV with LC activation (a 47% increase, ranging from 28% to 109%). A repeated-measures ANOVA was used to compare 1 min means for the time from 30 min prior to LC activation to 15 min post-activation. A second repeated-measures ANOVA compared 2 min means from 30 min pre-activation to 30 min post-activation. A significant time effect on amplitude was present when analyzing both 1 min means ( $F(45, 180) = 4.31, p < 0.01$ ) and 2 min means ( $F(29, 116) = 4.43, p < 0.01$ ). Post-hoc LSD analyses showed all points in the 30 min post-LC activation to differ significantly from all points within the 30 min baseline.

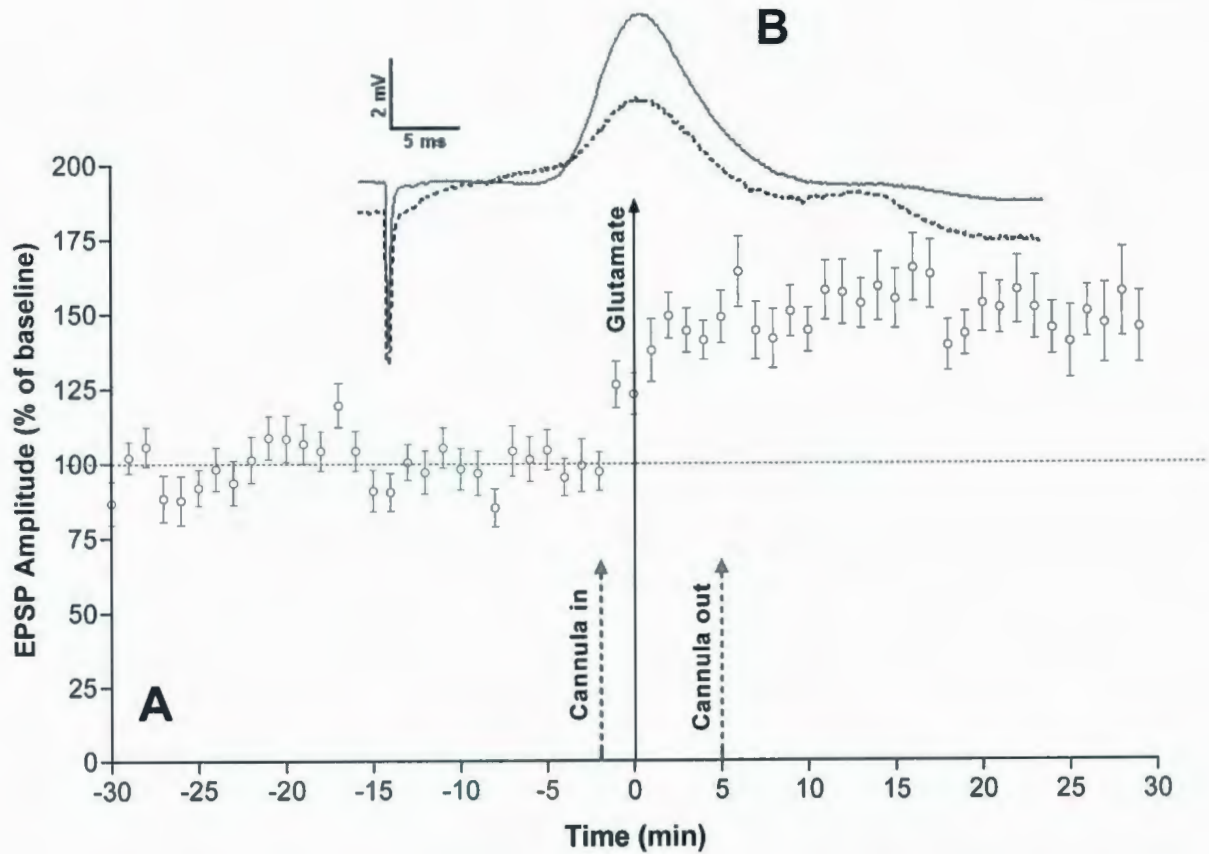


**Figure 3.7 Increase in LOT-evoked EPSP amplitude ( $n = 5$ ).**

A. A pop-up in LOT-evoked EPSP amplitude was observed following cannula insertion, and a significant increase of 47% above baseline followed LC activation. 1 min means, standard error indicated. B. Example LOT-evoked waveforms from animal with glutamatergic activation of LC. Dashed line is LOT-evoked potential recorded during baseline. Solid line is LOT-evoked potential recorded 30 min post-LC activation. Amplitude measured from baseline at stimulus artifact..

### 3.3.5 LOT-evoked EPSP slope

LOT-evoked EPSP slope increased in all animals from 0.31 mV/ms to 0.48 mV/ms, a 56% increase (ranging from 20 to 132%). A repeated-measures ANOVA was used to compare 1 min means for the time from 30 min prior to LC activation to 15 min post-activation. A second repeated-measures ANOVA compared 2 min means from 30 min pre-activation to 30 min post-activation. Similar to EPSP amplitude, a significant time effect on LOT-evoked EPSP slope was present when analyzing both 1 min means ( $F(45,180) = 4.19, p < 0.01$ ) and 2 min means ( $F(29,116) = 4.25, p < 0.01$ ), and post-hoc LSD analyses showed all points in the 30 min post-LC activation to differ significantly from all points within the 30 min baseline (see Figure 3.8).

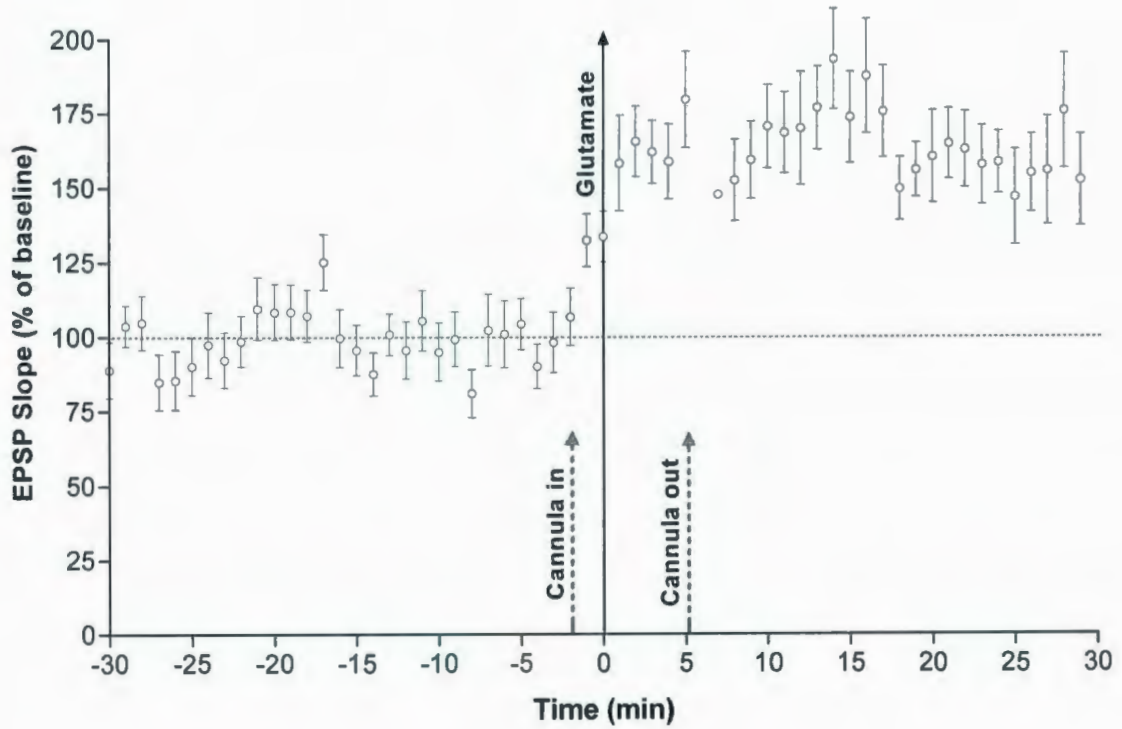


**Figure 3.8 Increase in LOT-evoked EPSP slope ( $n = 5$ ).**

A significant 56% increase in LOT-evoked EPSP slope was observed in all animals following LC activation. A pop-up in slope was observed at cannula insertion. 1 min means, standard error indicated.

### **3.3.6 LOT-evoked EPSP latency to peak**

LOT-evoked latency to peak also increased slightly in all animals (see Figure 3.9), from 17.6 ms to 18.4 ms (a 4% increase, ranging from 1% to 9%). A repeated-measures ANOVA was used to compare 1 min means for the time from 30 min prior to LC activation to 15 min post-activation. A second repeated-measures ANOVA compared 2 min means from 30 min pre-activation to 30 min post-activation. A significant time effect on latency was present when analyzing both 1 min means ( $F(45,180) = 1.68, p < 0.01$ ) and 2 min means ( $F(29,116) = 2.20, p < 0.01$ ). Post-hoc LSD analyses indicated that significant differences from baseline were present between 5 and 25 minutes post-LC activation.

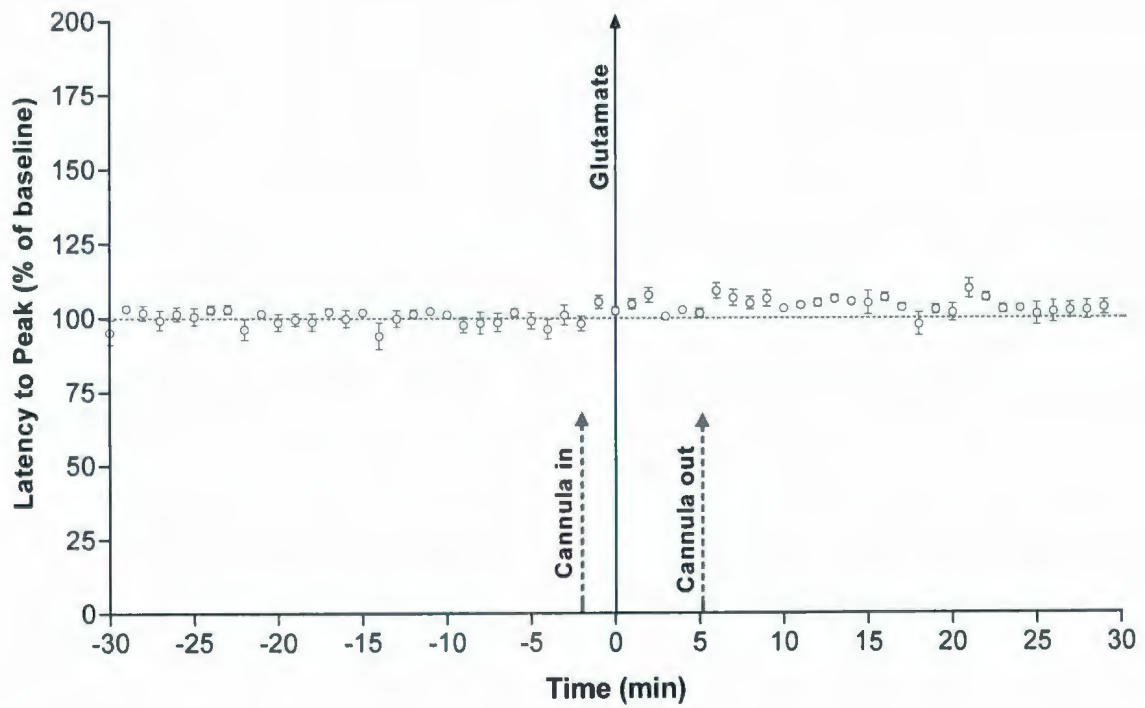


**Figure 3.9** LOT-evoked EPSP latency to peak ( $n = 5$ ).

A small but significant increase in LOT-evoked EPSP latency was observed following LC activation. 1 min means, standard error indicated.

### **3.3.7 Input-output analyses**

PP-evoked EPSP slope and population spike amplitude did not differ significantly between pre and post I-O curves (see Figures 3.10 and 3.11). LOT-evoked EPSP amplitude also remained unchanged between initial and final I-O curves (see Figure 3.12). The difference between pre and post LOT-evoked EPSP amplitude I-O curves was not significant ( $F(1,7) = 1.49, p = 0.26$ ).

The ratio of PP-evoked EPSP slope to population spike remained unchanged between initial and final I-O curves (see Figure 3.13).

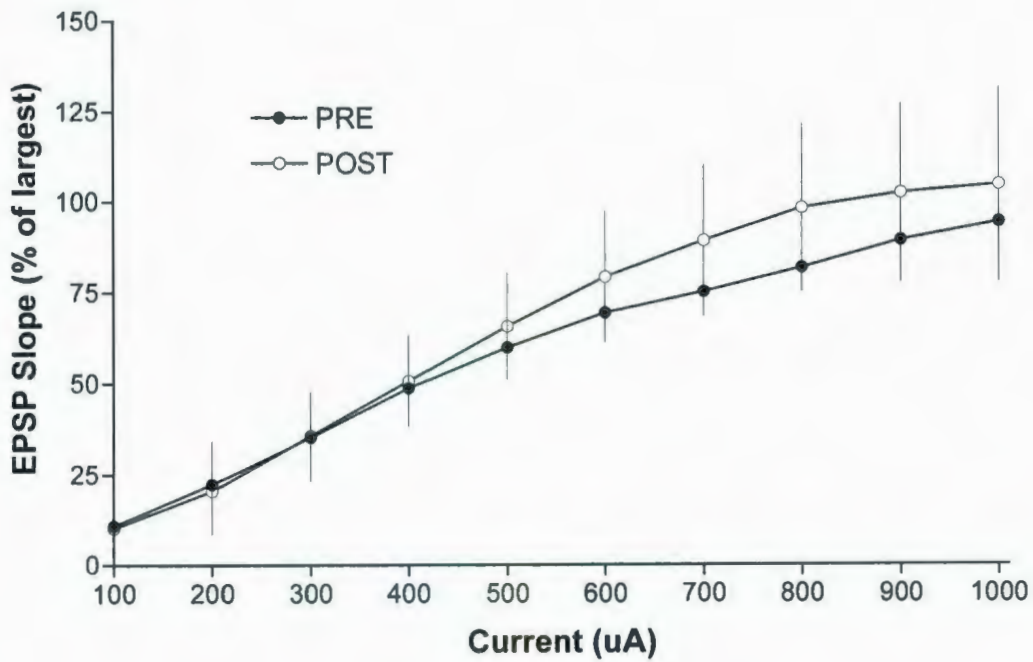


**Figure 3.10 PP-evoked EPSP slope input-output analysis**

I-O curves pre- and post-LC activation ( $n = 5$ ). The mean PP-evoked EPSP slope for each current intensity was converted to a percentage of the largest mean EPSP slope obtained during the pre-activation I-O curve. Data represent the group mean with SEM.

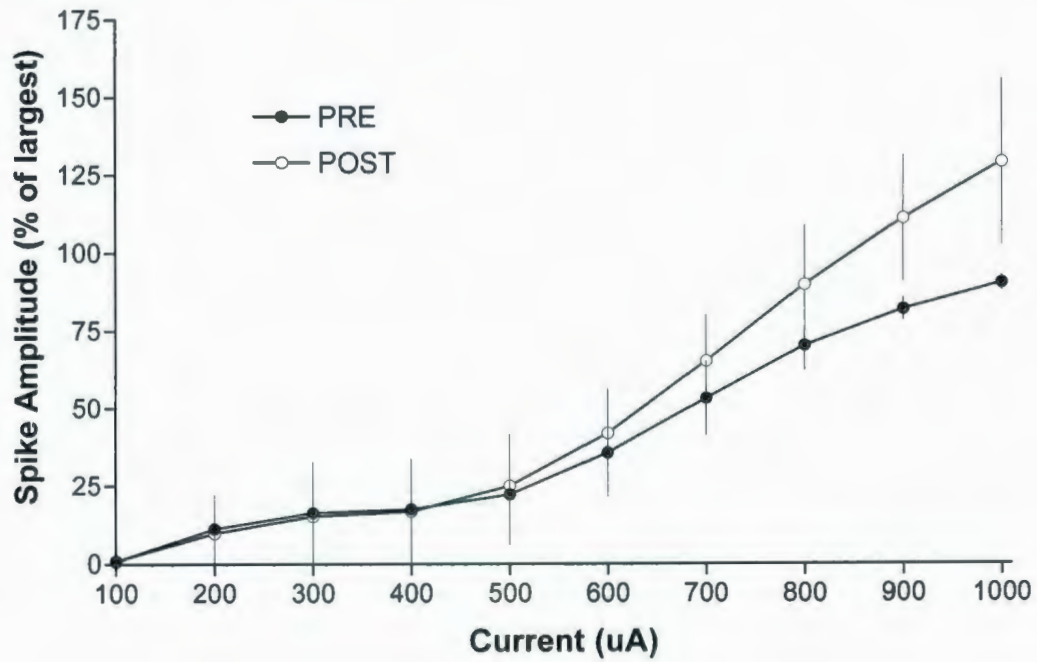


**Figure 3.11 PP-evoked population spike input-output analysis**

I-O curves pre- and post-LC activation ( $n = 5$ ). The mean PP-evoked population spike amplitude for each current intensity was converted to a percentage of the largest mean spike amplitude obtained during the pre-activation I-O curve. Data represent the group mean with SEM.

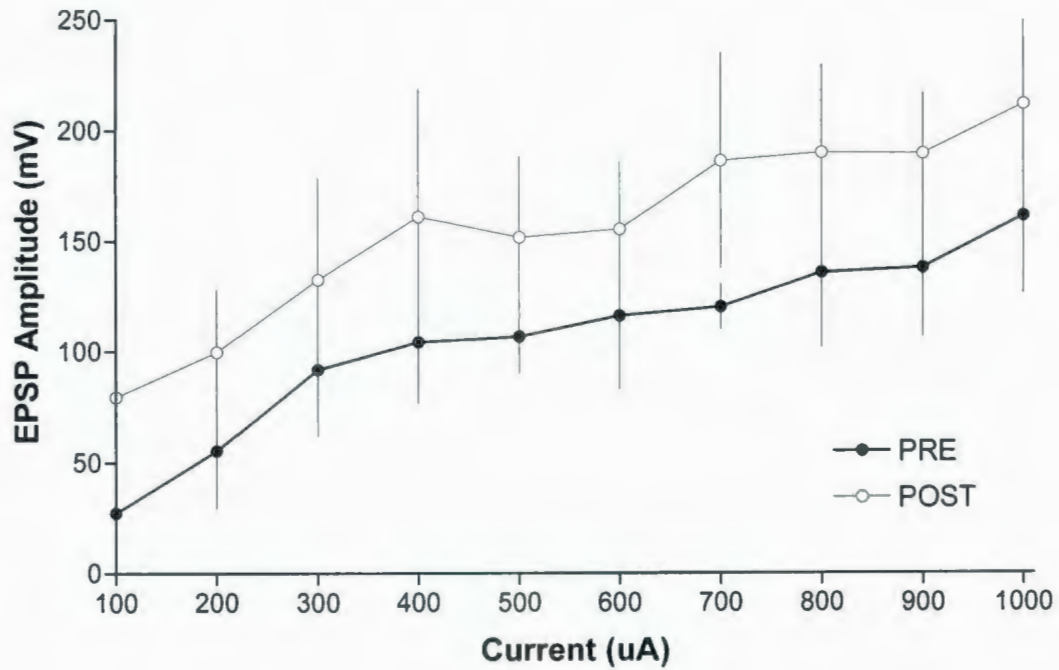


**Figure 3.12 LOT-evoked EPSP amplitude input-output analysis**

I-O curves pre- and post-LC activation ( $n = 5$ ). Mean LOT-evoked EPSP amplitude, group means with SEM.

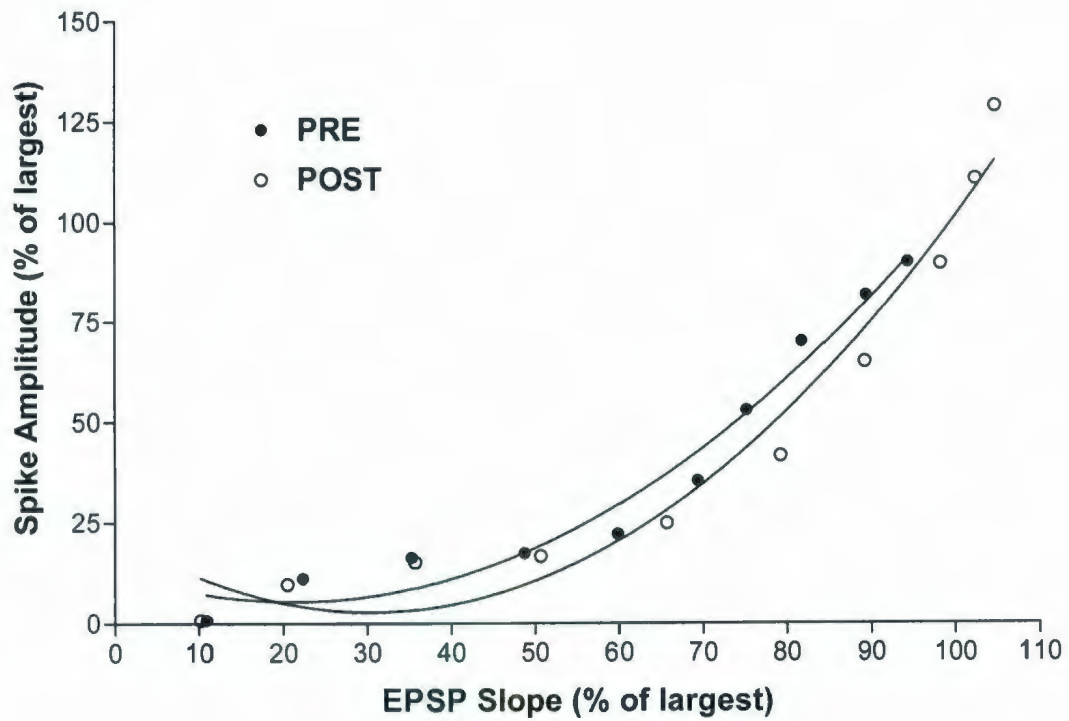


**Figure 3.13 PP-evoked EPSP slope/population spike ratio**

E-S coupling ratio for glutamate animals ( $n = 5$ ), PRE responses recorded 1 hr pre- and POST responses recorded 30 min post-LC activation.

### ***3.3.8 Histology and electrode placements***

Animals were included in the study on the basis of proximity of dye injection to LC; based on previous experience cannula tips located within 300  $\mu\text{m}$  of the Nissl-identified nucleus of the locus coeruleus were considered successful. Dye proximity to LC was measured in 30  $\mu\text{m}$  sagittal tissue sections and compared to adjacent cresyl violet-stained sections. Cannula placements were within the LC in three animals and approximately 200  $\mu\text{m}$  posterior in the remaining two (see Figure 3.14). One of the animals with posterior cannula placement was in the negative-change population spike group, while the other was in the no-change group.

LOT potentials were similar, although variable, in all animals, and lesions were present within LOT in all subjects. Electrophysiological data (positive-going waveform with negative-going population spike) obtained during I-O curves indicated recording micropipette positions within the granule cell layer of the DG in all animals. Population spike latencies were indicative of PP stimulating electrode placements within the medial perforant path.

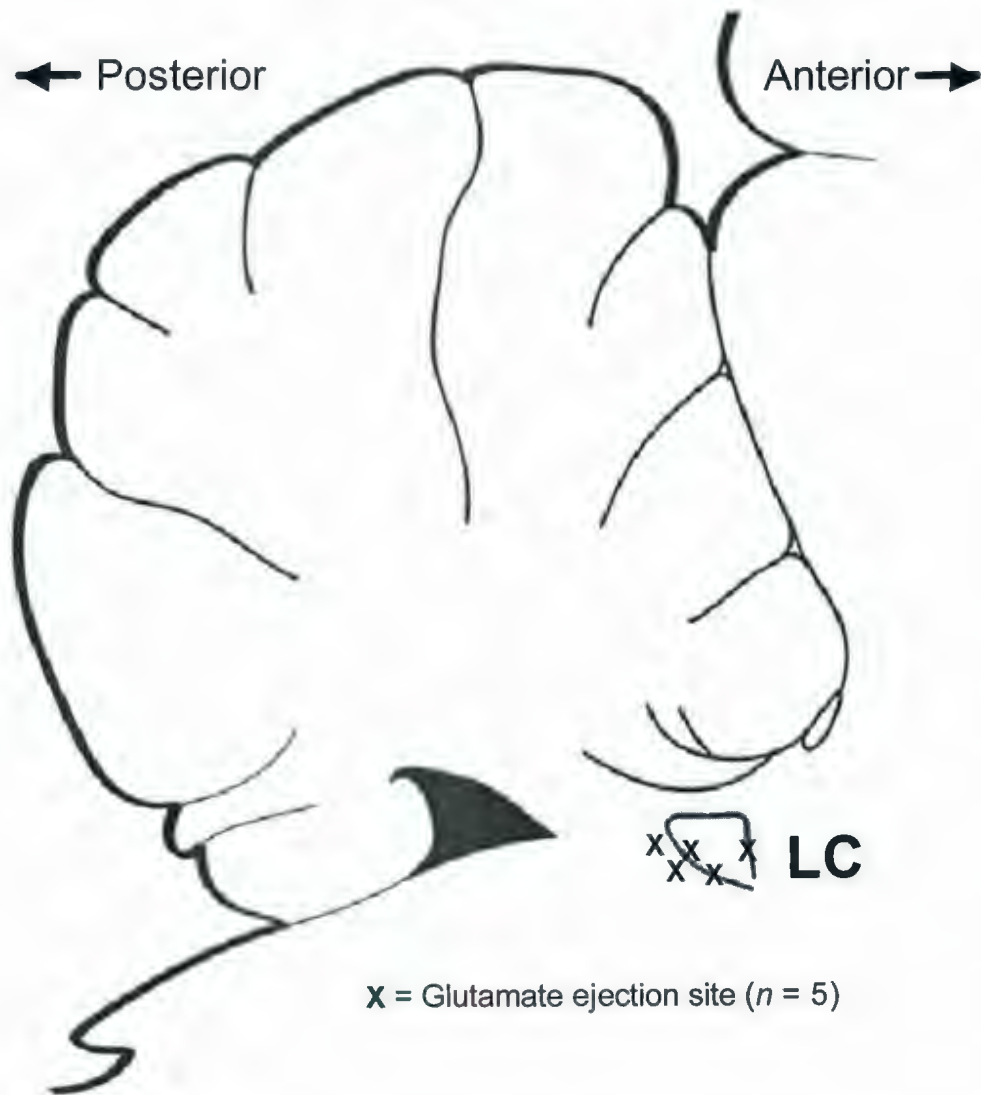


**Figure 3.14 Experiment 2 LC cannula ejection sites**

Locations of dye marking cannula ejection sites near LC, determined with 30 micron sagittal sections through brainstem/cerebellum.

### **3.4 Discussion**

Experiment 1 demonstrated a strong, long-term (3 hr) potentiation of the medial PP evoked potential, with no accompanying evidence of depression of the lateral (LOT) evoked DG potential. To investigate whether the lack of pairing between NE release and LOT stimulation may have been responsible for the failure to observe depression of the LOT evoked potential, more frequent LOT stimulation (10 s ISI) was used in Experiment 2.

In contrast to Experiment 1, Experiment 2 demonstrated an immediate and long-lasting (30 min) potentiation of the LOT evoked DG potential, while no potentiation of the medial PP evoked potential was observed.

In the group ( $n = 5$ ) as a whole, the amplitude of the PP-evoked population spike did not differ significantly from baseline in the 30 min following activation of LC. Histology indicated cannula placements within or near LC in Experiment 2 similar to those seen in Experiment 1; however, the expected increase in PP-evoked population spike amplitude following LC activation did not occur. The group results were composed of two distinct groups of animals, those exhibiting a decline in spike amplitude following LC activation, and those demonstrating a weakly increased or unchanged amplitude.

In three animals, a significant decline in PP-evoked population spike was observed, while the remaining two animals did not differ significantly from baseline. In the 3 animals demonstrating a significant decline in spike amplitude, amplitude had returned to near-

baseline levels approximately 20 min after LC activation. In the remaining two animals, while the increase in spike amplitude was non-significant, it similarly returned to baseline levels after approximately 20 min. The short duration of change from baseline indicates an effect that, while following a much longer time course than the immediate changes observed by Babstock and Harley (1993), is shorter in duration than that observed *in vitro* (Dahl & Sarvey, 1989; Pelletier et al., 1994), in addition to being opposite in direction from expected.

Consistent with the failure of potentiation for the PP-evoked potential, the I-O curves for PP-evoked population spike amplitude did not differ significantly from initial to final data collection. Similar to Experiment 1, no change in PP-evoked EPSP slope was observed over the duration of recording, and the paired-pulse ratio (30 ms ISI) remained unchanged from the initial to the final I-O curves.

The LOT-evoked fEPSP amplitude and slope increased in all animals, in contrast with the expected depression predicted from prior *in vivo* and *in vitro* studies. This increase began in the minute immediately following glutamate activation of LC and remained potentiated for the duration of the recording period (30 min post LC activation). This effect contrasts with Babstock and Harley's (1993) findings and prior studies, which demonstrated an immediate depression of the LOT-evoked EPSP *in vivo* following PGI stimulation of LC, and a lasting depression *in vitro* following NE application (Dahl & Sarvey, 1989). While the I-O curves of LOT-evoked EPSP amplitude taken pre- and post-recording were not significantly different, this may have been due to the high variability of the LOT-evoked

potential and the small number of waveforms (3) collected at each current intensity.

The stimulation-to-peak latency of the LOT-evoked potential also increased slightly in all animals, with latency changes in the same range as previously observed by Babstock and Harley (1993). This increase in latency could be accounted for by the accompanying increase in size of the LOT-evoked EPSP.

While these results do not support sensory selectivity as suggested by Dahl, they are consistent with studies of tetanic LTP of the medial and lateral PP demonstrating competition for control of the hippocampal network (Doyère, Srebro & Laroche, 1997). The potentiation of the LOT-evoked EPSP amplitude and the failure to observe the expected increase in PP-evoked population spike amplitude could be due to heterosynaptic interactions between the two inputs, with the potentiation of one set of synapses depotentiating neighboring inputs.

High-frequency stimulation of either the medial or lateral PP can produce LTP, but the induction of LTP in one pathway leads to a concurrent long-lasting depression of responses evoked by stimulation of the other pathway (Doyère, Srebro & Laroche, 1997). This heterosynaptic depression lasts at least 3 hours following tetanization of the other pathway, and is smaller than the magnitude of LTP. However, heterosynaptic LTD is not observed if the test pathway has been previously tetanized (Abraham & Goddard, 1983).

A study of tetanic-induced heterosynaptic LTD and depotentiation of LTP in the awake rat

noted that heterosynaptic LTD and depotentiation were not symmetric on the two PP inputs: tetanic stimulation of the medial PP had only a small effect on the lateral PP, while induction of LTP on the lateral PP could induce a long-lasting and reversible heterosynaptic LTD at medial PP synapses, with the magnitude of medial PP depotentiation linearly correlated with the magnitude of lateral PP LTP (Doyère, Srebro & Laroche, 1997).

If a similar effect were present in NE-induced LTP in the DG, the failure to observe potentiation of the PP-evoked population spike in this second experiment could be accounted for by the strong facilitation of the LOT-evoked potential.

Additionally, in comparison to Experiment 1 (0.98 mean paired-pulse ratio in glutamate group at baseline levels of stimulation, 400-800  $\mu$ A), the greater PP-evoked EPSP slope paired-pulse ratio (30 ms ISI) seen in Experiment 2 (1.05 at baseline) might indicate a greater proportion of lateral fibers stimulated by the PP electrode. If the activation of medial fibers was weaker in Experiment 2, the difference might contribute to the lateral input's dominance over medial input in the second experiment. The lateral PP would have been activated with both the PP and LOT stimulations. A more selective medial composition of fibers stimulated in the first experiment together with weaker pairing with NE could have led to the domination of medial input.

The amplitude of the LOT-evoked potential was highly variable throughout recording in both experiments. In Experiment 1, facilitation of the PP-evoked DG potential was

observed while the LOT-evoked potential remained unchanged. In Experiment 2, facilitation of the LOT-evoked potential was observed while the PP-evoked potentials diminished or remained unchanged.

This disparity and the negative correlation between amplitude of the LOT-evoked and PP-evoked potentials found in the first experiment seem to support a competitive relationship between the lateral and medial inputs to the DG. This may indicate that the LC enhances the input it is paired with most strongly, consistent with the proposition that LC-NE screens input by enhancing responses to significant stimuli while reducing responses to non-significant stimuli, acting to increase the signal-to-noise ratio in hippocampus (Segal & Bloom, 1976), and indicating also a possible facilitation of competitive interactions in the central nervous system.

## Chapter 4: Discussion

### 4.1 Overview of new outcomes

In Experiment 1, *in vivo* glutamatergic activation of LC combined with the novel use of alternating medial and lateral PP-mediated evoked potentials in the same animals (see Figure 4.1 for recording and stimulation configuration) initiated an immediate LTP of the medial PP-evoked population spike in the DG without accompanying depression of the lateral PP-evoked potential. The failure to observe depression of the lateral-evoked potential contrasts with both short-term *in vivo* (Babstock & Harley, 1993) and long-term *in vitro* (Dahl & Sarvey, 1989; Pelletier et al., 1994) findings which had demonstrated potentiation of the medial PP-evoked population spike accompanied by depression of the lateral PP-evoked potential. Here, as reported in other *in vivo* studies, the PP-evoked EPSP slope remained unchanged in the 3 hr post-LC activation, despite the increase in PP-evoked population spike amplitude.

However, Experiment 2, for the first time in an *in vivo* LC glutamate activation experiment, failed to observe potentiation of the medial PP-evoked potential, either of the EPSP or spike. Instead, a strong and immediate potentiation of the lateral PP-evoked potential (LOT-evoked EPSP in the DG) was seen. While the duration of post-LC activation recording was only 30 min, the robust increase in amplitude of the lateral PP-mediated EPSP indicated a possible long-term effect.

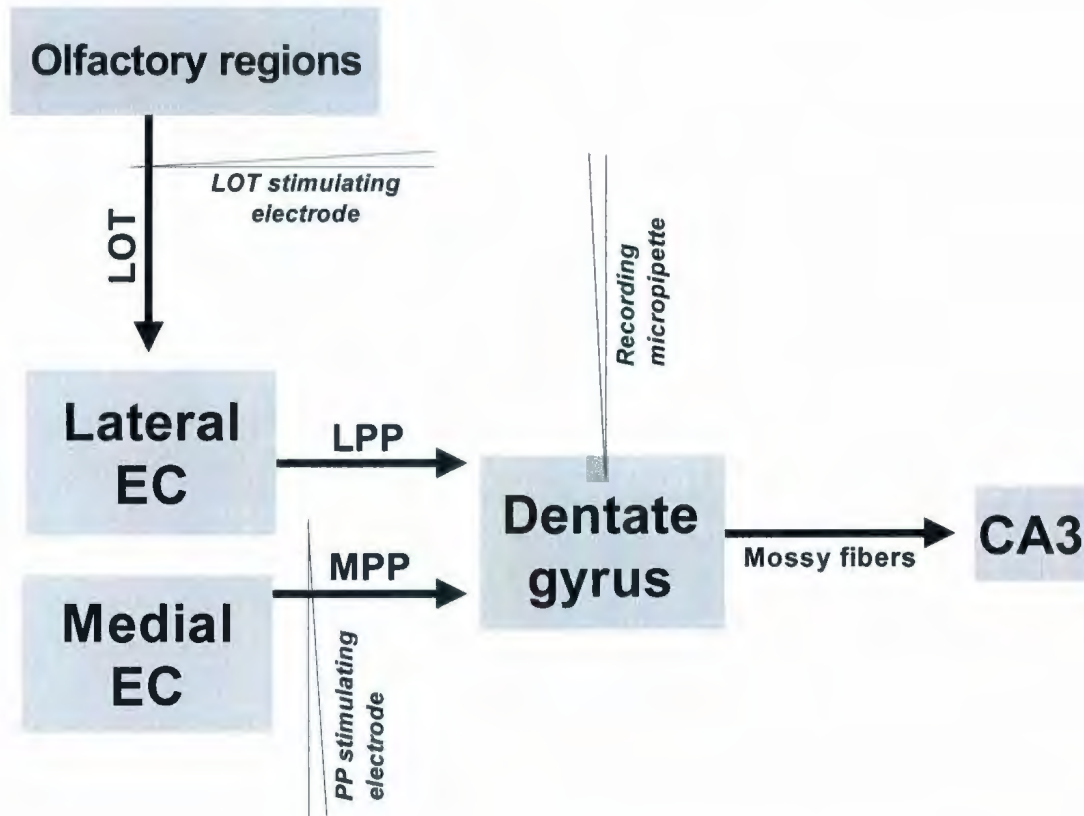


**Figure 4.1 Diagram of stimulation and recording configuration**

The LOT stimulating electrode is placed in the LOT. The PP stimulating electrode is placed in the medial PP (determined through electrophysiological properties of waveforms in I-O curves). The glass recording micropipette is placed in the granule cell layer of the DG (determined through properties of waveforms in I-O curves and histological analyses).

These results are novel in that previous *in vitro* and *in vivo* work has found both long- and short-term depression of the lateral PP, accompanied by potentiation of the medial PP input (either both the EPSP and population spike *in vitro* or population spike only *in vivo*). All studies of glutamate and electrical activation of LC or PGI have found medial PP spike potentiation. This is the first reported failure to observe potentiation of the medial population spike, and the first report of putative long-term potentiation of the lateral PP evoked potential via NE modulation.

## 4.2 Theoretical implications

### 4.2.1 Spatial v. olfactory selectivity

A role for LC activity in the selection of spatial over olfactory input to the hippocampus had been hypothesized. Previous *in vitro* (Dahl & Sarvey, 1989; Pelletier et al., 1994) and *in vivo* (Babstock & Harley, 1991) work supported this hypothesis, demonstrating both long- and short-term enhancement of the medial (spatial) PP potential with concurrent depression of the lateral (olfactory) potential.

The first demonstration of *in vitro* pathway-selective modifications of synaptic responses in the DG came from Dahl and Sarvey (1989), who induced potentiation of medial PP-evoked EPSPs and population spikes, and depression of lateral PP-evoked potentials with a low concentration of NE. Dahl and Sarvey's differential effects, produced by extensive perfusion of NE in the hippocampal slice (30 min), were long-lasting (> 45 min), resembling a memory-like change in synaptic efficacy. Pelletier et al. (1994) later demonstrated that *in vitro* application of isoproterenol, a  $\beta$ -noradrenergic receptor agonist,

also induces long-lasting potentiation of the medial PP and long-lasting depression of the lateral PP, confirming the selectivity of medial and lateral PP responses. Similar to Dahl and Sarvey's (1989) and Pelletier et al.'s (1994) *in vitro* selectivity effects, *in vivo* a short-term (< 10 s), attention-like selective effect of NE upon the medial and lateral PP inputs to DG was observed (Babstock & Harley, 1993). The depression of LOT-evoked potentials was seen 40 ms after PGI stimulation, the same latency at which potentiation of the PP-evoked potential was seen in DG.

Taken together, these results had suggested that NE does not just enhance the incoming signal to the hippocampus with respect to noise, but instead selectively enhanced medial (spatial) input and depressed lateral (olfactory) input. In Experiment 1, the long-lasting potentiation of medial PP input accompanied by an unchanged LOT-evoked potential supported this hypothesis, demonstrating a long-term *in vivo* enhancement of medial (spatial) input over lateral (olfactory).

However, contrary to Experiment 1, in which LC-NE selectively enhanced putative spatial input over lateral olfactory input, in Experiment 2 the lateral (olfactory) input to DG was potentiated while the medial (spatial) input was suppressed. Experiment 2 provides the first observation of selectivity between the medial and lateral PP in which the lateral PP responses are potentiated and not the medial. This suggests that a modality biased selection of input by NE does occur consistently and disconfirms the spatial-over-olfactory selectivity hypothesis.

#### ***4.2.2 Network resetting***

Network resetting is another hypothesis about the overall functional role of NE release. As discussed above, the present experiments were undertaken to test the hypothesis that NE promotes processing of spatial (medial) rather than olfactory (lateral) input by the hippocampal network, which is one form that network resetting might take. A general network reset or functional switch role for monoamine neuromodulators such as NE was first proposed based on invertebrate data (Nusbaum et al., 2001) and has recently been highlighted as the main role of LC-NE release in vertebrates (Sara, 2009).

In 2005 Bouret and Sara proposed network reset as an overarching theory to account for the effects of LC-NE on attention, sensory, and memory retrieval processes. By comparison with the roles of neuromodulators in crustaceans, they suggested that neuromodulator release in response to environmental cues would interrupt existing neural network activity and encourage reorganization of networks to facilitate behavioral adaptation. Because LC cells fire to novel, salient stimuli, it is suggested that this “interrupt” signal is linked to attentional processes (Sara, 2009).

Nusbaum et al. (2001) reviewed invertebrate network switching studies and concluded that the neuromodulatory actions of amines and peptides demonstrate that networks are not hardwired, but instead are reconfigured by the modulatory environment, and that such modulatory substances released under appropriate behavioral conditions enable the disparate functions of neurons configured in different patterns to mediate multiple behaviors.

In an earlier mammalian study, Wiener, Paul, and Eichenbaum (1989) had recorded hippocampal unit activity while rats performed two different tasks relying on hippocampal function: a spatial navigation task and an odor-discrimination task. They found that the same hippocampal complex spike cells with place correlates in the spatial navigation task had highly selective behavioral correlates including odor information in the odor-discrimination task, a finding which supports the hypothesis that the hippocampus “remodels” itself to represent the salient task (Wiener, Paul, & Eichenbaum, 1989). The present data are consistent with this overall framework of network resetting, but the reset rule is not simply modality driven and instead, as suggested by Sara, is likely to be related to adaptive behavioral requirements as originally suggested in the signal-to-noise hypothesis.

#### ***4.2.3 Signal-to-noise ratio***

As discussed in the introduction, in 1970 Kety proposed that NE and the aroused state induced by novel stimuli facilitate novel or significant stimuli while suppressing non-significant stimuli, and that this state initiates the persistent facilitation of active synapses. Segal and Bloom (1976) then proposed that LC-NE acted to screen stimuli by enhancing responses to significant stimuli while reducing excitatory responses to non-significant stimuli, in effect increasing the signal-to-noise ratio in the hippocampus.

Consistent with evidence of NE modulation of hippocampal input through enhancement of the signal or suppression of noise, the medial PP input to DG has been enhanced by

application of NE, an effect which can be short-term (Babstock & Harley, 1993), supporting an attention-like change in processing, or, with sufficiently strong NE input, can be long-term (Neuman & Harley, 1983), supporting a memory-like effect.

These increases in DG granule cell excitability in response to PP input with the application of NE could represent enhanced responses to novelty, as the LC responds to sensory stimuli, especially novelty in the environment (Aston-Jones et al., 1995). However, a number of past studies of this effect did not distinguish between medial and lateral PP stimulation, instead using coordinates that would evoke a mixed or primarily medial response (DG population spike latency to peak is a distinguishing factor between medial and lateral).

The selective enhancement of medial PP input and depression of lateral PP input to the DG seen in prior studies (e.g. Dahl & Sarvey, 1989; Babstock & Harley, 1993) seemed to support the idea of LC-NE functioning to enhance specific signals (with medial (spatial) inputs constituting the signal and lateral (olfactory) input constituting the noise). However, the overall results of the present thesis are consistent with enhancement of a “significant” signal as originally proposed, with significance being determined by the strength of pairing with LC input. Thus, theoretically, the present results are consistent with both the modern network resetting hypothesis and the earlier signal-to-noise enhancement hypothesis. Both the degree of LC pairing and winner-take-all competitive effects, to be considered in the next section, likely interact to determine the “signal” that is enhanced.

### **4.3 Other observations**

#### ***4.3.1 EPSP slope potentiation***

With the clear lateral EPSP potentiation of Experiment 2, it is surprising that no PP slope potentiation was detected. Ratio data indicated that the PP slope was likely a mixture of medial and lateral fibers, but the effect of LOT responsive lateral fibers must have been small enough to lose the signal change in the noise. For Experiment 1, since the LOT EPSP remained unchanged one might have predicted an EPSP slope increase to be observed if the medial PP EPSP had increased. Instead, it appeared that only the medial PP evoked population spike increased. Further studies are needed which isolate the medial and lateral PP fibers for pairing with LC-NE to clarify slope effects.

The observation of enhanced medial PP-evoked population spike without a corresponding EPSP slope increase in Experiment 1 is similar to that in previous *in vivo* studies, which also failed to observe consistent potentiation of PP-evoked EPSP slope despite long-lasting potentiation of population spike amplitude. This has been interpreted as an increase in cell excitability without an accompanying increase in synaptic drive (Harley & Neuman, 1983). The failure to see a decrease in latency with the increase in population spike amplitude argues against an underlying change in the driving EPSP slope for the medial spike. In the initial studies of tetanic LTP, EPSP potentiation was observed, but was also often not sufficient to account for the change in population spike (Bliss & Lomo, 1973). This argues that mechanisms which promote long-term increases in spiking, independent of slope increases, occur in both NE-LTP and tetanus-induced LTP.

It has been suggested earlier that the differential effects of lateral and medial PP stimulation could result in medial PP-evoked EPSP slope potentiation being masked by lateral PP-evoked depression of EPSP slope. However, in Experiment 1 no depression of the lateral evoked potential was observed, yet the mixed medial/lateral EPSP was not increased. Another *in vivo* study (Walling & Harley, 2004), while also demonstrating similar spike amplitude potentiation without an increase in EPSP slope in the 3 hr following glutamatergic activation of LC, later found both PP slope and spike potentiation 24 hr post-LC activation, with the increase in slope accounting for the increase in spike. If competition between lateral and medial PP was responsible for the lack of EPSP slope potentiation one might expect this pattern to be consistent over time, whereas Walling and Harley observed it only in the 3 hr directly following LC activation, and not 24 hr later.

#### ***4.3.2 ACSF controls***

In Experiment 1, a control group of animals received an ACSF ejection in the LC in place of glutamate. ACSF ejections in the LC have not typically been used in past studies utilizing LC activation due to the possibility of mechanical stimulation of LC alone leading to increased NE release. Harley and Sara (1992), while investigating the cellular changes in the LC produced by glutamate activation, noted that in addition to DG population spike amplitude increasing with glutamate ejection in the LC, movement of the LC recording electrode in the LC region alone was sufficient to initiate spike amplitude potentiation in some cases. However, while mechanical stimulation of the LC through brief insertion of a cannula has been shown to cause widespread and intense

activation of *c-fos* throughout the ipsilateral forebrain in most regions known to receive noradrenergic projections from the LC, no response was shown in the hippocampus, which also receives LC afferents (Stone, Zhang, & Carr, 1995).

In Experiment 1 no changes in evoked potential parameters following ACSF ejection in the LC were observed. While the amplitude of PP-evoked population spike increased over time in the ACSF control group, the changes seemed time-dependent and unrelated to ACSF ejection, with amplitude rising consistently over the 7 hr recording period. The differences in parameters recorded in initial and final I-O curves would be consistent with the overall rising baseline, and suggest an increase in excitability over time. This would account for the magnitude of change observed in the ACSF control group, but not for the entirety of larger changes seen in the experimental group receiving glutamatergic activation of LC.

The failure to observe changes in parameters consistent with mechanical stimulation of the LC in ACSF control group animals would suggest that this protocol can successfully be used as a control condition in comparison to conditions utilizing chemical activation of LC.

#### ***4.3.3 Competition in the present experiments***

Several aspects of the current results seem to indicate a competitive interaction between the medial and lateral PP inputs to the DG. In Experiment 1, the medial PP evoked potential was enhanced while the lateral potential remained unchanged, and in

Experiment 2, the lateral potential was enhanced while the medial PP evoked potential remained unchanged. Additionally, data from individual ACSF control animals in Experiment 1 demonstrated a spontaneous selectivity of responses over the duration of the 7 hr recording period, with the amplitude of PP- and LOT-evoked potentials varying in opposition, again suggesting competitive interactions.

The methodology in Experiments 1 and 2 is novel in that the medial and lateral PP were stimulated alternately in the same animals, in combination with glutamatergic activation of LC, setting the stage for competitive interactions during NE release. While the paired-pulse ratio in Experiment 1 indicated a predominantly medial mix of fibers was stimulated by the PP electrode, in Experiment 2, the proportion of medial and lateral fibers being stimulated by the PP electrode was less clearly defined by the paired-pulse ratio.

The disparity in effects in Experiments 1 and 2 and the negative correlation between lateral and medial PP evoked potentials in the control animals of Experiment 1 support a competitive relationship between the medial and lateral DG inputs, one in which LC-NE enhances the input it is paired with most strongly, again consistent with the proposition that LC-NE screens input by enhancing responses to significant stimuli (signal) while reducing responses to non-significant stimuli (noise) in the hippocampus (Segal & Bloom, 1976).

#### **4.3.4 Heterosynaptic tetanic LTP and LTD of PP**

The present results are also consistent with studies of heterosynaptic tetanic LTP and LTD of the medial and lateral PP demonstrating competition for control of the hippocampal network (Doyère, Srebro, & Laroche, 1997). While tetanic LTP can be produced through high-frequency stimulation of either the medial or the lateral PP, the induction of LTP in one pathway leads to a concurrent long-lasting depression of responses evoked by stimulation of the other pathway (Dahl & Sarvey, 1989). Both LTP and LTD have forms that are dependent upon NMDA receptor activation, and perfusion of NMDA on the hippocampal slice is sufficient to induce LTP of the medial PP and LTD of the lateral PP evoked potentials of the DG (Rush, Rowan, & Anwyl, 2001).

In 1983 Abraham and Goddard demonstrated that tetanic stimulation of either the medial or lateral PP (with electrode positions identified by the characteristic shape and latency of evoked potentials recorded in the hilus) reliably depressed synaptic transmission in the other pathway for at least 3 hr in anaesthetized rats. This LTD was present regardless of whether LTP was elicited in the tetanized pathway, and in all cases the magnitude of LTD was less than the magnitude of LTP. LTD was not observed when the test pathway had previously been tetanized. Christie and Abraham (1992), with the same method of medial-lateral electrode positioning, used trains of high-frequency stimulation to induce LTP of the medial PP input to DG in anaesthetized rats, and found LTD of the lateral PP when test pulses were applied. Abraham, Bliss, and Goddard (1985) also noted that tetanization of the lateral PP induced LTP of the lateral PP and LTD of the un-tetanized medial PP, with medial and lateral electrode placements determined by analyzing the EPSP rise

times.

Doyère, Srebro, and Laroche (1997) investigated the characteristics of heterosynaptic LTD and depotentiation of LTP in the medial and lateral PP of the awake rat, finding that while tetanic stimulation of the medial PP had only a small effect on lateral PP responses, induction of LTP of the lateral PP could induce a long-lasting and reversible heterosynaptic LTD at inactive medial PP synapses. This medial PP LTD was linearly correlated with the magnitude of LTP induced in lateral PP synapses, and these effects were long-term, remaining present over multiple days of recording (Doyère, Srebro & Laroche, 1997).

If NE-induced LTP of the DG evoked potential functioned in a similar manner, the unexpected failure to observe potentiation of the PP-evoked population spike in Experiment 2 could be accounted for by the strong facilitation of the LOT-evoked potential. Conversely, in Experiment 1, facilitation of the PP-evoked DG potential was observed while the LOT-evoked potential remained unchanged. Since the only change between Experiments 1 and 2 was frequency of stimulation and increased pairing with LC activation, and because an increased level of NE in the DG is required for NE-LTP to occur, it is reasonable to suggest that the strength of the medial PP evoked potential (population spike) dominated the potentiation mechanism and outcompeted the LOT input to DG in Experiment 1. In Experiment 2, more frequent pairing earlier in the NE release process led to the LOT input dominating the network and outcompeting the medial input. This is consistent with high-frequency LTP studies, in which lateral LTP has

a stronger effect on medial synapses than the reverse.

This disparity could support a competitive relationship between the lateral and medial inputs to DG, in which the LC enhances the input it is paired with most strongly. While the inputs in Experiment 1 were weakly paired with LC-NE, paired-pulse data suggested the fibers stimulated by the “PP” electrode were more medial in origin. In Experiment 2, however, the paired-pulse data was less clear, and the increased pairing may have favored the lateral synapses in the fibers stimulated by the “PP” electrode as well as those stimulated by the LOT electrode.

#### ***4.3.5 Pairing of LC-NE and PP stimulation***

The contrasting results of Experiments 1 and 2 are suggested to be due to the different pairing of LC-NE and LOT stimulation used in each. While the method of LC stimulation (200 nl 0.5M glutamate ejection through cannula over 30 s) remained the same for both experiments, the rate of PP and LOT stimulation was increased in Experiment 2 (10 s ISI), from the 60 s ISI used in Experiment 1.

A critical pairing of PP stimulation with the transient minutes-long increase in hippocampal NE levels may be necessary to produce long-term effects, and the longer ISIs in Experiment 1 may have led to the failure to observe depression of the lateral PP-evoked DG potential.

Palamarchouk et al. (2000) used *in vivo* voltammetry to demonstrate that glutamate

infusion (100 nl of 0.1M glutamate infused over 60 s) into the LC increases the NE-like oxidation current in the rat hippocampus with a latency of about 30 s and a peak within 90 s of glutamate application. Similarly, Harley and Sara (1992) noted that with glutamate activation of the LC (100 nl 0.5M glutamate) and PP stimulation 1/10 s, DG population spike amplitude is increased, with it taking an average of 34 s following glutamate ejection for spikes to exceed the maximum control spike, and nearly all increases occurring within the first minute following glutamate ejection. Together, these results suggest a latency of ~30 s for effective increase in NE release in the hippocampus.

Microdialysis data indicates the presence of increased hippocampal NE over minutes following LC activation (orexin stimulation of LC raised hippocampal NE levels in the first 20 min sample, but not following samples; Walling et al., 2004), and Reid and Harley's (2009) data showed a failure to obtain medial PP LTP if LC is not activated during PP stimulation, with long-lasting potentiation of both EPSP slope and population spike amplitude occurring only when PP stimulation and LC activation co-occurred.

Harley, Lalies, and Nutt (1996) demonstrated that the concentration of NE in the DG was a determining factor in whether or not long-term spike potentiation would occur, with higher levels associated with NE-LTP and lower levels associated with only short duration potentiation. Similarly, Harley and Sara (1992) had earlier demonstrated that the number of LC cells activated is a factor in the initiation of hippocampal potentiation, with smaller volumes of glutamate (< 50 nl) producing increases in LC cell activity but not changes in PP-evoked population spike amplitude.

The pairing effect, arguing for a necessary increase in NE level paired with input (Reid & Harley, 2009), is consistent with the present interpretation that NE-induced memory effects occur for those inputs most strongly and consistently related to elevated hippocampal NE levels. Thus the lesser pairing in Experiment 1 may have been responsible for the failure to observe depression of the lateral PP-evoked DG potential, while the greater pairing in Experiment 2 actually produced potentiation of the lateral input, which may be sufficiently dominant to suppress medial input as seen in asymmetrical tetanus-induced LTP effects.

#### **4.4 Conclusions**

Altogether, the present results seem consistent with an interpretation in which the dominant input signal resets the network, with the dominant signal being the input most strongly and consistently related to elevated hippocampal NE levels. This contrasts with the prior interpretation in which LC-NE selectively enhances the medial (spatial) input while depressing the lateral (olfactory) input, but is congruent with the hypothesis that NE enhances the incoming signal to the hippocampus with respect to noise.

Experiment 2 provided the first observation of selectivity between the medial and lateral PP inputs to DG in which the lateral responses were enhanced, and not the medial. Again, this supports a competitive network reset model of medial and lateral PP interactions in which the signal paired most strongly with elevated LC-NE levels controls the network, similar to the interactions seen with high-frequency LTP of the medial and lateral PP. This

hypothesis is additionally supported by the negative correlation between medial and lateral PP evoked potentials seen spontaneously in the ACSF control animals of Experiment 1, where control of the network spontaneously cycled between medial and lateral dominance.

Because the only change between the two experiments was the frequency of stimulation and increase in pairing with LC activation, and increased level of NE in the DG is a requirement for the induction of NE-LTP, it is reasonable to suggest that the strength of the medial input dominated the potentiation mechanism and outcompeted the lateral input to DG in the first experiment. In the second experiment, the more frequent pairing of PP and LOT stimulation during LC-NE release may have led to the lateral input dominating the network and outcompeting the medial input. This would be consistent with studies of tetanic LTP, in which induction of LTP on the lateral PP has a stronger effect on medial synapses than the reverse.

Thus LC-NE does appear to promote resetting of the network, but as a function of signal selection based on the strength and pairing of inputs. Further experimentation will be required to investigate the proposed competitive selection mechanism, and its engagement by NE and possibly other neuromodulators.

## Chapter 5: References

- Abraham, W. C., Bliss, T. V., & Goddard, G. V. (1985). Heterosynaptic changes accompany long-term but not short-term potentiation of the perforant path in the anaesthetized rat. *Journal of Physiology* 363, 335-349.
- Abraham, W. C., & Goddard, G. V. (1983). Asymmetric relations between homosynaptic long-term potentiation and heterosynaptic long-term depression. *Nature* 305, 717-719.
- Abraham, W. C., & McNaughton, N. (1984). Differences in synaptic transmission between medial and lateral components of the perforant path. *Brain Research* 303, 251-260.
- Amaral, D. G., Scharfman, H. E., & Lavenex, P. (2007). The dentate gyrus: Fundamental neuroanatomical organization (dentate gyrus for dummies). *Progress in Brain Research* 163, 3-21.
- Amaral, D. G., & Witter, M. P. (1995). Hippocampal formation. In G. T. Paxinos (Ed.) *The Rat Nervous System* (pp. 443-493). San Diego: Academic Press.
- Assaf, S. Y., Mason, S. T., & Miller, J. J. (1979). Noradrenergic modulation of neuronal transmission between the entorhinal cortex and the dentate gyrus of the rat. *Journal of Physiology* 292, 52P.
- Aston-Jones, G., Shipley, M. T., & Grzanna, R. (1995). The locus coeruleus, A5 and A7 noradrenergic cell groups. In G. T. Paxinos (Ed.) *The Rat Nervous System* (pp. 183-213). San Diego: Academic Press.
- Babstock, D. M., & Harley, C. W. (1991). Paragigantocellularis stimulation induces  $\beta$ -adrenergic hippocampal potentiation. *Brain Research Bulletin* 28, 709-714.
- Babstock, D. M., & Harley, C. W. (1993). Lateral olfactory tract input to dentate gyrus is depressed by prior noradrenergic activation using nucleus paragigantocellularis stimulation. *Brain Research* 629, 149-154.
- Berridge, C. W., & Foote, S. L. (1991). Effects of locus coeruleus activation on electroencephalographic activity on neocortex and hippocampus. *Journal of Neuroscience* 11, 3135-3145.
- Biella, G., & De Curtis, M. (2000). Olfactory inputs activate the medial entorhinal cortex via the hippocampus. *Journal of Neurophysiology* 83, 1924-1931.
- Bliss, T., Collingridge, G., & Morris, R. (2007). Synaptic plasticity in the hippocampus. *The Hippocampus Book*, Oxford University Press, 343-474.

- Bliss, T. V. P., & Gardner-Medwin, A. R. (1973). Long-lasting potentiation of synaptic transmission in the dentate area of the unanaesthetized rabbit following stimulation of the perforant path. *Journal of Physiology* 232, 357-374.
- Bliss, T. V. P., Goddard, G. V., & Riives, M. (1983). Reduction of long-term potentiation in the dentate gyrus of the rat following selective depletion of monoamines. *Journal of Physiology* 334, 475-491.
- Bliss, T. V. P., & Lømo, T. (1973). Long-lasting potentiation of synaptic transmission in the dentate area of the anaesthetized rabbit following stimulation of the perforant path. *Journal of Physiology* 232, 331-356.
- Bouret, S., & Sara, S. J. (2005). Network reset: A simplified overarching theory of locus coeruleus noradrenaline function. *Trends in Neurosciences* 28, 574-582.
- Bramham, C. R., Bacher-Svendsen, K., & Sarvey, J. M. (1997). LTP in the lateral perforant path is  $\beta$ -adrenergic receptor-dependent. *NeuroReport* 8, 719-724.
- Bramham, C. R., Errington, M. L., & Bliss, T. V. P. (1988). Naloxone blocks the induction of long-term potentiation in the lateral but not the medial perforant pathway in the anesthetized rat. *Brain Research* 449, 352-356.
- Bramham, C. R., Milgram, N. W., & Srebro, B. (1991).  $\delta$  opioid receptor activation is required to induce LTP of synaptic transmission in the lateral perforant path in vivo. *Brain Research* 567, 42-50.
- Brown, R. A. M., Walling, S. G., Milway, J. S., & Harley, C. W. (2005). Locus coeruleus activation suppresses feedforward interneurons and reduces  $\beta$ - $\gamma$  electroencephalogram frequencies while it enhances  $\theta$  frequencies in rat dentate gyrus. *Journal of Neuroscience* 25, 1985-1991.
- Brun, V. H., Solstad, T., Kjelstrup, K. B., Fyhn, M., Witter, M.P, Moser, E. I., et al. (2008). Progressive increase in grid scale from dorsal to ventral medial entorhinal cortex. *Hippocampus* 18, 1200-1212.
- Burgard, E. C., Decker, G., & Sarvey, J. M. (1989). NMDA receptor antagonists block norepinephrine-induced long-lasting potentiation and long-term potentiation in rat dentate gyrus. *Brain Research* 482, 351-355.
- Burwell, R. D., & Amaral, D. G. (1998). Cortical afferents of the perirhinal, postrhinal, and entorhinal cortices of the rat. *Journal of Comparative Neurology* 398, 179-205.
- Cahill, L., & McGaugh, J. L. (1998). Mechanisms of emotional arousal and lasting declarative memory. *Trends in Neurosciences* 21, 294-299.

- Canning, K. J., Wu, K., Peloquin, P., Kloosterman, F., & Leung, L. S. (2000). Physiology of the entorhinal and perirhinal projections to the hippocampus studied by current source density analysis. *Annals of the New York Academy of Sciences* 911, 55-72.
- Chaulk, P. C., & Harley, C. W. (1998). Intracerebroventricular norepinephrine potentiation of the perforant path-evoked potential in dentate gyrus of anesthetized and awake rats: A role for both  $\alpha$ - and  $\beta$ -adrenoceptor activation. *Brain Research* 787, 59-70.
- Christie, B. R., & Abraham, W. C. (1992). NMDA-dependent heterosynaptic long-term depression in the dentate gyrus of anaesthetized rats. *Synapse* 10, 1-6.
- Clayton, E.C., & Williams, C. L. (2000). Glutamatergic influences on the nucleus paragigantocellularis: Contribution to performance in avoidance and spatial memory tasks. *Behavioral Neuroscience* 114, 707-712.
- Clement, E. A., Richard, A., Thwaites, M., Ailon, J., Peters, S., & Dickson, C. T. (2008). Cyclic and sleep-like spontaneous alternations of brain state under urethane anaesthesia. *Public Library of Science* 3(4), 1-16.
- Colino, A., & Malenka, R. C. (1993). Mechanisms underlying induction of long-term potentiation in rat medial and lateral perforant paths in vitro. *Journal of Neurophysiology* 69, 1150-1159.
- Collins, G. G., Probett, G. A., Anson, J., & McLaughlin, N. J. (1984). Excitatory and inhibitory effects of noradrenaline on synaptic transmission in the rat olfactory cortex slice. *Brain Research* 294, 211-223.
- Crutcher, K. A., & Davis, J. N. (1980). Hippocampal  $\alpha$ - and  $\beta$ -adrenergic receptors: Comparison of [3H]dihydroalprenolol and [3H]WB4104 binding with noradrenergic innervation in the rat. *Brain Research* 182, 107-117.
- Dahl, D., & Sarvey, J. M. (1989). Norepinephrine induces pathway-specific long-lasting potentiation and depression in the hippocampal dentate gyrus. *Proceedings of the National Academy of Sciences of the United States of America* 86, 4776-4780.
- Dahl, D., & Winson, J. (1985). Action of norepinephrine in the dentate gyrus. I. Stimulation of locus coeruleus. *Experimental Brain Research* 59, 491-496.
- Dolorfo, C. L., & Amaral, D. G. (1998). Entorhinal cortex of the rat: Topographic organization of the cells of origin of the perforant path projection to the dentate gyrus. *Journal of Comparative Neurology* 398, 25-48.
- Doyère, V., Srebro, B., & Laroche, S. (1997). Heterosynaptic LTD and depotentiation in the medial perforant path of the dentate gyrus in the freely moving rat. *Journal of*

*Neurophysiology* 77, 571-578.

- Ferbinteanu, J., Holsinger, R. M., & McDonald, R. J. (1999). Lesions of the medial or lateral perforant path have different effects on hippocampal contributions to place learning and on fear conditioning to context. *Behavioural Brain Research* 101, 65-84.
- Foote, S. L., Freedman, R., & Oliver, A. P. (1975). Effects of putative neurotransmitters on neuronal activity in monkey auditory cortex. *Brain Research* 86, 229-242.
- Fyhn, M., Molden, S., Witter, M. P., Moser, E. I., & Moser, M-B. (2004). Spatial representation in the entorhinal cortex. *Science* 305, 1258-1264.
- Gilbert, M. E., & Mack, C. M. (1999). Field potential recordings in dentate gyrus of anesthetized rats: Stability of baseline. *Hippocampus* 9, 277-287.
- Harley, C. W. (1987). A role for norepinephrine in arousal, emotion and learning?: Limbic modulation by norepinephrine and the Kety hypothesis. *Progress in Neuro-Psychopharmacology and Biological Psychiatry* 11, 419-458.
- Harley, C. W. (1991). Noradrenergic and locus coeruleus modulation of the perforant path-evoked potential in rat dentate gyrus supports a role for the locus coeruleus in attentional and memorial processes. *Progress in Brain Research* 88, 307-321.
- Harley, C. W. (2007). Norepinephrine and the dentate gyrus. *Progress in Brain Research* 163, 299-313.
- Harley, C. W., & Evans, S. (1988). Locus-coeruleus-induced enhancement of the perforant-path evoked potential. In C. D. Woody, D. L. Alkon, & J. L. McGaugh (Eds.) *Cellular Mechanisms of Conditioning and Behavioral Plasticity* (pp. 415-423). New York: Plenum Publishing Corporation.
- Harley, C. W., Lalies, M. D., & Nutt, D. J. (1996). Estimating the synaptic concentration of norepinephrine in dentate gyrus which produces  $\beta$ -receptor mediated long-lasting potentiation in vivo using microdialysis and intracerebroventricular norepinephrine. *Brain Research* 710, 293-298.
- Harley, C. W., & Milway, J. S. (1986). Glutamate ejection in the locus coeruleus enhances the perforant path-evoked population spike in the dentate gyrus. *Experimental Brain Research* 63, 143-150.
- Harley, C., Milway, J. S., & Lacaille, J-C. (1989). Locus coeruleus potentiation of dentate gyrus responses: Evidence for two systems. *Brain Research Bulletin* 22, 643-650.
- Harley, C. W., & Sara, S. J. (1992). Locus coeruleus bursts induced by glutamate trigger delayed perforant path spike amplitude potentiation in the dentate gyrus. *Experimental*

*Brain Research* 89, 581-587.

- Hebb, D. O. (1949). *The organization of behavior*. New York, NY: John Wiley & Sons.
- Hjorth-Simonsen, A. (1972). Projection of the lateral part of the entorhinal area to the hippocampus and fascia dentata. *Journal of Comparative Neurology* 146, 219-232.
- Hjorth-Simonsen, A., & Jeune, B. (1972). Origin and termination of the hippocampal perforant path in the rat studied by silver impregnation. *Journal of Comparative Neurology* 144, 215-232.
- Hunsaker, M. R., Mooy, G. G., Swift, J. S., & Kesner, R. P. (2007). Dissociations of the medial and lateral perforant path projections into dorsal DG, CA3, and CA1 for spatial and nonspatial (visual object) information processing. *Behavioral Neuroscience* 121, 742-750.
- Jones, B. E., & Moore, R. Y. (1977). Ascending projections of the locus coeruleus in the rat. II. Autoradiographic study. *Brain Research* 127, 23-53.
- Kemp, A., & Manahan-Vaughan, D. (2006). Hippocampal long-term depression: Master or minion in declarative memory processes? *Trends in Neuroscience* 30, 111-118.
- Kemp, A., & Manahan-Vaughan, D. (2008).  $\beta$ -adrenoceptors comprise a critical element in learning-facilitated long-term plasticity. *Cerebral Cortex* 18, 1326-1334.
- Kerr, K. M., Agster, K. L., Furtak, S. C., & Burwell, R. D. (2007). Functional neuroanatomy of the parahippocampal region: The lateral and medial entorhinal areas. *Hippocampus* 17, 697-708.
- Kesner, R. P., Lee, I., & Gilbert, P. (2004). A behavioral assessment of hippocampal function based on a subregional analysis. *Reviews in the Neurosciences* 15, 333-351.
- Kety, S. S. (1970). The biogenic amines in the central nervous system: Their possible roles in arousal, emotion and learning. In F. O. Schmitt (Ed.) *The Neurosciences Second Study Program* (pp. 324-335). New York: Rockefeller University Press.
- Kloosterman, F., van Haeften, T., & da Silva, F. H. L. (2004). Two reentrant pathways in the hippocampal-entorhinal system. *Hippocampus* 14, 1026-1039.
- Lacaille, J.-C., & Harley, C. W. (1985). The action of norepinephrine in the dentate gyrus: Beta-mediated facilitation of evoked potentials in vitro. *Brain Research* 358, 210-220.
- Lipton, P. A., & Eichenbaum, H. (2008). Complementary roles of hippocampus and medial entorhinal cortex in episodic memory. *Neural Plasticity* 2008, 1-8.

- Loy, R., Koziell, D. A., Lindsey, J. D., & Moore, R. Y. (1980). Noradrenergic innervation of the adult rat hippocampal formation. *Journal of Comparative Neurology* 189, 699-710.
- McNaughton, B. L. (1980). Evidence for two physiologically distinct perforant pathways to the fascia dentata. *Brain Research* 199, 1-19.
- McNaughton, B. L., & Barnes, C. A. (1977). Physiological identification and analysis of dentate granule cell responses to stimulation of the medial and lateral perforant pathways in the rat. *Journal of Comparative Neurology* 175, 439-454.
- Milner, T. A., Shah, P., & Pierce, J. P. (2000).  $\beta$ -adrenergic receptors primarily are located on the dendrites of granule cells and interneurons but also are found on astrocytes and a few presynaptic profiles in the rat dentate gyrus. *Synapse* 36, 178-193.
- Moore, R. Y., & Bloom, F. E. (1979). Central catecholamine neuron systems: Anatomy and physiology of the norepinephrine and epinephrine systems. *Annual Review of Neuroscience* 1979 2, 113-168.
- Mueller, A. L., Hoffer, B. J., & Dunwiddie, T. V. (1981). Noradrenergic responses in rat hippocampus: Evidence for mediation by alpha and beta receptors in the in vitro slice. *Brain Research* 214, 113-126.
- Mueller, A. L., Kirk, K. L., Hoffer, B. J., & Dunwiddie, T. V. (1982). Noradrenergic response in rat hippocampus: Electrophysiological actions of direct- and indirect-activating sympathomimetics in the in vitro slice. *Journal of Pharmacology and Experimental Therapeutics* 223, 599-605.
- Munro, C. A. M., Walling, S. G., Evans, J. H., & Harley, C. W. (2001).  $\beta$ -adrenergic blockade in the dentate gyrus in vivo prevents high frequency-induced long-term potentiation of EPSP slope, but not long-term potentiation of population spike amplitude. *Hippocampus* 11, 322-328.
- Neuman, R. S., & Harley, C. W. (1983). Long-lasting potentiation of the dentate gyrus population spike by norepinephrine. *Brain Research* 273, 162-165.
- Nusbaum, M. P., Blitz, D. M., Swensen, A. M., Wood, D., & Marder, E. (2001). The roles of co-transmission in neural network modulation. *TRENDS in Neurosciences* 24, 146-154.
- Palamarchouk, V. S., Zhang, J.-J., Zhou, G., Swiergiel, A. H., & Dunn, A. J. (2000). Hippocampal norepinephrine-like voltammetric responses following infusion of corticotropin-releasing factor into the locus coeruleus. *Brain Research Bulletin* 51, 319-326.

- Pelletier, M. R., Kirkby, R. D., Jones, S. J., & Corcoran, M. E. (1994). Pathway specificity of noradrenergic plasticity in the dentate gyrus. *Hippocampus* 4, 181-188.
- Rick, J. T., & Milgram, N. W. (1999). Instability of dentate gyrus field potentials in awake and anesthetized rats. *Hippocampus* 9, 333-339.
- Reid, A. T., & Harley, C. W. (2009). An associativity requirement for locus coeruleus-induced long-term potentiation in the dentate gyrus of the urethane-anesthetized rat. *Experimental Brain Research*, 10.1007/s00221-009-1955-6.
- Rush, A. M., Rowan, M. J., & Anwyl, R. (2001). Application of *N*-methyl-D-aspartate induces long-term potentiation in the medial perforant path and long-term depression in the lateral perforant path of the rat dentate gyrus in vitro. *Neuroscience Letters* 298, 175-178.
- Sara, S. J. (2009). The locus coeruleus and noradrenergic modulation of cognition. *Nature Reviews Neuroscience* 10, 211-223.
- Sara, S. J., Vankov, A., & Hervé, A. (1994). Locus coeruleus-evoked responses in behaving rats: A clue to the role of noradrenaline in memory. *Brain Research Bulletin* 35, 457-465.
- Sarvey, J. M., Burgard, E. C., & Decker, G. (1989). Long-term potentiation: Studies in the hippocampal slice. *Journal of Neuroscience Methods* 28, 109-124.
- Segal, M., & Bloom, F. E. (1976a). The action of norepinephrine in the rat hippocampus. III. Hippocampal cellular responses to locus coeruleus stimulation in the awake rat. *Brain Research* 107, 499-511.
- Segal, M., & Bloom, F. E. (1976b). The action of norepinephrine in the rat hippocampus. IV. The effects of locus coeruleus stimulation on evoked hippocampal unit activity. *Brain Research* 107, 513-525.
- Sewards, T. V., & Sewards, M. A. (2003). Input and output stations of the entorhinal cortex: Superficial vs. deep layers or lateral vs. medial divisions? *Brain Research Reviews* 42, 243-251.
- Stanton, P. K., & Sarvey, J. M. (1985). Blockade of norepinephrine-induced long-lasting potentiation in the hippocampal dentate gyrus by an inhibitor of protein synthesis. *Brain Research* 361, 276-283.
- Stanton, P. K., & Sarvey, J. M. (1985b). Depletion of norepinephrine, but not serotonin, reduces long-term potentiation in the dentate gyrus of rat hippocampal slices. *Journal of Neuroscience* 5, 2169-2176.

- Stanton, P. K., & Sarvey, J. M. (1987). Norepinephrine regulates long-term potentiation of both the population spike and dendritic EPSP in hippocampal dentate gyrus. *Brain Research Bulletin* 18, 115-119.
- Steward, O. V. (1976). Topographic organization of the projections from the entorhinal area to the hippocampal formation of the rat. *Journal of Comparative Neurology* 167, 285-314.
- Steward, O., & Scoville, S. A. (1976). Cells of origin of entorhinal cortical afferents to the hippocampus and fascia dentata of the rat. *Journal of Comparative Neurology* 169, 347-370.
- Stone, E. A., Zhang, Y., & Carr, K. D. (1995). Massive activation of *c-fos* in forebrain after mechanical stimulation of the locus coeruleus. *Brain Research Bulletin* 36, 77-80.
- Swanson, L. W., & Hartman, B. K. (1975). The central adrenergic system. An immunofluorescence study of the location of cell bodies and their efferent connections in the rat utilizing dopamine  $\beta$ -hydroxylase as a marker. *Journal of Comparative Neurology* 163, 467-506.
- Walling, S. G., & Harley, C. W. (2004). Locus ceruleus activation initiates delayed synaptic potentiation of perforant path input to the dentate gyrus in awake rats: A novel  $\beta$ -adrenergic- and protein synthesis-dependent mammalian plasticity mechanism. *Journal of Neuroscience* 24, 598-604.
- Walling, S. G., Nutt, D. J., Lalies, M. D., & Harley, C. W. (2004). Orexin-A infusion in the locus ceruleus triggers norepinephrine (NE) release and NE-induced long-term potentiation in the dentate gyrus. *Journal of Neuroscience* 24, 7421-7426.
- Wiener, S. I., Paul, C. A., & Eichenbaum, H. (1989). Spatial and behavioral correlates of hippocampal neuronal activity. *Journal of Neuroscience* 9, 2737-2763.
- Wilson, R. C., & Steward, O. (1978). Polysynaptic activation of the dentate gyrus of the hippocampal formation: An olfactory input via the lateral entorhinal cortex. *Experimental Brain Research* 33, 523-534.
- Woodward, D. J., Moises, H. C., Waterhouse, B. D., Hoffer, B. J., & Freedman, R. (1979). Modulatory actions of norepinephrine in the central nervous system. *Federation Proceedings* 38, 2109-2116.
- Young, W. S., & Kuhar, M. J. (1980). Noradrenergic  $\alpha_1$  and  $\alpha_2$  receptors: Light microscopic autoradiographic localization. *Proceedings of the National Academy of Sciences of the United States of America* 77, 1696-1700.





